이학박사학위논문

성상세포와 남성생식세포의 분화 과정에서 Cep215 의 기능에 관한 연구

Studies on the roles of Cep215 in differentiation of astrocytes and male germ cells

2022 년 8 월

서울대학교 대학원

생명과학부

강 동 희

성상세포와 남성생식세포의 분화 과정에서

Cep215 의 기능에 관한 연구

Studies on the roles of Cep215

in differentiation of astrocytes and male germ cells

지도교수 이 건 수

이 논문을 이학박사 학위논문으로 제출함
2022 년 8 월

서울대학교 대학원
생명과학부

강 동 희

강동희의 이학박사학위논문을 인준함
2022 년 8 월

위 원 장 공 영 윤 (인)

부위원장 이 건 수 (인)

위 원 김 재 범 (인)

위 원 강 찬 희 (인)

위 원 성 영 훈 (인)

Studies on the roles of Cep215 in differentiation of astrocytes and male germ cells

A dissertation submitted in partial
fulfillment of the requirement
for the degree of

DOCTOR OF PHILOSOPHY

to the Faculty of
School of Biological Sciences
at
Seoul National University
by

Dong Hee Kang

Date Approved:
August, 2022

_____
_____
_____
_____
_____

ABSTRACT

Studies on the roles of Cep215 in differentiation of astrocytes and male germ cells

Dong Hee Kang

Department of Biological Sciences

The Graduate School

Seoul National University

Centrosome is a subcellular organelle that functions as a microtubule organizing center in animal cells. Centrosomes play roles in several cellular processes, such as cell morphogenesis, mitosis, and cilia formation. A centrosome consists of a pair of centrioles surrounded by proteinous matrix called pericentriolar material (PCM). Cep215, one of major PCM proteins, recruits the γ-tubulin ring complex for microtubule organization. Cep215 is also involved in microtubule organization outside the centrosome. Although the cellular functions of Cep215 have been extensively studied, its specific roles at diverse tissues are relatively less known. During my predoctoral period, I investigated the roles of Cep215 in the brain and testis tissues.

In chapter I, I investigated the roles of Cep215 in astrocyte differentiation using the P19 embryonic carcinoma cells and the mouse hippocampal primary cells. Cep215 was detected in the processes of astrocytes in addition to the centrosomes. Deletion of *Cep215* in P19 cells caused the defects in differential morphogenesis of astrocytes, but did not affect

neuronal differentiation, cell proliferation, and cell fate determination. I found that the microtubule organizing function of Cep215 is critical for the glial process formation. Based on these results, I propose that Cep215 organizes microtubules for glial process formation during astrocyte differentiation.

In chapter II, I investigated the roles of Cep215 in male germ cell development using the KO mouse in which *Cep215* was totally removed by targeting specific sites at both the first and last introns. The *Cep215* KO mice had microcephaly-like defects as reported previously. In addition, *Cep215* KO testes were smaller than the wild type testes, suggesting defects in male germ cell development. In fact, the *Cep215* KO testes were devoid of post-meiotic germ cells. Spermatogenesis in *Cep215* KO mouse was arrested at prophase I and the spermatocytes were vulnerable to cell death. It is surprising that the centrosomes of *Cep215*-deleted germ cells appeared to be intact, suggesting that the defects in progression of meiosis by *Cep215* deletion may be not caused by abnormal centrosomes. Rather, the tight and gap junctions of Sertoli cells were disorganized and the intercellular bridges among germ cells were reduced in the *Cep215* KO testes. Based on the results, I propose that germ cell defects are attributed, in part, to disorganized architecture of the *Cep215* KO testis.

Considering the cellular role of Cep215 in the microtubule organization at centrosomes, it is astonishing that *Cep215*-deleted tissues generated such diverse phenotypes. This research provides an example how diverse cellular functions are regulated by a simple change of the centrosome protein.

Keywords : Centrosome, Cep215, microtubules, differentiation, astrocyte, male germ cell

Student number : 2017-24251

CONTENTS

LIST OF FIGURES

보존용 학위논문 정오표

페이지	정정 전	정정 후
p. 43	Figure 14	Figure 22

BACKGROUNDS

1. Centrosome

Centrosome is a non-membranous organelle which consists of two centrioles and pericentriolar materials (PCM) (Doxsey, 2001). This small organelle was firstly discovered by Boveri in 1888 (Fig. 1; Scheer, 2014). It was reported that the centrosome located at the center of the microtubule network, so it has been called microtubule organizing center (MTOC) in the cells. Since the centrosome has different kinds of functions during cell cycle, mutation of centrosomal proteins are related to various human diseases such as cancer, ciliopathy, and microcephaly (Bettencourt-Dias et al., 2011).

1.1. Structure of centrosome

The centrosome is composed of two centrioles and surrounded by PCM (Fig. 2; Doxsey, 2001). The centriole has a cylindrical structure with 9-fold symmetrically arranged microtubules (Azimzadeh and Marshall, 2010). A pair of centrioles is composed of the mother and daughter centrioles, which have different structure and functions. Mother centriole has distal and subdistal appendages, while daughter centriole does not. These centrioles are linked by intercentrosomal linker proteins during interphase. Two centrioles are embedded in PCM that is a complex of several centrosomal proteins. The core components of PCM, such as Pericentrin, CEP215, NEDD1, CEP192 and γ-tubulin form toroidal structures surrounded the centrioles (Fig. 2; Lawo et al., 2012; Woodruff et al., 2014). Especially, γ-tubulin acts as a template of microtubule via formation of γ-tubulin ring complex (γ-TuRC) with several GCP proteins (Kollman et al., 2011). In onset of mitosis, the centrosome undergoes PCM maturation,

a process of drastic accumulation of PCM proteins to increase the microtubule organizing activity (Kim and Rhee, 2014).

1.2. Functions of centrosome

The centrosome can nucleate microtubules via recruitment of γ-tubulin so that the centrosome acts as a major microtubule organizing center in the cells. However, the function of centrosome varies depending on the cell cycle (Fig. 3). In interphase, centrosome makes microtubules for maintaining the cellular morphology, cell polarity and providing tracks for motor-driven transport of vesicles and organelles (Meiring et al., 2020; Roper, 2020). When the cells enter the mitosis, the centrosome functions as spindle poles to segregate the chromosomes precisely into two daughter cells. Also, the centriole become a basal body to form the cilium in G0 phase (Mahjoub, 2013).

During embryogenesis, the centrosome can act as a determinant of cell fate in neuronal development. In early stage of neurogenesis, neural stem cells (NSCs) divide symmetrically to proliferation. When the NSCs start to differentiate into neuron, NSCs undergo asymmetric division which means that the fate of two daughter cells is not identical. One of daughter cells which inherited daughter centriole is induced neuronal differentiation, another daughter cell given mother centrioles remains as NSC (Fig. 4; Paridaen and Huttner, 2014). In addition, centrosome also determines neuronal polarity (de Anda et al., 2005)

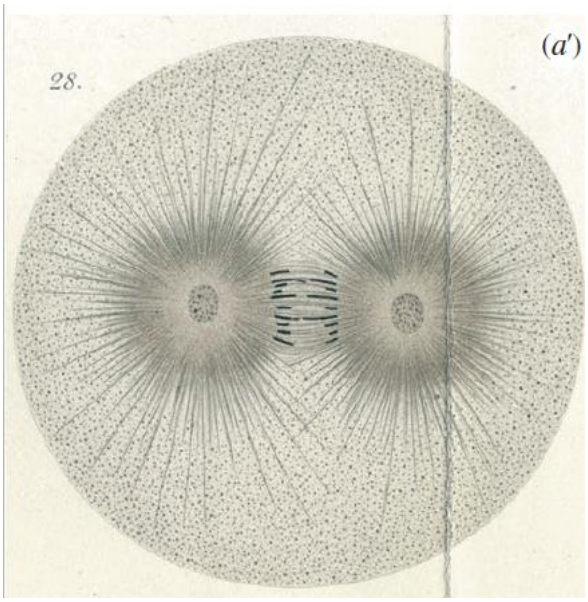

Figure 1. Boveri's drawing of the centrosome Boveri observed and described the centrosome in *Echinus microtuberculatus* during first cleavage. Astral microtubules appear to radiate out from the centrosome. (Scheer, 2014)

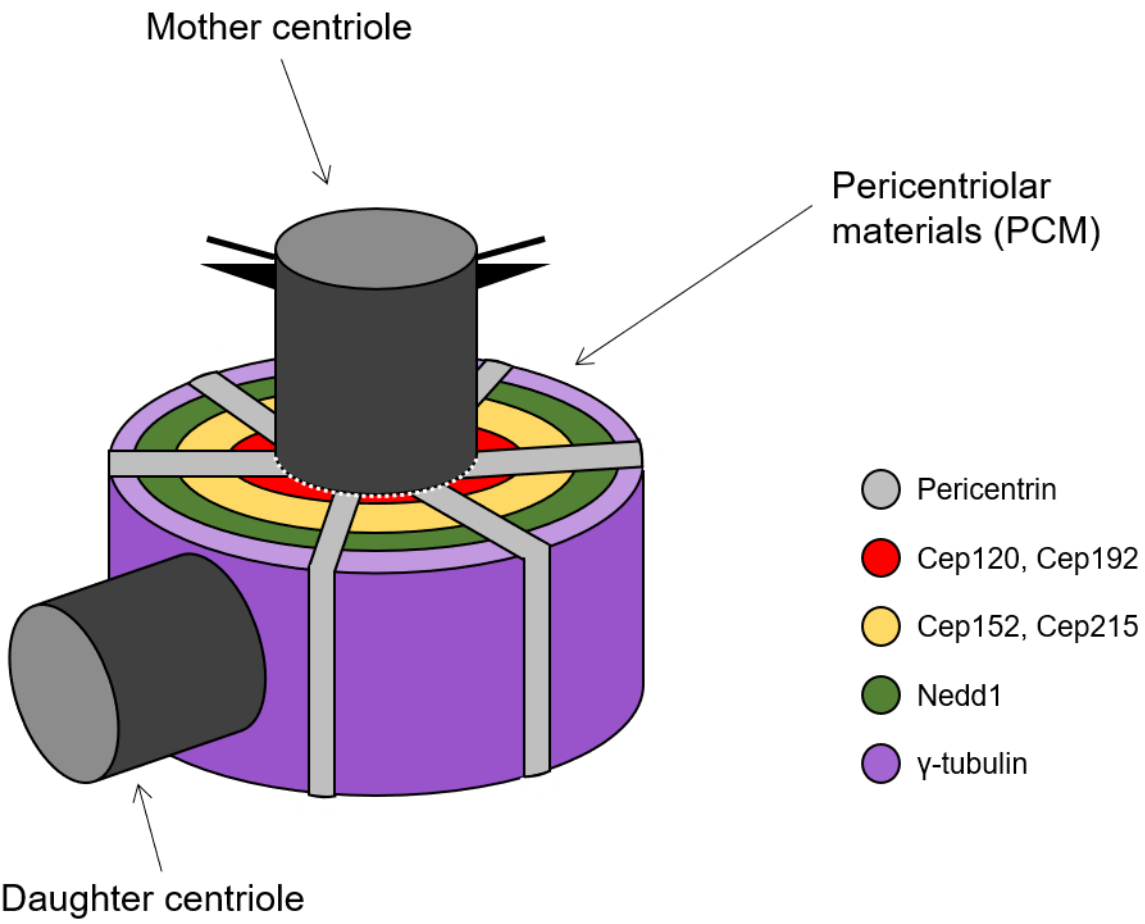

Figure 2. The structure of centrosome The basic structure of centrosome is composed of mother centriole, daughter centriole and surrounded pericentriolar materials (PCM). Major components of PCM proteins (Pericentrin, Cep120, Cep192, Cep152, Cep215, Nedd1, and γ-tubulin) are organized in toroidal structures (modified from Lawo et al., 2012).

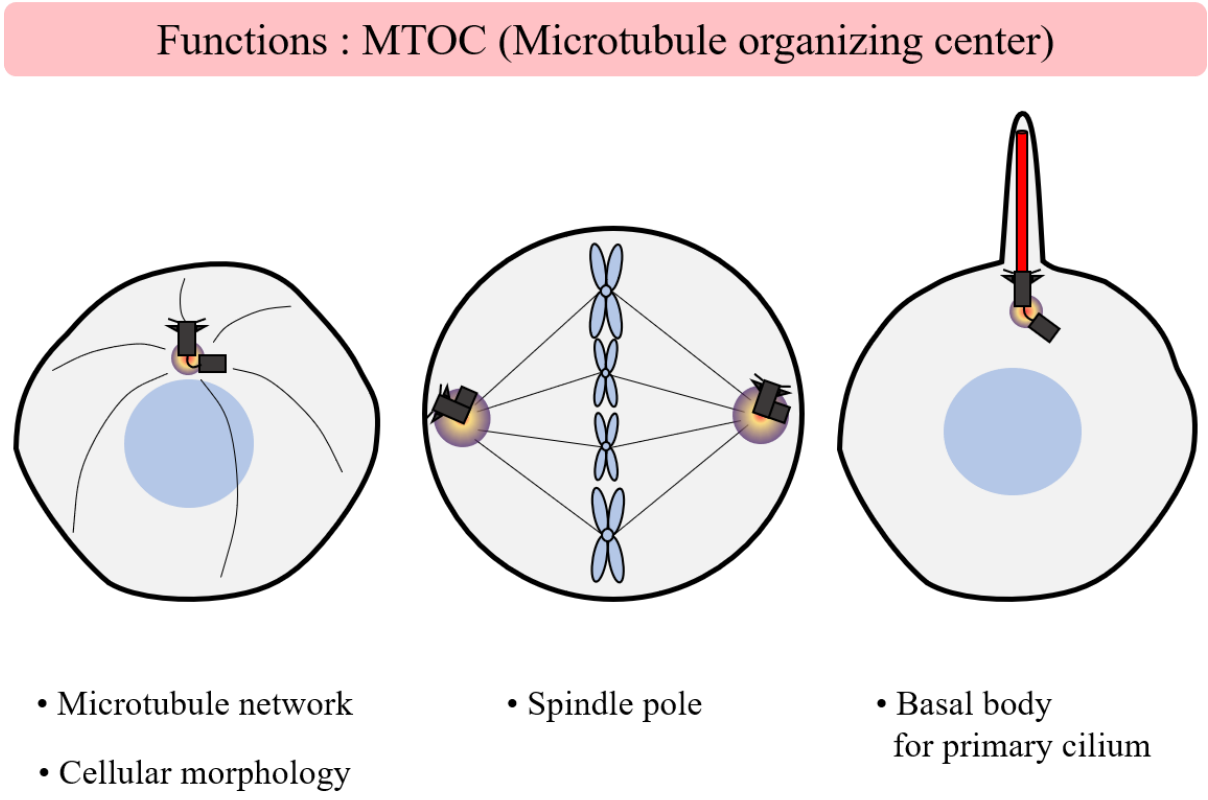

Figure 3. The functions of centrosome The function of centrosome varies depending on the cell cycle. In interphase, centrosome acts as MTOC and maintains the microtubule network and cellular morphology. The centrosome is also involved in bipolar spindle formation during mitosis. Mother centriole is served as basal body for primary cilia formation in quiescent cells

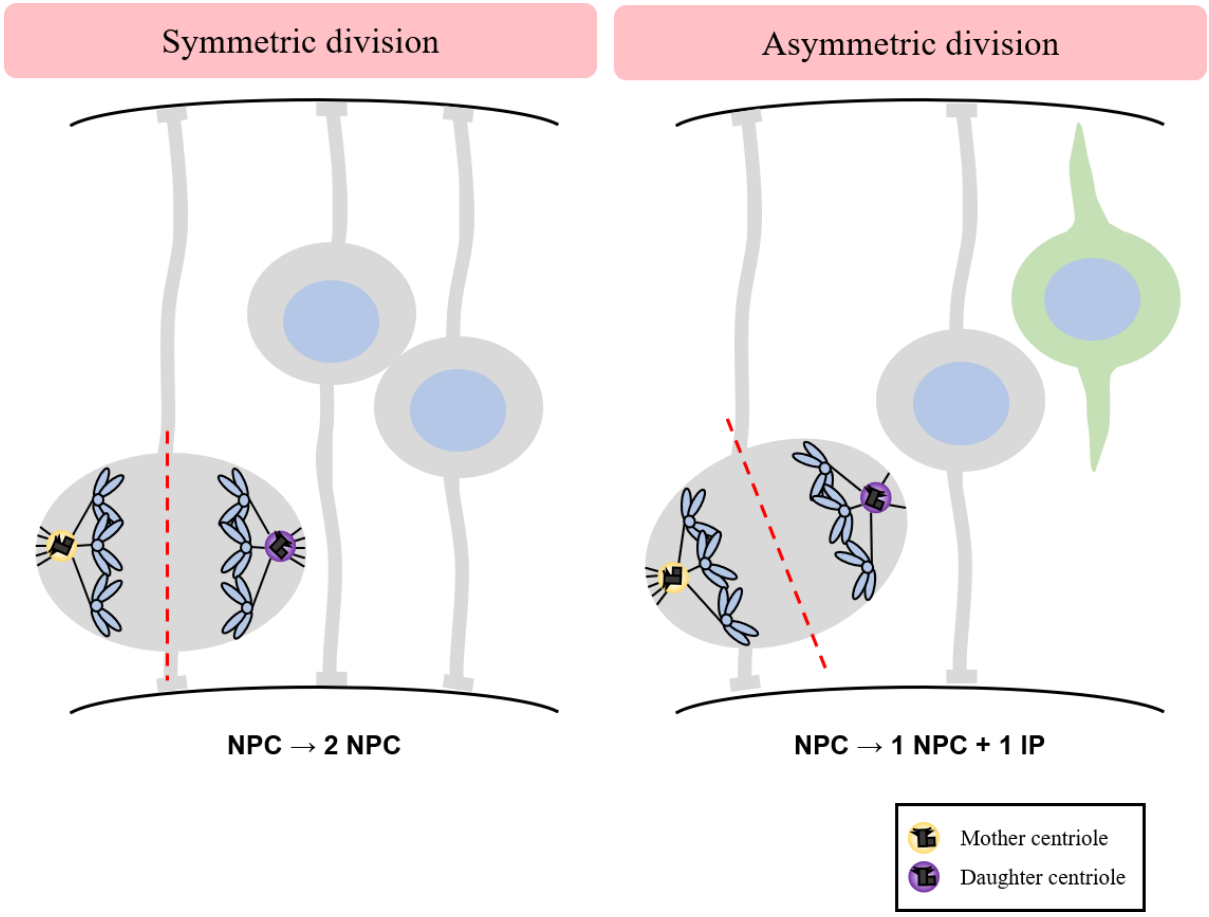

Figure 4. Symmetric and asymmetric division of neural stem cells Neural stem cells proliferate in early stage of neurogenesis by symmetric division. When the stem cells start to neural differentiation, the cells divide asymmetric and cell fate is decided by the centrosome. The daughter cells with mother centriole continue to remain neuronal progenitor cells (NPC) while another daughter cells obtained daughter centriole differentiate intermediate progenitor (IP). (modified from Paridaen and Huttner, 2014).

2. The functions of Cep215

2.1 Microtubule nucleation

Microtubule is one of the essential cytoskeleton and made up of α- and β- tubulins. Although the extension of microtubule is active process, the γ-TuRC is needed for scaffold of tubulin dimers to nucleate microtubule (Oakley et al, 2015). Many proteins that regulate microtubule nucleation have been reported, including Cep215. Cep215, which is also known as Cdk5rap2, is a scaffold protein of other PCM proteins. Cep215 is firstly reported as an activator of neuronal CDK5, but further studies discovered that Cep215 is one of the centrosomal proteins which can recruit and activate γ-TuRC for microtubule nucleation (Fig. 5; Ching et al., 2000; Fong et al., 2008; Choi et al., 2010).

Cep215 has two conserved motifs, CM1 and CM2 (Fig. 6; Barrera et al., 2011). CM1 domain can interact γ-TuRC and this interaction is necessary for the microtubule nucleation. CM2 motif is important for the interactions of Cep215. Through this domain, Cep215 can bind with several proteins, such as Pericentrin or AKAP450, and locate at the centrosome and golgi (Wang et al., 2010). Collectively, Cep215 can nucleate microtubule at specific locations through the various interactions.

2.2 Spindle formation

The major function of centrosome in mitosis is bipolar spindle formation. In the onset of mitosis, PCM expands their size to increase the microtubule organizing activity and the centrosome is separated into two spindle poles. In this context, the interactions of Cep215 with several proteins are necessary for making a functional bipolar spindle. Cep215 regulates the dynein-dynactin complex which transports selected centrosomal proteins, such as PCM-1 and CG-NAP, along the microtubules (Lee and Rhee, 2010). Cep215 also functions as scaffold of other PCM proteins through the interaction with Pericentrin during centrosome maturation (Fig.

7; Kim and Rhee, 2014). Deletion of Cep215 or Pericentrin showed that accumulation of Cep215 and Pericentrin is important for recruitment of γ-tubulin at the spindle pole and formation of bipolar spindle (Kim and Rhee, 2014). In addition, Cep215 binds with HSET to prevent the detachment of centrosome from the spindle pole (Chavali et al., 2016).

2.3. Neuronal differentiation

It is reported that mutations in several centrosomal proteins, including Cep215, cause microcephaly (Bond et al., 2006; Phan and Holland, 2021). Many papers showed that Cep215 regulates the division of NSCs. Mutation or deletion of Cep215 in NSC causes mitotic defects, such as changed mitotic spindle orientation, and induces asymmetric division. These defects led to premature neuronal differentiation. As a result, cell death was induced in prematurely differentiated neuron. Because the number of NSC and differentiated neurons was significantly decreased, the brain size was reduced, as a result (Fig. 8; Buchman et al., 2010; Lizarraga et al., 2010). It is also reported that interaction between Cep215 and Pericentrin plays a role in this process (Buchman et al., 2010). Along with the role of Cep215 in NSC, Cep215 also regulate the morphology of neurons. Centrosomin, a *Drosophila* ortholog of Cep215, can regulate the dendrite branching in dendritic arborization neurons of *Drosophila* through its microtubule organizing activity (Yalgin et al., 2015).

2.4. The phenotypes of *Cep215* mutant mice

The most well-established mutant mouse of Cep215 is *Cep215*$^{an/an}$ mutant mouse. Hertwig's anemia (an) mutant was reported by Hertwig in 1942, and this mutant mouse were identified among the progeny of a heavily irradiated male mouse (Hertwig, 1942; Barker and Bernstein, 1983). *Cep215*$^{an/an}$ mutant mouse has an in-frame deletion of exon 4 that later turn out to be important for the microtubule nucleation activity of Cep215, and showed microcephaly (Lizarraga et al.,2010). Because Cep215 is known to causative gene for

microcephaly, the role of Cep215 in the neural stem cell or neurons have been studied the most (described above). In addition to the role of Cep215 in NSC, it is also reported that Cep215 is essential for dendritic development and synaptogenesis of neocortical layer 2/3 pyramidal neurons in mouse (Zaqout et al., 2019). Along with the studies on the brain development, the involvement of Cep215 in development of several organs are discovered using this mutant mouse. It is reported that *Cep215*$^{an/an}$ mutant showed developmental defects in eye and testis (Zaqout et al., 2017, 2020).

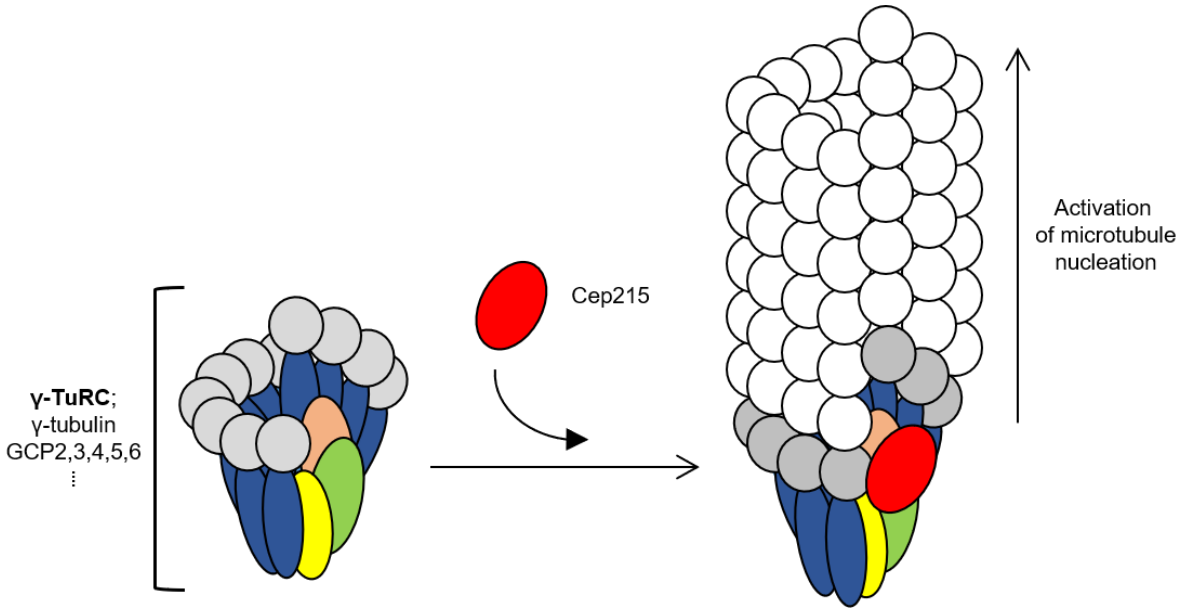

Figure 5. Model for activation of microtubule nucleation by Cep215 When γ-tubulin recruits GCP proteins and assembles to γ-tubulin ring complex (γ-TuRC), CM1 motif of Cep215 binds to γ-TuRC to stimulate the microtubule nucleation. (modified from Choi et al., 2010).

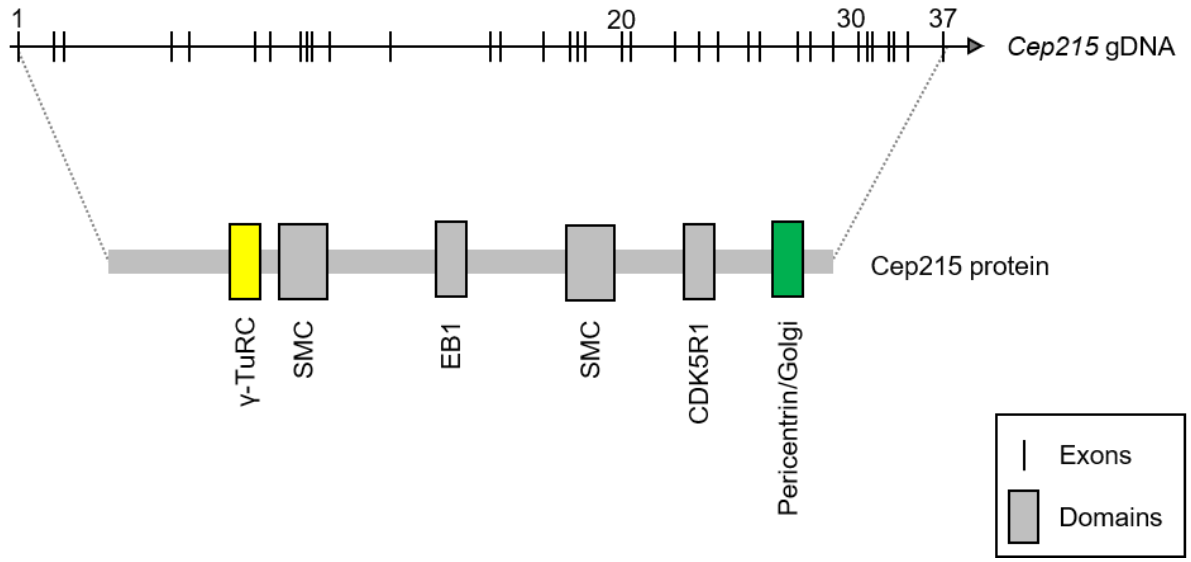

Figure 6. Domains of Cep215 Cep215, one of Centrosomin family, has conserved domains, CM1 and CM2 (yellow box and green box, respectively). CM1 domain mediates γ-TuRC binding and CM2 domain mediates the localization of Cep215 in centrosome and Golgi (modified from Issa et al., 2013)

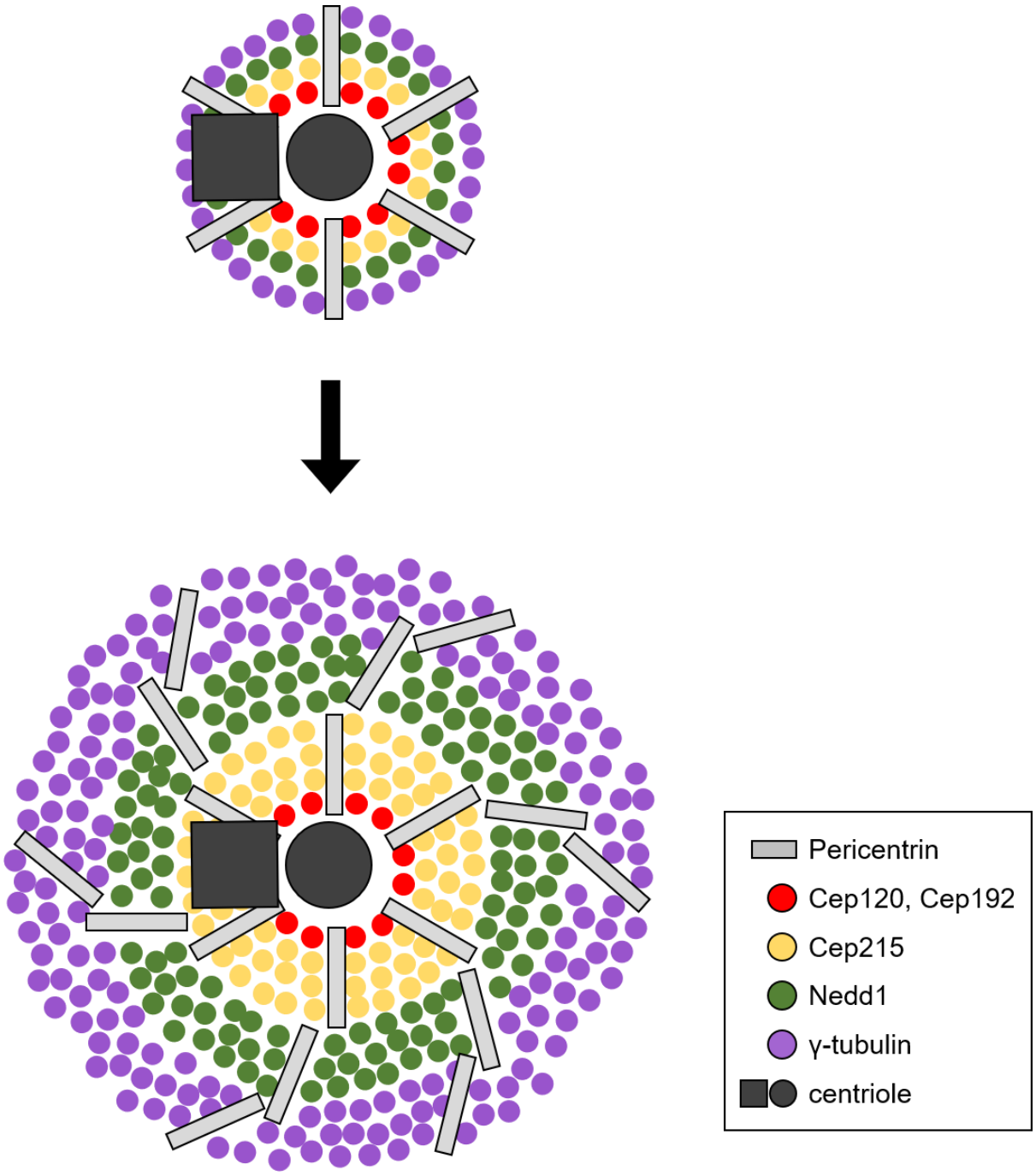

Figure 7. Model for the PCM maturation Cep215 and pericentrin function as a scaffold of other PCM proteins, especially γ-tubulin, to increase microtubule organizing activity prior to mitosis. (modified from Kim and Rhee, 2014)

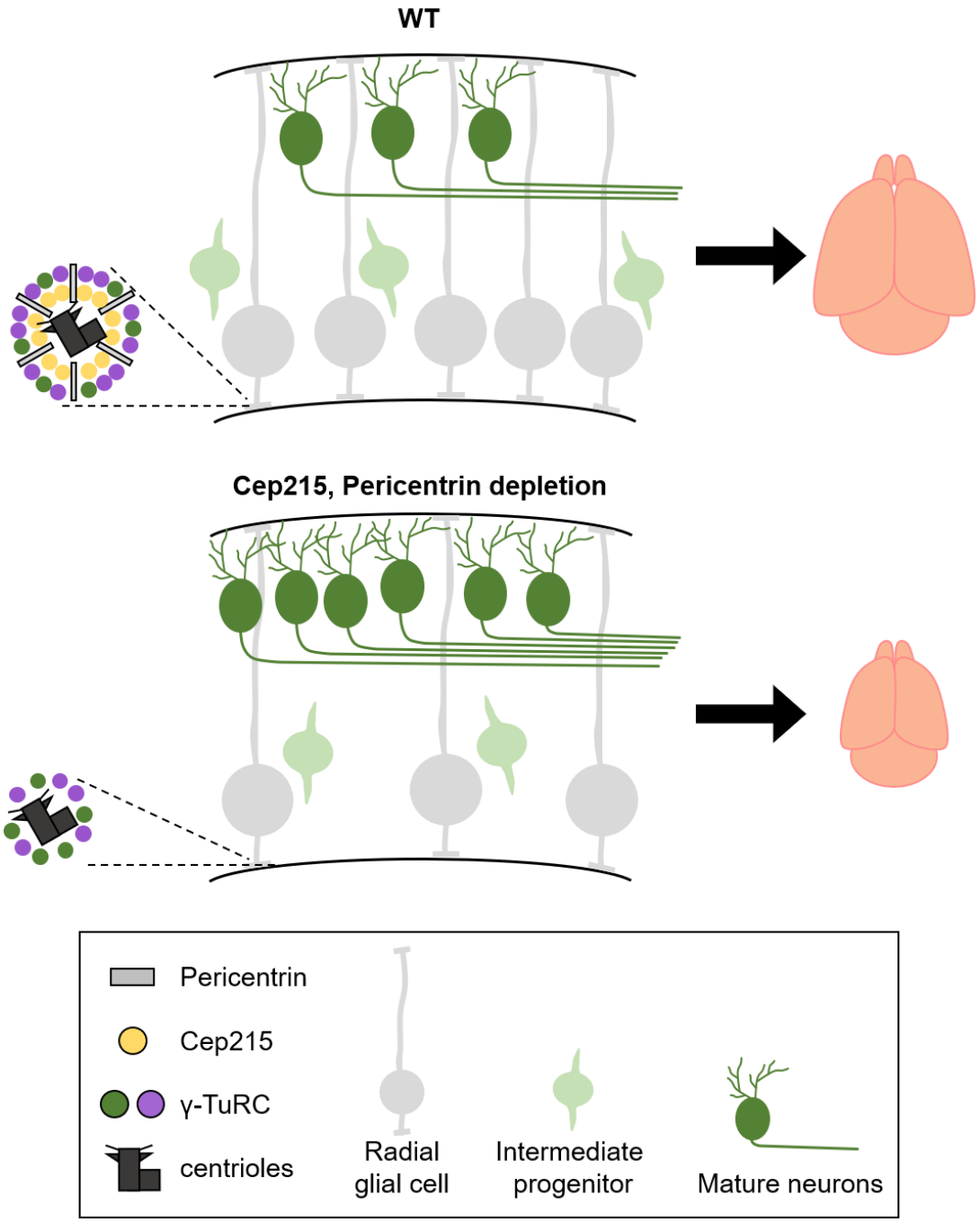

Figure 8. Model of Cep215 and pericentrin functions in neurogenesis When Cep215 or pericentrin was depleted, the balance between proliferation and differentiation of neural stem cell is broken so that the cells undergo premature neurogenesis. In conclusion, the pool of neural stem cells is depleted and the brain size is reduced. (modified from Buchman et al., 2010)

Chapter I.

Roles of Cep215 in morphological differentiation of astrocytes

ABSTRACT

Cep215 is a centrosome protein which is involved in microtubule organization. Cep215 is also placed at specific subcellular locations and organizes microtubules outside the centrosome. *Cep215* is a causal gene of microcephaly with premature neurogenesis and cell death. However, importance of Cep215 in other brain cell types, such as astrocytes, has not been elucidated yet. Here, I report that Cep215 is involved in morphological differentiation of astrocytes. Defects in morphological differentiation of astrocytes was observed not only in the *Cep215*-deleted P19 cells but also in the *Cep215*-depleted embryonic hippocampal culture. I confirm that the microtubule organizing function of Cep215 is critical for the glial process formation. However, Cep215 is not involved in the regulation of cell proliferation nor cell specification. Based on the results, I propose that Cep215 organizes microtubules for glial process formation during astrocyte differentiation

INTRODUCTION

Microtubule is an important building block for cellular morphogenesis. During neurogenesis, microtubules are nucleated from the centrosome in early phase (Stiess et al., 2010). However, in late phase, the centrosome loses its microtubule organizing activity as soon as it loses pericentriolar material (PCM) proteins (Stiess et al., 2010). Instead, non-centrosomal microtubules play critical roles for neuronal morphogenesis (Ori-McKenney et al, 2012). It is known that microtubule nucleating factors, such as Tpx2 and the Haus complex, locally regulate microtubule nucleation outside the centrosome (Chen et al., 2017b; Cunha-Ferreira et al., 2018). Non-centrosomal microtubule organization is also observed in other differentiated cells as well (Muroyama and Lechler, 2017; Paz and Luders, 2018).

Cep215 (also known as Cdk5rap2) is a major PCM protein with at least two functional domains: CM1 is essential for interaction with γ-tubulin ring complex (γ-TuRC) (Fong et al., 2008) and CM2 is essential for interaction with specific centrosome proteins, such as pericentrin and Akap450 (Wang et al., 2010). It is also known that Cep215 can interact with other cellular proteins (Fong et al., 2008). The structural information suggests that Cep215 is a recruiter of γ-TuRC to specific loci, including the centrosome (Paz and Luders, 2018). For example, Cep215 forms complex with the microtubule plus-end tip and organizes microtubules at the cell periphery (Fong et al., 2009; Fong et al., 2017). *Centrosomin* (*Cnn*), a *Drosophila* ortholog of *Cep215*, can be alternatively spliced to generate testis-specific isotype protein, Cnn-T (Chen et al., 2017a). Cnn-T includes a mitochondria-binding domain instead of the centrosome binding domain and organizes microtubules at the mitochondria in *Drosophila* sperm (Chen et al., 2017a).

Mutations in *CEP215* have been reported among microcephaly patients (Abdullah et al., 2017; Alfares et al., 2018; Nasser et al., 2020). *Cep215* mutations in mice are similar to the human conditions with reduced brain size and a strikingly thin neocortex already at early stages

of neurogenesis (Zaqout et al, 2019). Depletion of Cep215 in mouse embryo brain revealed precocious neurogenesis with an increase in cell cycle exit (Buchman et al, 2010). The *Hertwig's anemia* (*an*) mouse which has a genomic inversion at exon 4 of *Cep215* was previously reported a macrocytic, hypoproliferative anemia and leukopenia with a high level of spontaneous aneuploidy (Eppig and Barker, 1984). Microcephaly was also observed in the *Cep215*$^{an/an}$ mice (Lizarraga et al., 2010). In the brain of *Cep215*$^{an/an}$ mouse, the neural stem had defects in spindle axis formation, the timing of neurogenesis, and cell survival as same as *Cep215* depletion (Lizarraga et al., 2010). Mutations in *Cnn* promoted extra branching of dendrite via regulation of the microtubule nucleation at the Golgi complex of specific *Drosophila* neurons (Yalgin et al., 2015). Therefore, Cep215 is critical for proliferation and differentiation of neuronal progenitor cells as well as of other stem cells.

Brain tissues consist of neurons and glial cells both of which are originated from radial glial cells. During embryogenesis, neural stem cells undergo differentiation in early stage, and start glial differentiation into astrocytes and oligodendrocytes at late stage (Bond et al., 2020). Astrocyte, a major glial cell, contains a small soma and extensive branches and fine processes with a unique intermediate protein, glial fibrillary acidic protein (Gfap) (Ventura and Harris, 1999). Gfap, a building block of astrocyte processes, is known to move along the microtubules (Leduc and Etienne-Manneville, 2017b). However, it remains to be understood how microtubules contribute to morphogenesis of astrocytes.

In this study, I investigated the involvement of Cep215 in glial process formation during astrocyte differentiation. My results revealed that Cep215 is located at the glial processes as well as centrosomes and plays an essential role in glial process formation by regulation of microtubule organization.

MATERIALS & METHODS

Cell culture and induction of differentiation

Cell culture and differentiation method were performed following Yoon et al (Yoon et al., 2009) with minor modifications. The P19 mouse embryonic carcinoma cells were maintained in DMEM (Welgene) supplemented with 10% FBS (Welgene) and antibiotics (ANT-MPT; Invivogen) at 37°C. To induce differentiation of P19 cells, 1.0×10^5 cells/ml were suspension cultured in 100mm bacterial petri dishes, and treated with 1μM all trans-retinoic acid (R2656; Sigma) once a day for 4 days. Four days later, the aggregated embryoid bodies were dissociated with pre-warmed 0.05% trypsin-0.53mM EDTA (Welgene). Dissociated cells were replated on the poly-L-lysine (P4707; Sigma) coated dishes with 3.2×10^5 cells/ml for astrocyte differentiation, and on the poly-L-lysine / laminin coated dishes with 1.2×10^4 cells/ml for neuronal differentiation. In case of the microtubule regrowth assays and EB1-GFP comet assays, 2.4×10^5 cells/ml were seeded on the coated dishes to prevent the cells from peeling off. The seeded cells were maintained in DMEM supplemented with 10% FBS for glial differentiation or with B27 supplement for neuronal differentiation. To estimate the Gfap- or Tuj1- positive population, the number of Gfap or Tuj1 expressing cells were counted among all nuclei in several microscopic fields. And then, Cells with mesh-like structures of Gfap or Tuj1 around the cell body were counted as cells without processes. Cells with long and thick processes and protrusions from their cell body were counted as cells with processes.

The primary culture using mouse embryo in this study were permitted by Institutional Animal Care and Use Committee at Seoul National University (SNU-181219-2-4). Mouse hippocampal cultures were prepared from E18 mouse embryos of either sex as modified protocols from Beaudoin et al. (Beaudoin et al., 2012). Dishes and coverslips were coated with 0.1mg/ml poly-D-lysine solution diluted by borate buffer. Dissociated hippocampi tissues were treated with papain (1.2mg/ml) for 20 min at 37°C. The tissues were then mechanically

dissociated by titration with a micropipette tip. Hippocampal cells 4 or 8×10^4 cells/ml were plated in MEM (Welgene) supplemented with 0.6% glucose (Sigma), 1mM sodium pyruvate (Sigma), antibiotics (ANT-MPT; Invivogen), 2mM L-glutamine (Welgene) and 10% FBS (Welgene) for 4-5 hours before exchange with a neurobasal medium (Gibco) containing 0.5mM L-glutamine and B27 supplement (Gibco). The cells were maintained in a 5% CO_2 incubator at 37°C for up to 12 days. At DIV4 and DIV11, a half of the original media was discarded and replaced with fresh neurobasal media supplemented with 0.5mM glutamine and B27 supplement.

Generation of *Cep215* stable cell lines in base of knockout cells

To generate P19 cell lines stably expressing the *Flag-Cep215* constructs, the plasmid DNA was transfected in P19 cells using Lipofectamine 3000 (Invitrogen) according to the manufacturer's instruction. The *Cep215*-deleted cell lines stably expressing *Flag-Cep215* constructs were generated using 800μg/ml of G418 (Calbiochem) selection.

Plasmids and RNA interference

The wild type and F75A mutant *CEP215* cDNA were initially subcloned into *pCMV10-3×Flag* vector. Then, the *CMV* promoter was replaced to *SV40* promoter (*pSV40-3×Flag*) to regulate the expression level of ectopic proteins as much as endogenous Cep215. The *EB1* cDNA was subcloned into *pEGFP-N1* vector. The siRNA specific to mouse *Cep215* (5'-CUCA GUGCAGUGAGGCUAUUATT-3') was purchased from ST Pharm, and was transfected using RNAiMAX (Invitrogen) according to the manufacturer's instruction. Non-specific control siRNA (5'-GCAATCGAAGCTCGGCTAC-3') was used.

Reverse Transcription and quantitative real-time RT-PCR (qRT-PCR)

qRT-PCR analysis was performed following Yoon et al. (Yoon et al., 2017) with minor modifications. Total RNA was isolated from undifferentiated or differentiated P19 cells at the

indicated days using TRIzol reagent (Invitrogen) following the protocol of the manufacturer. Reverse transcription was conducted with random hexamers. Real-time PCR was carried out with the Applied Biosystems (Carlsbad, CA) 7300 Real Time PCR System. The primer sequences are listed in Table 1. Real-time PCR was conducted in triplicate, and the experiment was repeated three times. Relative mRNA expression level was determined with the comparative Ct method and normalized to endogenous Gapdh.

Table 1. Primer sequences for qRT-PCR.

Gene	Sequence	Reference
Gfap	F : 5'-AAG CCA AGC ACG AAG CTA ACG A-3' R : 5'-TTG AGG CTT TGG CCC TCC-3'	Mamber et al., 2012
Sox9	F : 5'-AGG AAG CTG GCA GAC CAG TA-3' R : 5'-TCC ACG AAG GGT CTC TTC TC-3'	Hosokawa et al., 2015
Nfia	F : 5'-GGC ATA CTT TGT ACA TGC AGC-3' R : 5'-ACC TGA TGT GAC AAA GCT GTC C-3'	Bunt et al., 2015
Neurofilament	F : 5'-TGA TGT CTG CTC GCT CTT TC-3' R : 5'-CTC AGC TTT CGT AGC CTC AAT-3'	Mohammad et al., 2016
Ngn1	F : 5'-GAC ACT GAG TCC TGG GGT TC-3' R : 5'-GTC GTG TGG AGC AGG TCT TT-3'	Sanchez-Martin et al., 2013
NeuroD1	F : 5'-GGA GGA GGA GGA TCA AAA GC-3' R : 5'-TGG GTC TTG GAG TAG CAA GG-3'	Sanchez-Martin et al., 2013
Gapdh	F : 5'-TCA AGA AGG TGG TGA AGC AG-3' R : 5'-AGG TGG AAG AGT GGG AGT TG-3'	Yoon et al., 2017

Immunoblot analyses

Protein sampling and immunoblot analysis were performed following Shin et al (Shin et al., 2015) with minor modifications. In brief, the undifferentiated and differentiated P19 cells

were lysed using RIPA buffer (150mM NaCl, 1% Triton X-100, 0.5% sodium deoxycholate, 0.1% SDS, 50mM Tris-HCl at pH 8.0, 10mM NaF, 1mM Na_3VO_4, 1mM EDTA and 1mM EGTA) containing a protease inhibitor cocktail (P8340; Sigma-Aldrich) for 10min on the ice. Cell lysates were centrifuged with 12,000 rpm for 10 min at 4℃. The supernatants were mixed with 4×SDS sample buffer (250mM Tris-HCl at pH 6.8, 8% SDS, 40% glycerol and 0.04% bromophenol blue) and 400mM DTT (0281-25G; Amresco). Mixtures were boiled for 5 min and the protein samples were subjected to SDS-polyacrylamide gel electrophoresis. The gel was transferred to a nitrocellulose membrane. The membrane was blocked with 5% skim milk in 0.1% TBST (Tris-buffered saline TBS with 0.1% Tween 20) for 1-2 h. The membrane was incubated with primary antibody overnight at 4˚C. The membrane was incubated with horseradish peroxidase-conjugated secondary antibody for 30-40 min at room temperature. The ECL solution was treated onto the membrane, and then exposed to an X-ray film.

Immunostaining and image processing

Immunostaining analysis was performed following Shin et al (Shin et al., 2015) with minor modifications. In brief, the cells on the coverslip were fixed with cold methanol for 10 min on ice and washed with phosphate-buffered saline (PBS) 3 times. The fixed cells were blocked with 3% bovine serum albumin in 0.5% PBST (PBS with 0.5% Triton X-100) for 30 min, incubated with the primary antibody for 1 h. After washing with 0.1% PBST (PBS with 0.1% Triton X-100) 3 times, the cells were incubated with the secondary antibody for 30 min, and then washed with 0.1% PBST 3 times. The coverslips were mounted on a slide glass using Prolong gold mounting solution (Invitrogen) after DAPI incubation.

In case of triple staining, the permeabilization step is necessary. For permeabilization, the cells were fixed and incubated with 0.1% PBST for 10 min. The cells were incubated with primary (rabbit Cep215 or rabbit γ-tubulin antibodies and mouse Tuj1 or mouse Cetn2 antibodies) and secondary (anti-rabbit-488nm- and anti-mouse-647nm-fluorescent-conjugated) antibodies as same with method mentioned above. Then, the third (mouse Tuj1 and mouse

Gfap) antibodies were prepared with Zenon Alexa fluor labeling kit (Z25005; Invitrogen) following the protocol of the manufacturer. The cells were incubated with conjugated antibody for 2-3h and mounted on a slide glass. The cells were incubated with DAPI and mounted on a slide glass.

The immunostained cells were observed using fluorescence microscope with a CCD (Qi-cam Fast 1394; Qimaging) camera and processed with ImagePro 5.0 (Media Cybernetics, Inc.), Adobe Photoshop software and ImageJ software. The intensity of centrosomal proteins levels was measured using ImageJ software by drawing the circle including the centrosome area, and background was excluded by drawing same size circle in the nearest cytoplasm.

BrdU incorporation assay

The P19 cells were treated with BrdU (30μM) for 24 h, fixed with cold methanol for 10 min on the ice and washed with PBS 3 times. For permeabilization, the cells were incubated with 0.1% PBST for 10 min. To denature DNA structure, the cells were incubated with pre-warmed 2N HCl at 37℃ for 20 min and neutralized with 0.1M borate buffer. The samples were subjected to immunostaining analysis with the BrdU antibody (B8434; Sigma).

Antibodies

The Cep215 antibody were previously described (Lee and Rhee, 2010) or purchased (06-1398; Millipore). The antibodies against Tuj1 (MMS-435P-100; Covance), neurofilament 68 (13-0400; Invitrogen), Gfap (#3670; Cell Signaling), Sox9 (AB5535; Millipore), Nfia (HPA006111; Sigma), Flag (F3165; Sigma-Aldrich) and α-tubulin (ab18251; Abcam) were commercially purchased. The rabbit γ-tubulin (ab11317; Abcam) were used for immunocytochemistry and mouse γ-tubulin (ab11316-100; Abcam) was used for immunoblot. The antibodies against centrin-2, centrobin and Gapdh were purchased from Millipore, Abcam and Invitrogen, respectively. The Alexa-fluorescence secondary antibodies were purchased

from Invitrogen. The mouse and rabbit IgG-HRP antibodies were purchased from Sigma and Millipore, respectively.

Microtubule regrowth assay

To depolymerize microtubules, P19 cells and *Cep215*-deleted cells in differentiation day 12 were treated nocodazole (1.65μM) for 1 h. To induce microtubule repolymerization, the cells were incubated with pre-warmed fresh medium for 10 min, and immediately fixed with 4% paraformaldehyde in PEM buffer (80mM PIPES pH6.9, 1mM $MgCl_2$, 5mM EGTA, 0.5% Triton X-100) for 10 min at room temperature. The fixed cells were incubated with 0.3% PBST for 5 minutes to increase permeability and subjected to immunostaining. The length and the number of centrosomal microtubules were measured manually using NeuronJ software which is a sort of ImageJ plug-in.

EB1-GFP comet assay

To acquire the time-lapse images, the P19 cells, *Cep215*-deleted cells, and Flag-CEP215-rescued cells were differentiated into glial cell in 35mm confocal dishes. To express the EB1-GFP protein, differentiated cells were transfected using Lipofectamine 3000 (Invitrogen) according to the manufacturer's instruction at differentiation day 11. Twenty-four hours after transfection, the cells were transferred to the chamber which is pre-warmed at 37℃ of Delta Vision (GE Healthcare Life Sciences). The fluorescence of EB1 was observed under a Delta Vision, equipped with a camera (CoolSNAP HQ, Roper Scientific) and a 60× 1.4 NA UPlanSApo oil objective lens (Olympus). Time-lapse images were acquired every 1 second for 1 min. SoftWoRX was used to analyze the obtained images. Microtubules were marked by their directions. Anterograde microtubules mean the EB1 comets emanating from the centrosome, and retrograde microtubule mean the EB1 comets moving toward the centrosome.

The microtubule density was determined by counting the number of EB1-GFP comets in entire area of the cells. The number of EB1 comets were normalized with the cell area using

ImageJ software. The movements of EB1-GFP comets were tracked manually using ImageJ plugin, MTrack2. Twenty cells in each groups were measured.

Statistical analyses

For statistical analyses, experiments were independently performed three times. To calculate *P* values, all data were analyzed using the Prism 6 software (GraphPad Software) including unpaired two-tailed *t*-test, one- or two-way analysis of variant (ANOVA). In the case of ANOVA, the Tukey's post-test was performed if *p* value is lower than 0.05.

All measured fluorescent intensities, the length and the number of microtubule were displayed with box-and-whiskers plots in Prism 6 (lines, median; vertical boxes, values from 25^{th} and 75^{th}; down error bars, 10^{th} value, up error bar, 90^{th} value; circle, outliers).

RESULTS

The importance of Cep215 in astrocyte differentiation of P19 cells

P19 cells are mouse embryonic carcinoma cells which can differentiate into neurons and astrocytes with retinoic acid (RA), and into muscle cells with DMSO (Fig. 9a). In this study, I treated P19 cells with RA to differentiate into neurons and glial cells at early and late stages, respectively (Jones-Villeneuve et al., 1982) (Fig. 9b). I investigated the involvement of Cep215 during differentiation of neuron and astrocytes, using the *Cep215*-deleted P19 cells. Deletions of *Cep215* was confirmed with immunoblot and immunostaining analyses (Fig. 10a, b).

First, I examined effects of *Cep215* deletion on differentiation of astrocytes. Gfap, a marker for astrocytes, started to be expressed in day 12 after RA induction (Fig. 11a). However, the Gfap levels were significantly reduced in the *Cep215*-deleted P19 cells (Fig. 11a). Furthermore, the proportion of cells with glial processes was also significantly reduced (Fig. 11b, c). These results suggest that Cep215 is essential for astrocyte differentiation.

I also examined effects of the *Cep215* deletion on differentiation of neurons. The differentiated cells were immunostained with antibodies specific to Tuj1 and neurofilament68, neuronal marker proteins. The neuronal markers started to be expressed in day 5, immediately after P19 cells were cultured in the neuron-inducing medium containing B27 supplement (Fig. 12a, b). *Cep215*-deleted P19 cells were differentiated into neurons as effectively as the control cells (Fig. 12a-d). Neurite formation was not affected by the *Cep215* deletion, either (Fig. 12c, d). These results suggest that Cep215 is not critical for neuronal differentiation of P19 cells.

Cell proliferation and cell fate determination of *Cep215*-deleted P19 cells

Gfap expression would be reduced if the *Cep215*-deleted cells proliferated less than the control cells. To rule out the possibility, I determined the proliferation activity of *Cep215*-

deleted cells using bromodeoxyuridine (BrdU) incorporation assays (Fig. 13a). I treated *Cep215*-deleted P19 cells with BrdU for 24 h and counted the number of BrdU-positive cells. As expected, the number of BrdU-positive cells decreased after glial differentiation (Fig. 13a, b). However, I did not observe any difference in the proliferation activities of the wild type and *Cep215*-deleted cells in both the undifferentiated and differentiated conditions. It indicates that deletion of *Cep215* does not affect proliferation of P19 cells.

Cell fate is determined by expression of a specific set of genes at early stages. For glial cell determination, Sox9 is one of the initiators and Nfia is one of the downstream determinants (Stolt et al., 2003; Deneen et al., 2006; Kang et al., 2012). For neuronal cell differentiation, Ngn1 and NeuroD1 are known as cell fate initiators (Ma et al., 1998; Bertrand et al., 2002). To identify whether the cell fate of *Cep215*-deleted P19 cells was altered, I observed expression of selected cell fate determinants in P19 cells undergoing differentiation. Quantitative reverse transcription PCR (qRT-PCR) analysis revealed that *Sox9* expression was immediately induced and *Nfia* expression followed in both wild type and *Cep215*-deleted P19 cells (Fig. 14a). Similar expression kinetics were also observed at the protein levels (Fig. 14c). However, expression of Gfap, a structural protein for astrocytes, appeared reduced in *Cep215*-deleted cells at both the mRNA and protein levels (Fig. 14a, c). These results indicate that Cep215 is not involved in cell fate determination toward astrocytes but is necessary for expression of Gfap for morphological differentiation. I also determined the expression of neuronal cell determinants, Ngn1 and NeuroD1, in P19 cells. The results showed that both *Ngn1* and *NeuroD1* were immediately expressed in both of control and Cep215 deleted P19 cells after RA treatment (Fig. 14b). I did not observe a significant difference in their expression and Nf-L, a structural protein for neuronal cells, in wild type and *Cep215*-deleted cells. (Fig. 14b) These results show that Cep215 is not involved in cell fate determination and differentiation of neuronal cells.

Reduction of the microtubule organizing activity in *Cep215*-deleted P19 cells

Microtubule nucleation is the best-known function of Cep215 in the centrosome (Fong, et al., 2008). Therefore, I state the hypothesis that the microtubule organization activity at the centrosome is essential for the morphological differentiation of astrocytes. To test the hypothesis, I performed microtubule regrowth assay with the *Cep215*-deleted P19 cells. The differentiated P19 cells were treated with nocodazole for 1 h to dissolve the cellular microtubules (Fig. 15a). When the cells were transferred into a fresh medium, microtubules started to grow mostly from the centrosomes, and also in the cytoplasm (Fig. 15a). I measured the total length and the number of microtubules at the centrosomes. The results showed that the length and number of newly nucleated microtubules at the centrosome were significantly reduced in the *Cep215*-deleted astrocytes (Fig. 15b, c). These results suggest that Cep215 is needed for microtubule nucleation at the centrosome in the differentiated P19 cells.

I also determined microtubule formation activity in P19 cells using the EB1-GFP protein. EB1 protein is a family of microtubule plus-end tracking protein and used as a marker for the plus ends of microtubules. Using live images of EB1 comets, I estimated the movement of microtubules. I observed that the density of growing microtubules was significantly reduced in *Cep215*-deleted cells and was recovered with ectopic Flag-Cep215 (Fig. 16a, b). These result indicate that Cep215 is essential for microtubule organization in differentiated astrocytes.

Importance of interaction between Cep215 and γ-TuRC for glial differentiation

Cep215 can bind and recruit γ-tubulin at the centrosome, which is necessary for effective microtubule nucleation (Fong et al., 2008). Because the microtubule organization of differentiated astrocytes was suppressed in *Cep215*-deleted condition, I examined the importance of the Cep215 as a recruiter of the γ-tubulin ring complex (γ-TuRC) during astrocyte differentiation. A point mutant of Cep215 at phenylalanine 75 position ($Cep215^{F75A}$) is reported to have a defect in interaction with γ-TuRC (Choi et al., 2010). I rescued the knockout P19 cells with the *Cep215* mutant construct and determined astrocyte differentiation. Immunoblot analysis confirmed that comparable amounts of ectopic Cep215 proteins were

expressed (Fig. 17a). The results also showed that the cellular levels of Gfap were rescued with Flag-Cep215, but not with Flag-Cep215^{F75A} (Fig. 17a, b). Furthermore, the ectopic Cep215^{F75A} hardly rescued the glial process formation activity (Fig. 17b, c). These results suggest that Cep215 interaction with γ-TuRC is critical for astrocyte differentiation.

Subcellular localization of Cep215 in primary cultured astrocytes

The results with P19 cells revealed that Cep215 is required for morphological differentiation of astrocytes. I wished to confirm these observations in primary culture cells from mouse embryonic hippocampus. First, I determined subcellular distribution of Cep215 in the hippocampal cells. The immunostaining analysis revealed that the specific signals of Cep215 were mainly detected at the centrosome and was not limited to the centrosomes but were also detected at the processes of astrocytes (Fig. 18). In case of neurons, I observed Cep215 signals in the cell body of Tuj1-positive cells rather than the centrosome (Fig. 18). These immunostaining results showed that the expression patterns of Cep215 depended on the cell types.

I determined the centrosomal levels of Cep215 during a prolonged culture of hippocampal cells. I observed that the centrosomal levels of Cep215 increased in astrocytes (Fig. 19 a, b). However, the opposite was the case in neurons as previous published results (Fig. 19a, c). I estimated the expression patterns of γ-tubulin. Similar expression patterns were observed in the centrosomal levels of γ-tubulin (Fig. 19d-f). These results suggest that Cep215 may differentially function during morphogenesis in astrocytes and neurons.

Depletion of Cep215 in mouse hippocampal cells

To test the hypothesis in which Cep215 may be involved in astrocyte morphogenesis, I transfected siRNA specific to mouse *Cep215* (*siCep215*) into the primary hippocampal cells. Depletion of Cep215 in astrocytes and neurons was confirmed by immunostaining analyses of the centrosomes (Fig. 20a, b). At the same time, I observed that the number of astrocytes

without glial processes increased after depletion of Cep215 (Fig. 20a, c). On the other hand, Cep215 depletion did not affect neurite formation (Fig. 20a, d). These results indicate that Cep215 has a role in morphological differentiation of primary astrocytes as in case of P19 cells.

It is known that the specific interaction of Cep215 with pericentrin (Pcnt) is critical for microtubule organization of the centrosomes, especially during mitosis (Kim and Rhee, 2014). I determined the centrosomal levels of Pcnt and γ-tubulin in Cep215-depleted astrocytes (Fig. 21a). The results showed that the centrosomal levels of γ-tubulin were reduced in Cep215-depleted astrocytes, whereas those of Pcnt were not (Fig. 21b, c). These results suggest that depletion of Cep215 might cause reduction of the microtubule organizing activity of the centrosomes in astrocytes, which results in defects in process formation.

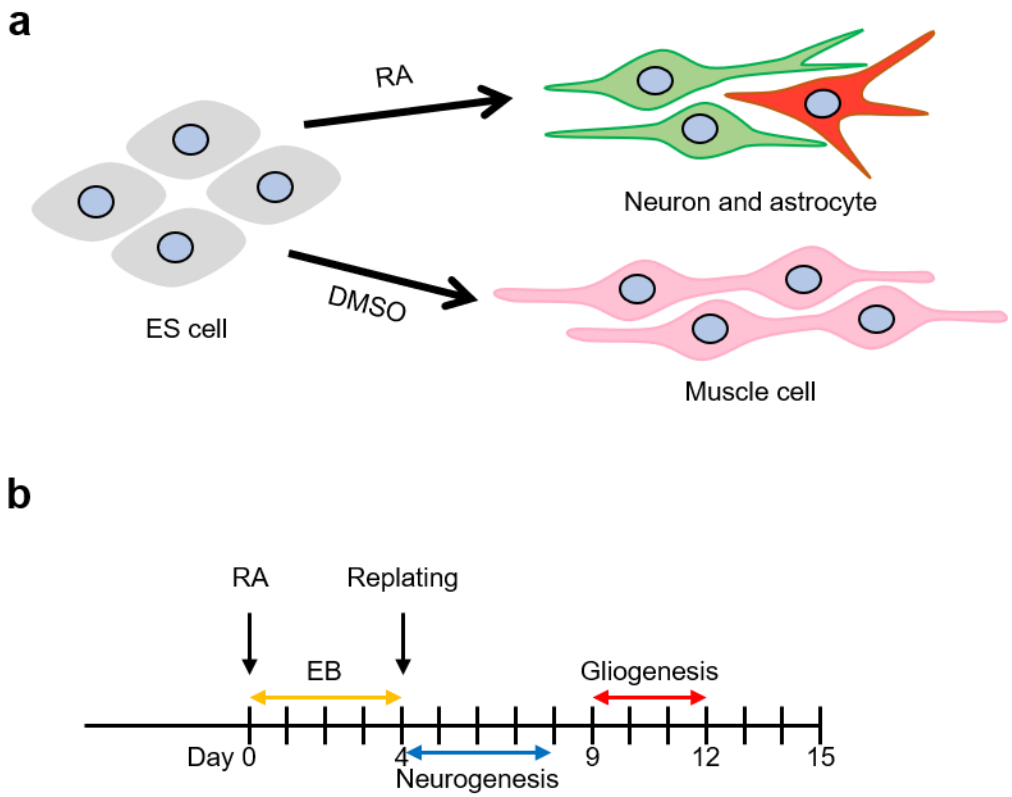

Figure 9. The experimental scheme for differentiation of P19 cells (**a**) P19 was derived from a mouse embryonic carcinoma cell. P19 cells can differentiate into neurons and astrocytes with retinoic acid (RA), and into muscle cells with DMSO. (**b**) P19 cells are treated with RA for 4 days to induce embryoid body (EB) and cultured for up to 15 days. Neurogenesis occurs at the early stage of differentiation (D4-8) whereas gliogenesis occurs at the late stage of differentiation (D9-12).

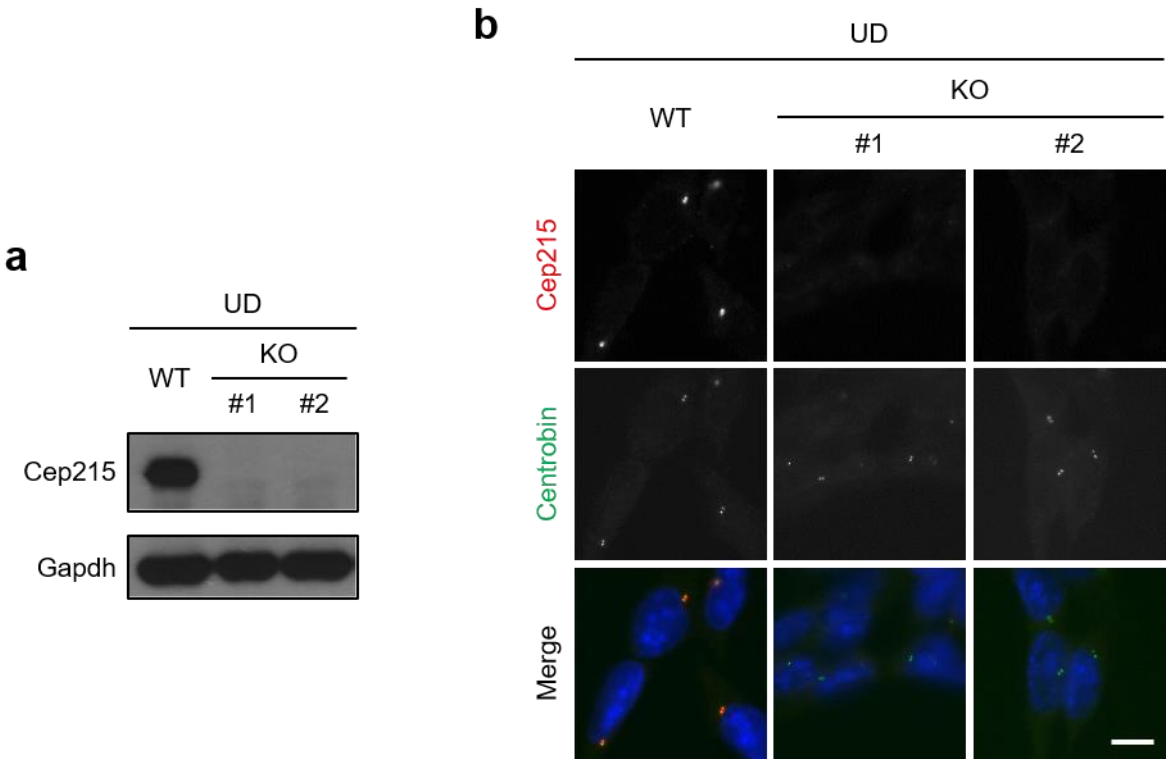

Figure 10. *Cep215* deletions in P19 cells *Cep215* was deleted in P19 cells with the CRISPR-Cas9 method. Two *Cep215*-deleted cell lines (#1 and #2) were subjected to immunoblot (**a**) and coimmunostaining (**b**) analyses with antibodies specific to Cep215, Gapdh, and centrobin. Nuclei were stained with DAPI (blue). Scale bar, 10μm.

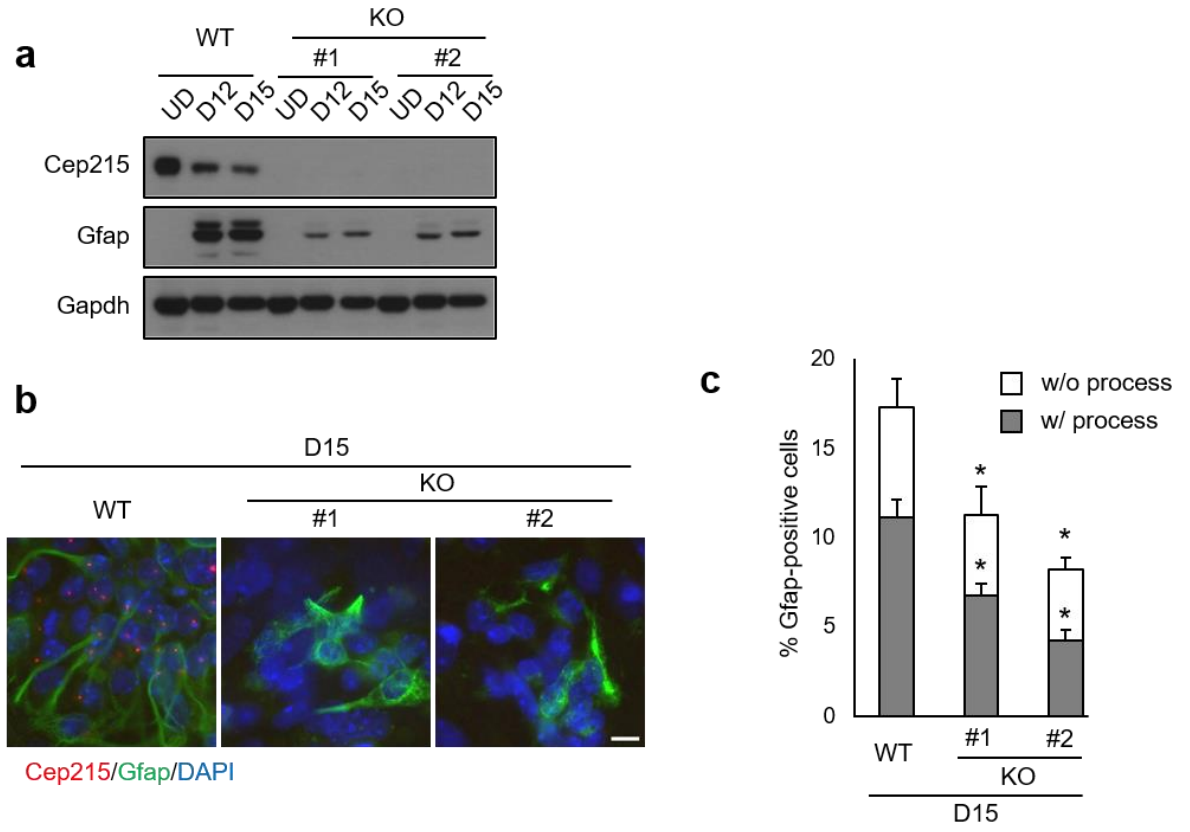

Figure 11. Astrocyte differentiation of the *Cep215*-deleted P19 cells (**a**) The *Cep215*-deleted P19 cells (KO #1 and #2) were differentiated and subjected to immunoblot analyses with antibodies specific to Cep215, Gfap and Gapdh. (**b**) The same cells at D15 were coimmunostained with the Cep215 and Gfap antibodies. Nuclei were stained with DAPI (blue). Scale bar, 10μm. (**c**) The number of Gfap-positive cells with or without glial processes were counted. Greater than 5600 cells per experimental group were counted in three independent experiments. The statistical analysis was performed by two-way ANOVA. Error bars, SEM. *, P<0.05.

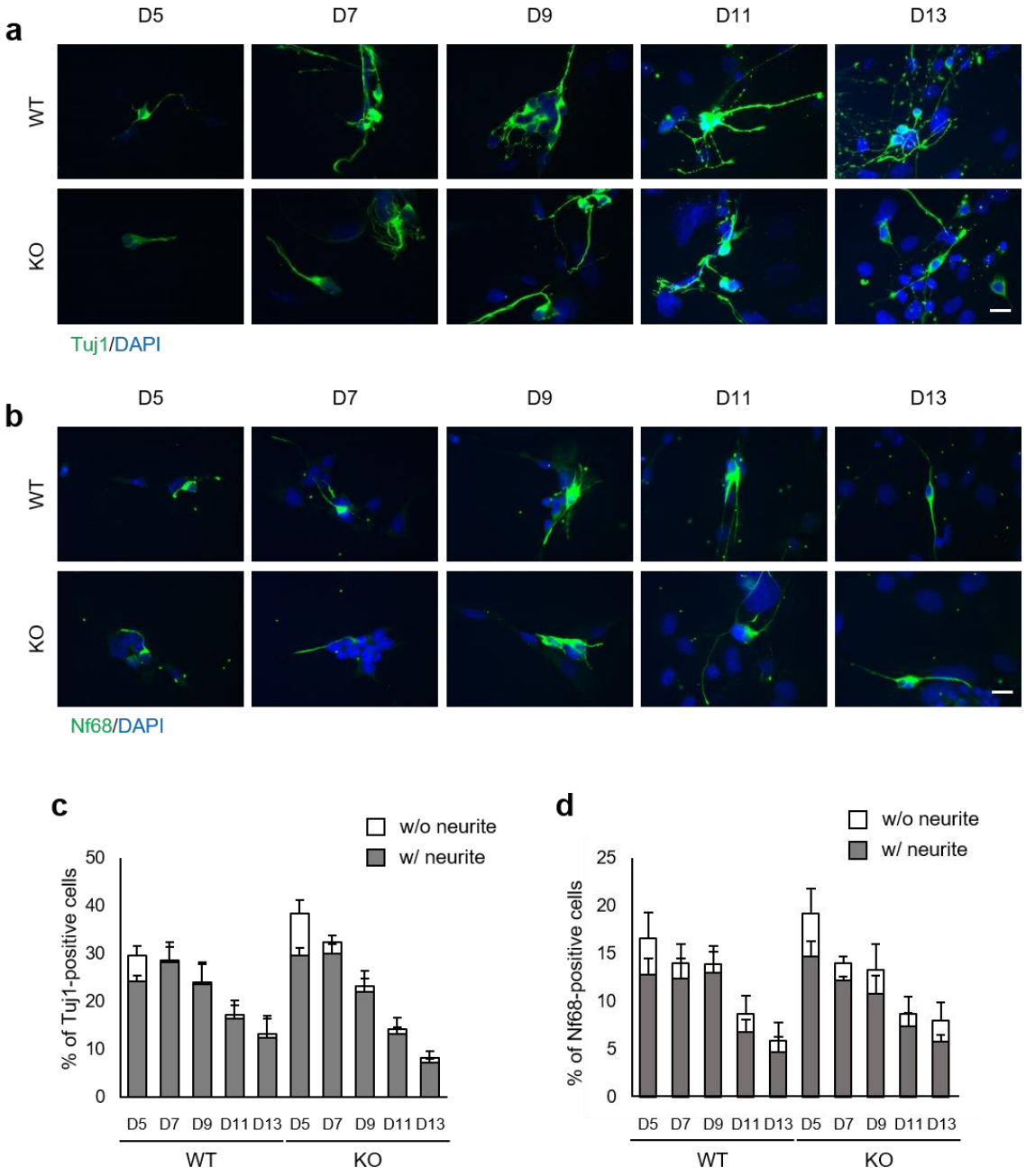

Figure 12. Neuronal differentiation of the *Cep215*-deleted P19 cells Wild type (WT) and *Cep215*-deleted (KO) P19 cells were induced to neuronal differentiation using a neuron culture medium. (**a**, **b**) P19 cells at indicated days of differentiation were coimmunostained with the antibodies specific to Tuj1 (**a**) and Nf68 (**b**) (green). Nuclei were stained with DAPI (blue). Scale bar, 20μm. (**c**, **d**) The number of Tuj1-positive cells (**c**) and Nf68-positive cells (**d**) with or without neurites were counted. Greater than 300 cells per experimental group were counted in three independent experiments. The statistical analysis was performed by two-way ANOVA. Error bars, SEM.

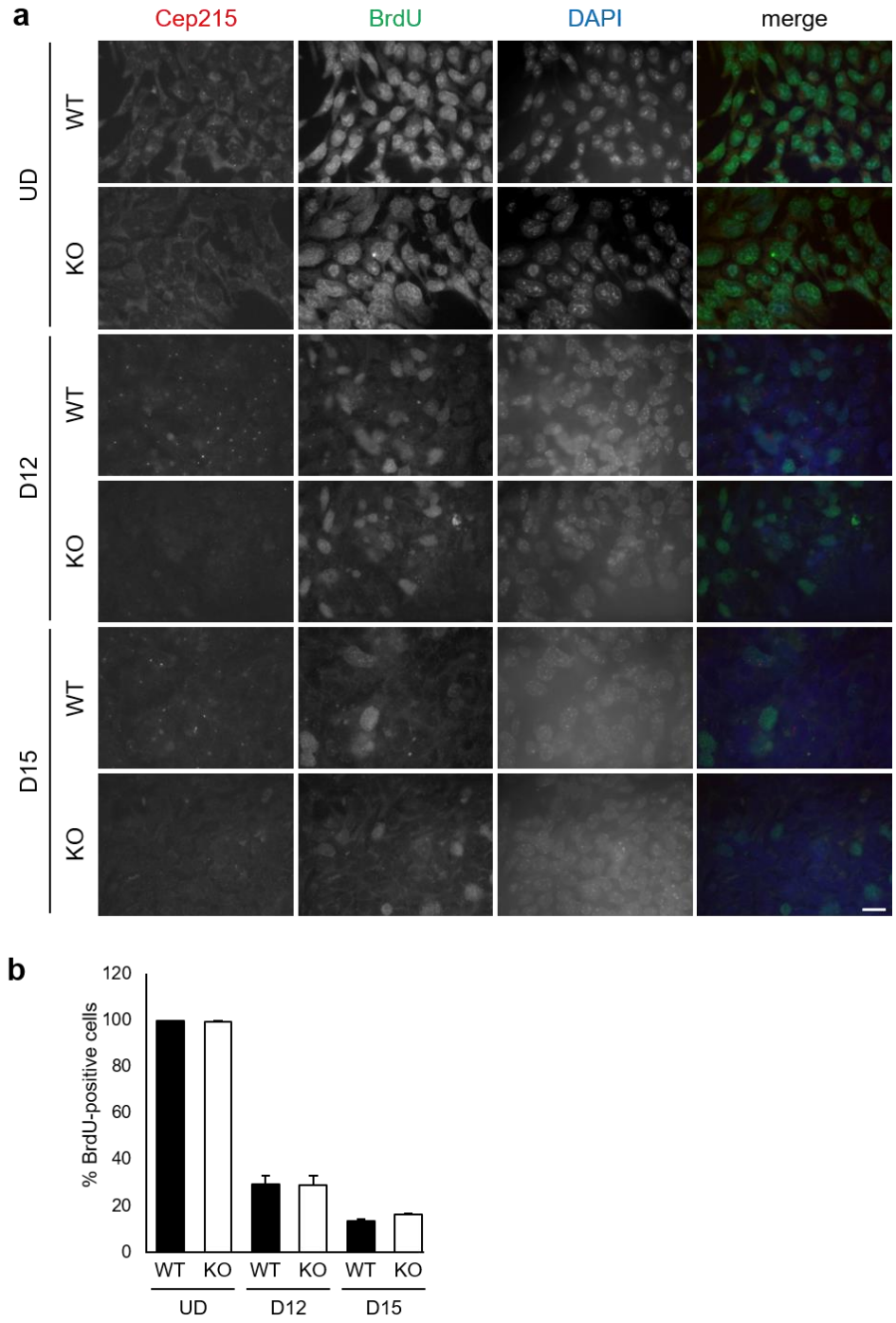

Figure 13. The proliferation activities of the *Cep215*-deleted P19 cell (**a**) Undifferentiated (UD) and differentiated (D12 and D15) P19 cells were incubated with BrdU (30μM) for 24 h and were subjected to comimmunostaining analysis with the antibodies specific to BrdU (green) and Cep215 (red). Nuclei were stained with DAPI (blue). Scale bars, 20μm. (**b**) The number of BrdU-positive cells at the indicated days were counted. Greater than 3000 cells per experimental group were counted in three independent experiments. The statistical analysis was performed by unpaired *t*-test. Error bars, SEM.

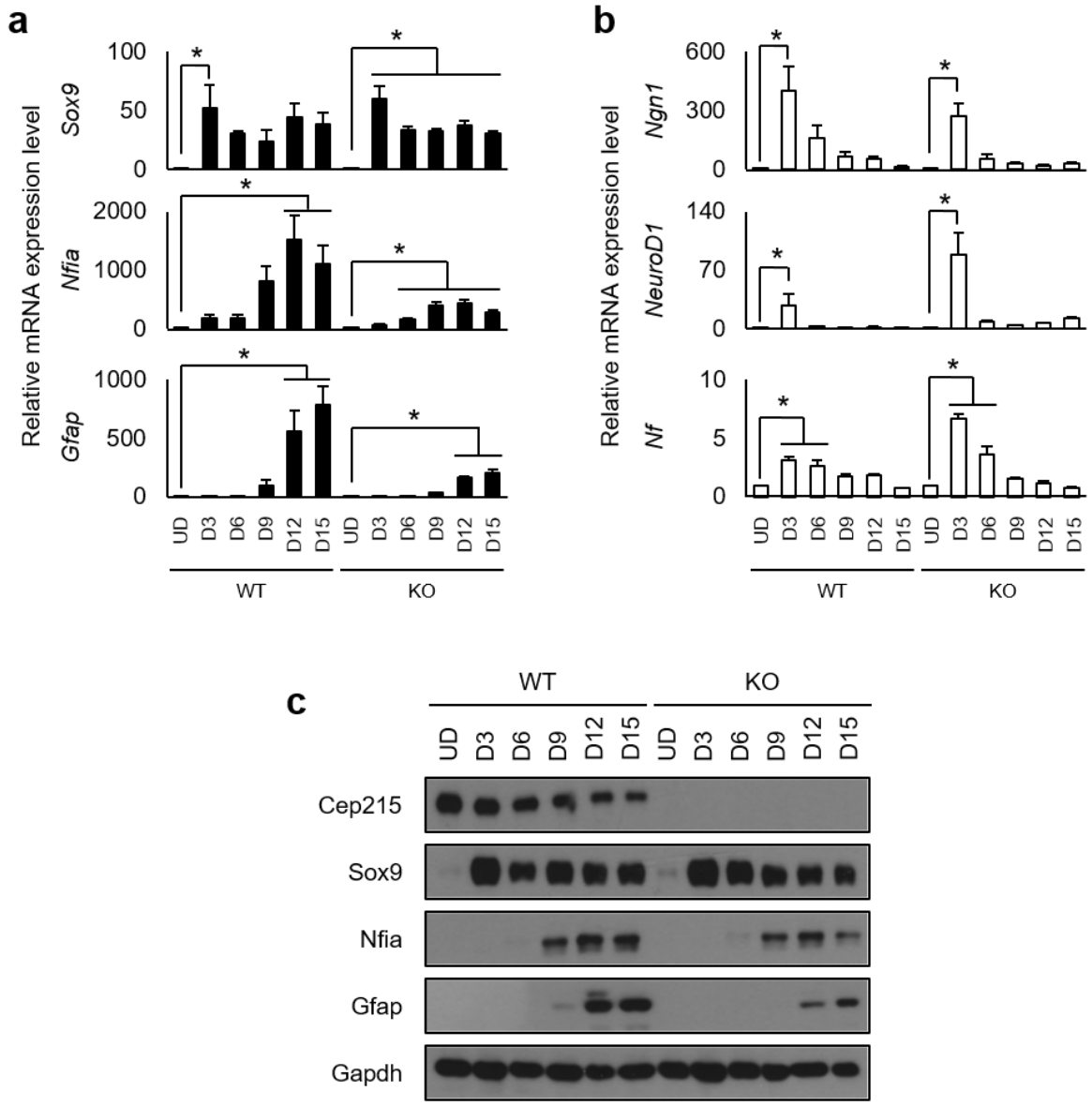

Figure 14. The expression of the cell fate determinants in *Cep215*-deleted P19 cells The wild type (WT) and *Cep215*-deleted (KO) P19 cells were differentiated for up to D15. (**a**, **b**) The cells at indicated days of differentiation were subjected to qRT-PCR analysis with *Sox9*, *Nfia*, and *Gfap* for glial cell fate (**a**) and *neurogenin1* (*Ngn1*), *NeuroD1*, and *neurofilament* (*Nf*) for neuronal cell fate (**b**) determinant genes. Relative mRNA levels of the genes were normalized to the *Gapdh* levels, and compared to the levels of the undifferentiated (UD) cells. (**c**) The protein levels of the glial cell fate determinants were analyzed with immunoblot using the antibodies specific to Cep215, Sox9, Nfia, Gfap and Gapdh. (**a**, **b**) The statistical analysis was performed by one-way ANOVA. Error bars, SEM. *, P<0.05.

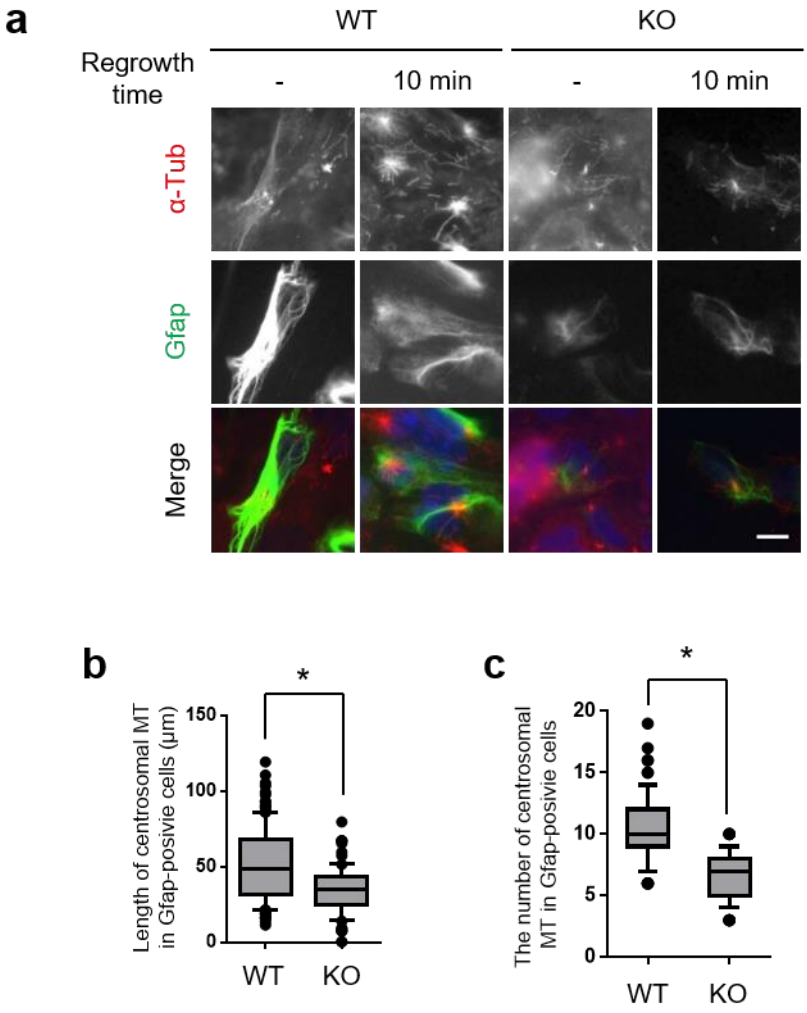

Figure 15. The microtubule regrowth assays in the *Cep215*-deleted P19 cells (**a**) *Cep215*-deleted P19 cells at D12 were treated with nocodazole for 1 h and transferred to a fresh medium for microtubule regrowth. Ten minutes later, the cells were subjected to coimmunostaining analysis with antibodies specific to α-tubulin (red) and Gfap (green). Nuclei were stained with DAPI (blue). Scale bar, 10μm. (**b**, **c**) Total length of centrosomal microtubules (**b**) and the number of centrosomal microtubules (**c**) were determined. Greater than 60 cells per experimental group were measured in three independent experiments. The statistical significance was determined by unpaired *t*-test. Error bars, SEM. *, P<0.05.

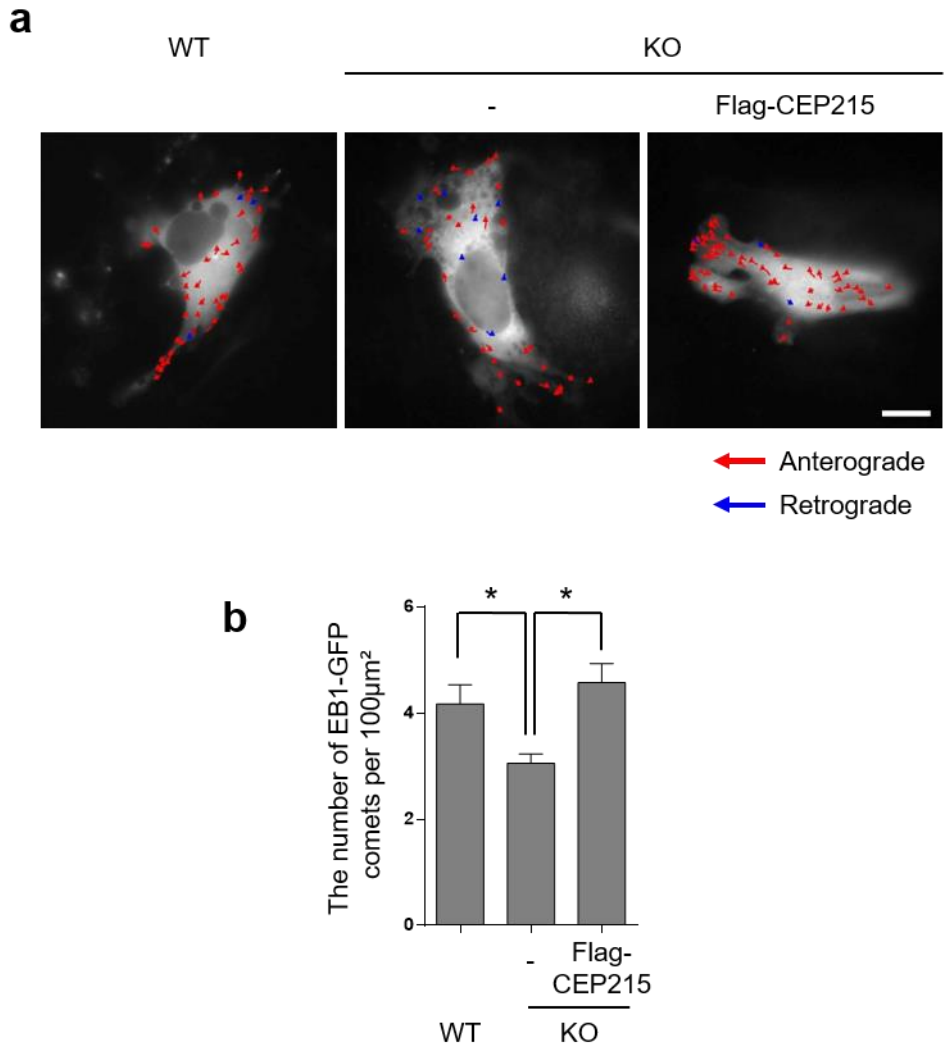

Figure 16. The live imaging of EB1 proteins in the *Cep215*-deleted P19 cells (**a**) EB1-GFP was transfected into *Cep215*-deleted P19 cells with and without ectopic Flag-CEP215. The movements of EB1 comets were traced and indicated as red and blue arrows for anterograde and retrograde directions, respectively. Scale bar, 10μm. (**b**) The number of EB1-GFP signals was counted and normalized with cell area. Twenty cells per experimental group were measured in three independent experiments. The statistical significance was determined by one-way ANOVA. Error bars, SEM. *, $P<0.05$.

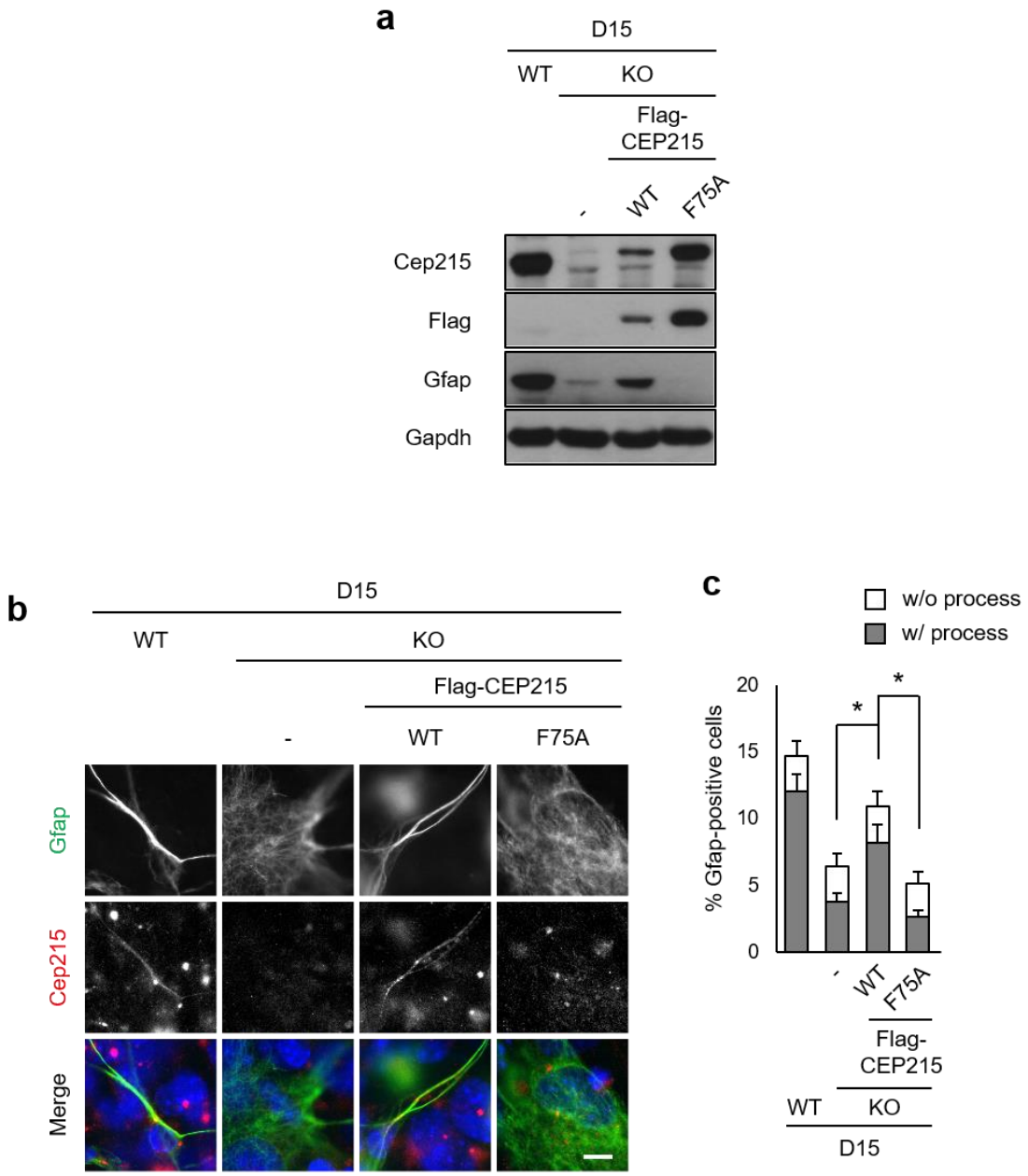

Figure 17. Importance of Cep215 interaction with γ-TuRC in glial differentiation *Cep215*-deleted P19 cells were stably transfected with Flag-CEP215 (WT) and Flag-CEP215^{F75A} (F75A). (**a**, **b**) The cells at D15 were subjected to immunoblot (**a**) and coimmunostaining (**b**) analyses with antibodies specific to Cep215, Flag, Gfap and Gapdh. Nuclei were stained with DAPI (blue). Scale bar, 10μm. (**c**) The number of Gfap-positive cells with or without glial processes were counted. Greater than 1400 cells per experimental group were counted in three independent experiments. The statistical analysis was performed by two-way ANOVA. Error bars, SEM. *, P<0.05.

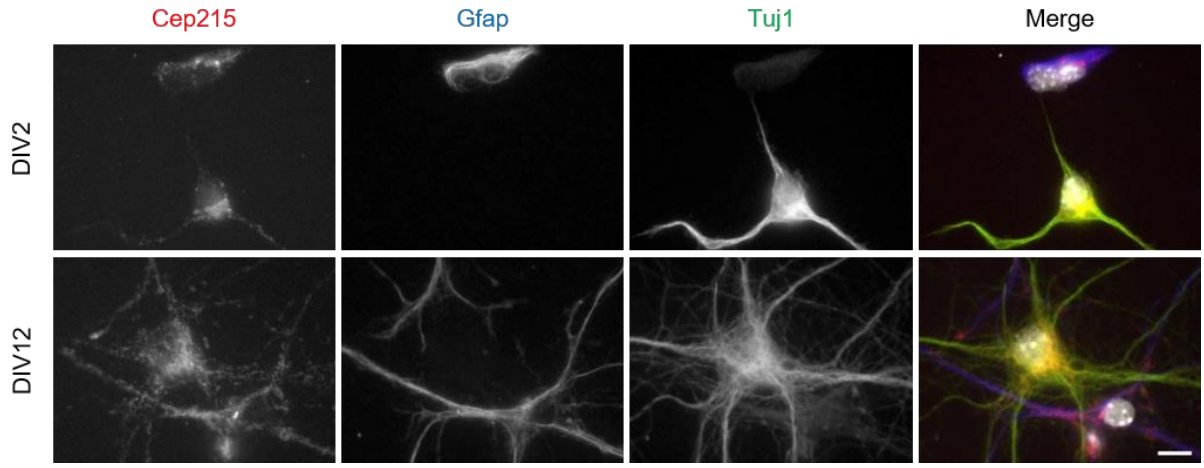

Figure 18. Subcellular distribution of Cep215 in mouse embryonic hippocampal cells Mouse hippocampi at embryonic day 18 (E18) were dissected for primary cultures. The hippocampal cells were cultured to early (DIV2) and late (DIV12) developmental stages. The cells were coimmunostained with antibodies specific to Cep215 (red), Gfap (blue) and Tuj1 (green). Nuclei were stained with DAPI (white). Scale bar, 10μm. DIV: days in vitro.

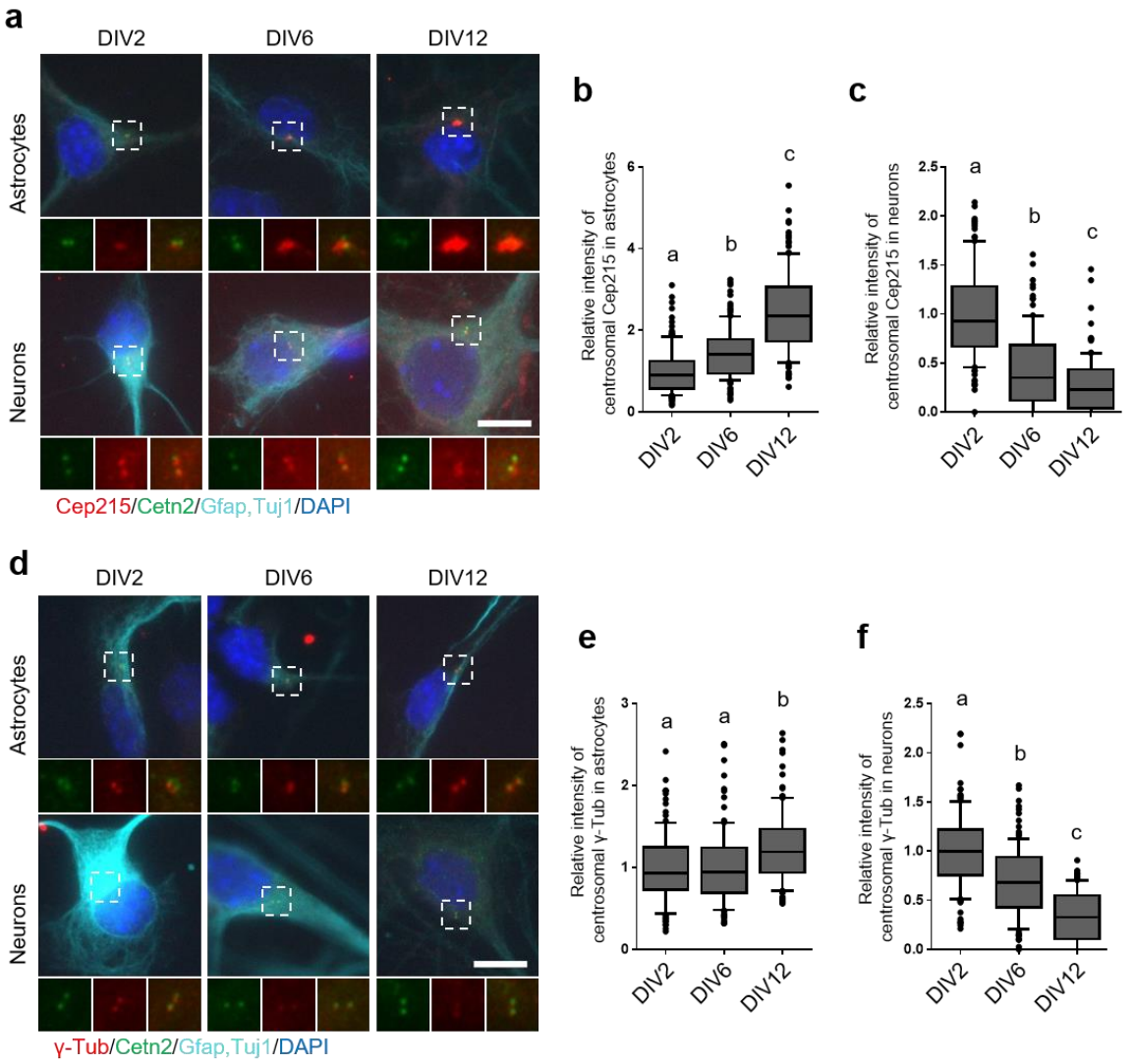

Figure 19. Expression patterns of Cep215 and γ-tubulin during differentiation of primary astrocytes and neurons (**a**) Cultured mouse embryonic hippocampal cells at DIV2, 6 and 12 were coimmunostained with antibodies specific to Cep215 (red) and centrin-2 (green) along with the cell type markers (Gfap or Tuj1, cyan). (**b**, **c**) Intensities of the centrosomal Cep215 signals were measured in astrocytes (**b**) and neurons (**c**). (**d**) Cultured mouse embryonic hippocampal cells at DIV2, 6 and 12 were subjected to coimmunostaining analysis with antibodies specific to γ-tubulin (red) and centrin-2 (green) along with cell markers (Gfap or Tuj1, cyan). (**e**, **f**) Intensities of the centrosomal γ-tubulin signals were measured in astrocytes (**e**) and neurons (**f**). (**a, c**) Nuclei were stained with DAPI (blue). Scale bar, 10μm. (**b, c, e, f**) Greater than 90 cells per experimental group were measured in three independent experiments. The statistical significance was analyzed using one-way ANOVA and is indicated by lower cases ($P<0.05$).

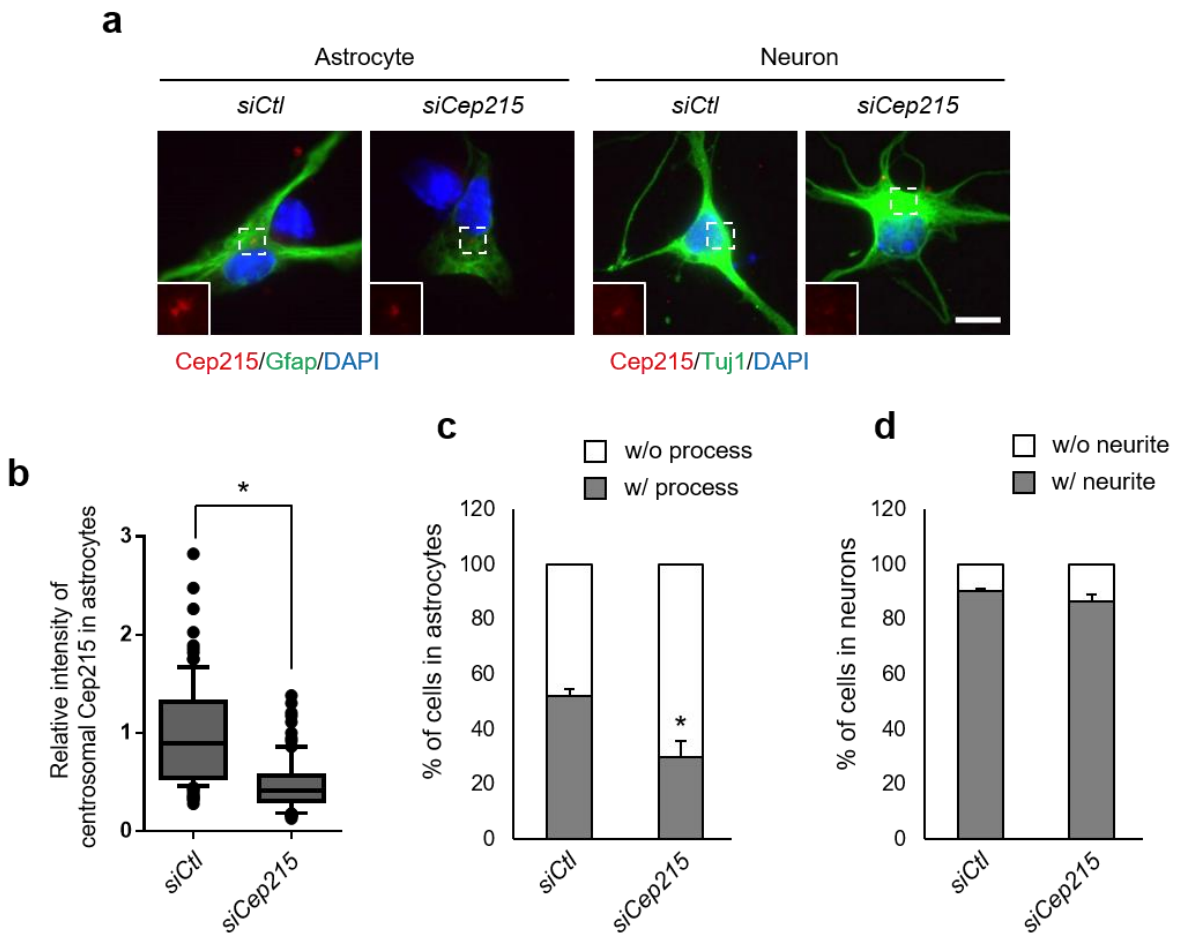

Figure 20. The involvement of Cep215 in morphological differentiation of mouse hippocampal cells Cep215 in primary hippocampal cells was depleted with specific siRNA (*siCep215*) transfection at DIV1. (**a**) The cells at DIV3 were subjected to coimmunostaining analysis with antibodies specific to Cep215 (red) along with Gfap or Tuj1 (green). Nuclei were stained with DAPI (blue). Scale bar, 10μm. (**b**) Intensities of the centrosomal Cep215 signals in astrocytes were measured. Greater than 90 cells per experimental group were estimated in three independent experiments. (**c**, **d**) The number of Gfap-positive (**c**) and Tuj1-positive (**d**) cells with or without processes was counted. More than 420 cells per experimental group were counted in three independent experiments. The statistical significance was determined by unpaired *t*-test. Error bars, SEM. *, P<0.05.

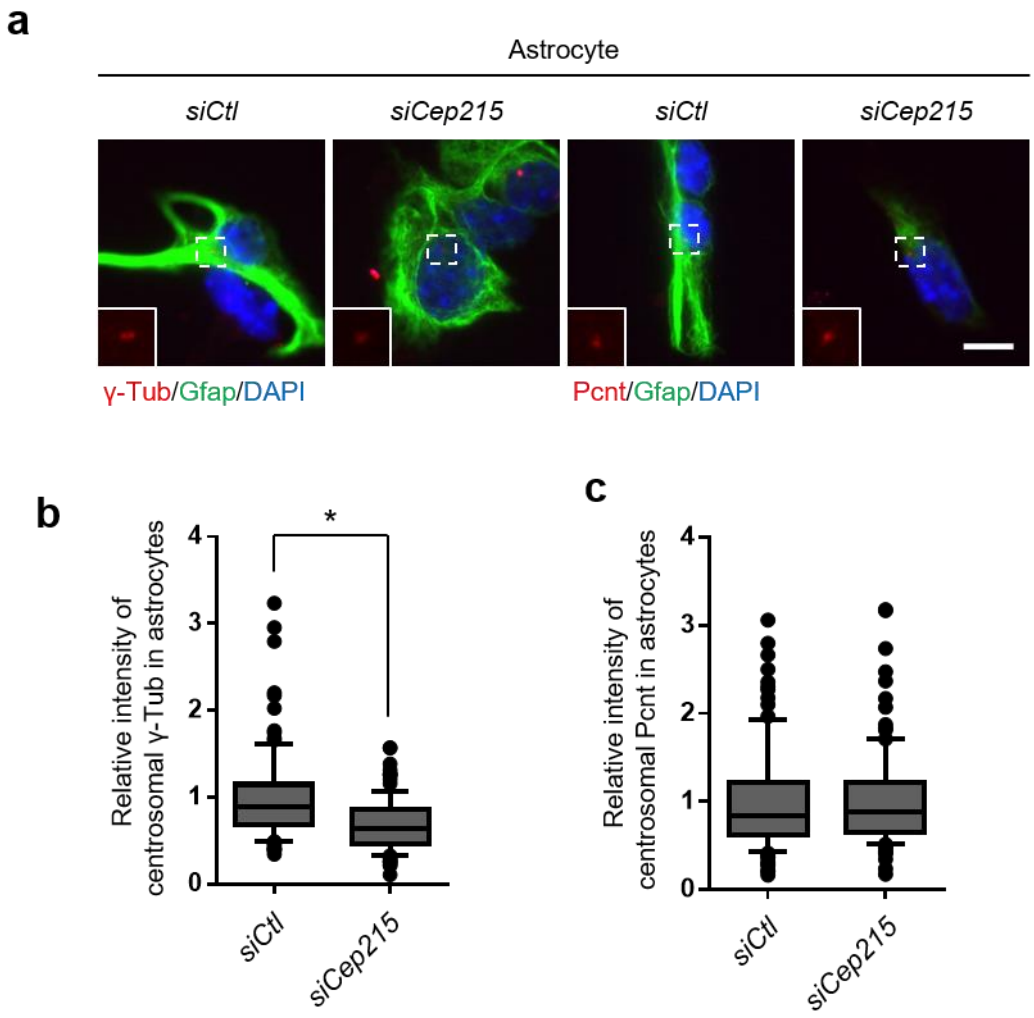

Figure 21. Reduction of centrosomal γ-tubulin in Cep215-depleted primary astrocytes Cep215 in primary hippocampal cells was depleted with specific siRNA (*siCep215*) transfection at DIV1. (**a**) The Cep215-depleted hippocampal cells at DIV3 were subjected to coimmunostaining analysis with γ-tubulin or pericentrin (Pcnt) (red) along with Gfap (green). Nuclei were stained with DAPI (blue). Scale bar, 10μm. (**b**, **c**) Intensities of the centrosomal γ-tubulin (**b**) and Pcnt (**c**) signals were measured in Cep215-depleted astrocytes. Greater than 90 cells per experimental group were estimated in three independent experiments. The statistical significance was determined by unpaired *t*-test. Error bars, SEM. *, P<0.05.

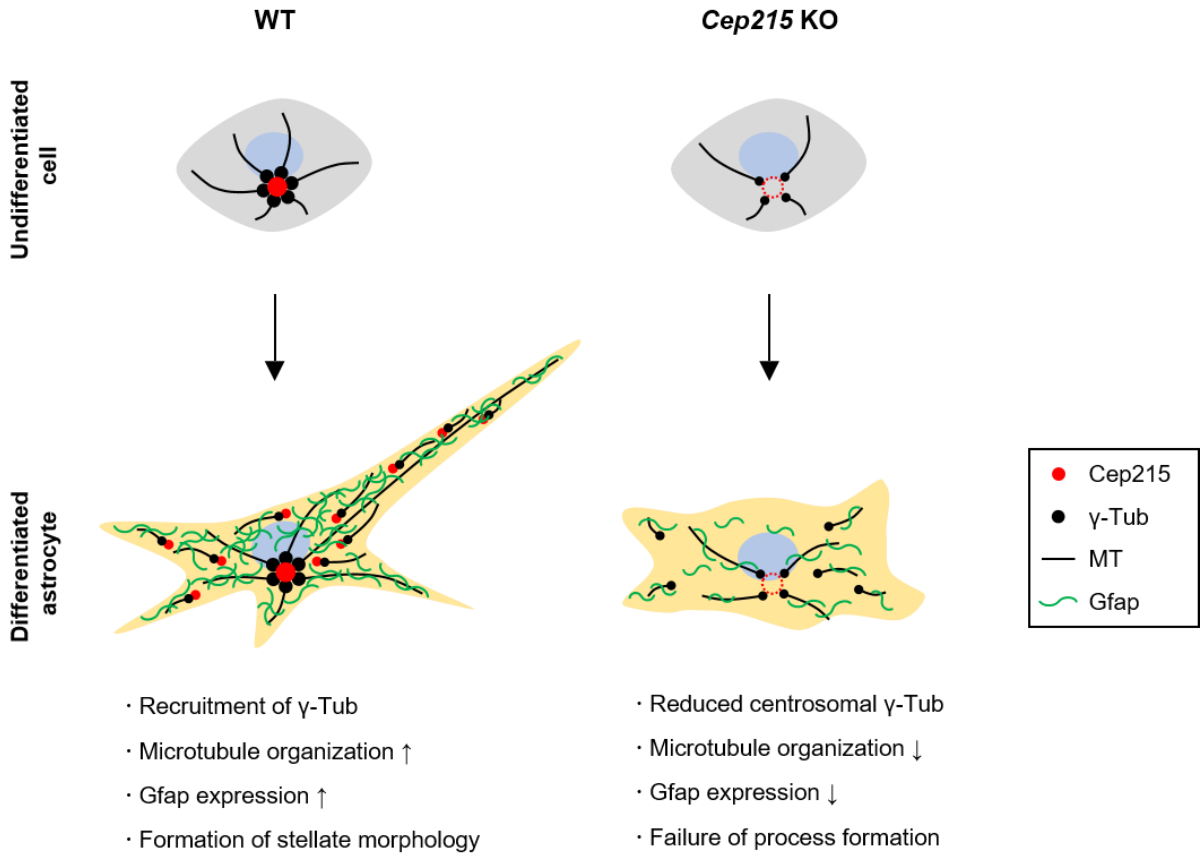

Figure 14. Model for the role of Cep215 in morphological differentiation of astrocytes During astrocyte differentiation, the centrosomal Cep215 recruits γ-tubulin at the centrosome for a dense organization of microtubules. Active microtubule nucleation is necessary to form processes of astrocytes and to make a stellate morphology. However, the *Cep215*-deleted cells cannot effectively gather γ-tubulin to the centrosome so that the microtubule organizing activity in the centrosome is suppressed. Astrocytes with a reduced activity of microtubule nucleation do not form processes with a fibroblast-like morphology.

DISCUSSION

In this work, I investigated the involvement of Cep215 in morphological differentiation of astrocytes. Cep215 localized at the glial processes as well as at the centrosomes in primary hippocampal astrocytes. Furthermore, the formation of glial processes was suppressed in the *Cep215*-deleted P19 cells. Similar phenotypes were also observed in astrocytes in the embryonic hippocampal culture. Cep215^{F75A} mutant which did not interact with γ-tubulin could not rescue the phenotypes and microtubule organizing activity of differentiated astrocytes was suppressed in *Cep215*-deleted P19 cells. These results indicate that Cep215 is essential for glial process formation during differentiation of astrocytes via regulation of microtubule organization.

The major biological function of Cep215 is to recruit γ-TuRC at specific sites of the cell for microtubule organization (Fong et al., 2017). In fact, I observed a significant reduction of the microtubule organization activity in the *Cep215*-deleted P19 cells even after astrocyte differentiation (Fig. 15). The microtubule organizing function of Cep215 should be critical for the glial process formation, since the ectopic Cep215^{F75A} protein could not rescue the *Cep215* deletion phenotypes in astrocyte differentiation of P19 cells (Fig. 17). Since the cellular distribution of Cep215 is not limited to the centrosome, it is likely that the deletion phenotypes of *Cep215* are partly attributed by cytoplasmic Cep215. It was already known that Cep215 controls the cytoplasmic microtubule organization (Choi et al., 2010). Likewise, the regrowth of cytoplasmic microtubule should to be reduced in *Cep215*-deleted astrocytes compared to wild type P19 cells (Fig. 15a). These results imply that Cep215 may regulate the organization of microtubule in astrocytes in both the centrosome and cytoplasm. Further experiments are needed to clarify the role of non-centrosomal Cep215 in glial differentiation.

Importance of cytoplasmic microtubule organization in cell morphogenesis has been demonstrated in number of tissues (Sanchez and Feldman, 2017). For example, the cytoplasmic

γ-tubulin in mature neurons increases to maintain the microtubule nucleating activity in the axon (Sanchez-Huertas et al., 2016). I propose that Cep215 is also observed in glial process of astrocytes. It is possible that Cep215 anchors γ-TuRC at the glial processes using a specific subcellular organelle whose identity remains to be discovered. However, we do not rule out the possibility that microtubules may be nucleated at the centrosome and transported to the intended location through existing microtubule networks (Ahmad et al., 1999). In accord, the centrosomal levels of Cep215 significantly increased in mouse hippocampal culture (Fig. 11), and microtubule organizing activity of centrosome was still functional for microtubule organization during astrocyte differentiation (Fig. 15).

Specific roles of microtubules in glial process formation have not been fully understood yet. Microtubules may extend the cell periphery for glial process formation. Microtubules, then, provide an intracellular transport route for glial process formation. For example, mitochondria should be distributed along the glial processes. In fact, mitochondria are aligned with and transported along microtubules in cultured astrocytes (Kremneva et al., 2013). Gfap is also known to be transported through microtubules when astrocytes start to extend the glial processes (Leduc and Etienne-Manneville, 2017a, b). I observed that *Cep215* deletion suppressed the cellular Gfap levels (Fig. 11). I suspect that *Gfap* expression may be stimulated when cell periphery is extended by microtubule networks. Both *Gfap* mRNA and protein could be transported through microtubules to install glial processes during gliogenesis (Medrano and Steward, 2001; Sakers et al., 2017).

Cep215 is one of causal genes of microcephaly (Bond et al., 2005). A mouse genetic study revealed that Cep215 is essential for proliferation and differentiation of neurons during brain development (Buchman et al., 2010). Nonetheless, it remains elusive how microcephaly is developed by *Cep215* mutations. It was initially proposed that defects in spindle pole orientation reduce population of neuronal stem cells during brain development (Fish et al., 2006). It was later proposed that extensive cell death might cause reduction of brain cell number during development (Endoh-Yamagami et al., 2010). In *Drosophila*, Cnn is known to be

important for dendrite morphogenesis (Yalgin et al., 2015). Therefore, Cep215 is likely to be involved in multiple stages of neuronal differentiation during brain development.

My work proposes another possibility that defects in glial differentiation might contribute to microcephaly development in *Cep215* mutant patients. Astrocytes are the most abundant cell types in the central nervous system with a remarkable heterogeneity both in morphology and function. In the past, astrocytes were believed to act as passive supporting cells for neuronal connections and tissue homeostasis. However, recent works revealed that astrocytes play diverse roles in the brain, such as the formation of neural networks, neurotransmitter recovery, extracellular ion maintenance, and detoxification (Chandrasekaran et al., 2016). Morphology of glial processes is very diverse depending on where they reside in the brain. The positioning, size, and anatomical complexity of protoplasmic astrocytes make these cells well-suited to interaction with neurons and synaptic elements in the brain. In fact, defects in astrocyte differentiation are known to link to neurological disease including diverse neurodegenerative diseases and neurodevelopmental disorders (Chandrasekaran et al., 2016). In the future, it is worth to investigate specific functions of Cep215 in astrocytes in vivo.

Chapter II.

Roles of Cep215 in male germ cell development

ABSTRACT

In order to investigate specific roles of Cep215 in diverse tissues, I used the KO mouse in which specific sites at the first and the last introns of *Cep215* were double-targeted by CRISPR gRNAs to remove most of the *Cep215* gene. The *Cep215* KO mice had microcephaly-like defects as reported previously. In addition, *Cep215* KO testes were smaller than the wild type testes, suggesting defects in male germ cell development. In fact, The *Cep215* KO testes were devoid of post-meiotic germ cells. Spermatogenesis in the *Cep215* KO mouse was arrested at prophase I and the spermatocytes were vulnerable to cell death. It is surprising that the centrosomes in the *Cep215*-deleted germ cells appeared to be intact, suggesting that the defects in progression of meiosis by *Cep215* deletion may be not caused by a defect in centrosome functions. Rather, the tight and gap junctions of Sertoli cells were disorganized and the intercellular bridges among germ cells were reduced in the *Cep215* KO testes. Based on the results, I propose that the germ cell defects are attributed, in part, to disorganized architecture of the *Cep215* KO testis.

INTRODUCTION

Centrosome is an intracellular organelle whose major function is forming microtubule networks in the cells. Conservation of this small organelle in most animal cells implies the importance of centrosome in many cellular processes. The centrosome is thought to be essential for the normal embryonic development, as it plays a role in cell division by forming a bipolar spindle pole and separating the DNA contents into exactly two daughter cells. In surprise, however, most phenotypes of the mice having mutations in centrosomal proteins are focused on a few organs. The most popular phenotypes caused by mutations of centrosomal proteins is malformation of brain. Many papers suggest a close relationship between dysfunction of centrosome and survival, and further, differentiation of neural stem cells (Robinson et al., 2020; Phan and Holland, 2021). In addition to brain, the dysfunction of centrosome is closely related to gametogenesis (Schatten and Sun, 2011, 2018). In some cases, mutant mice show in both of microcephaly and developmental defects in male reproductive organ (Marjanovic et al., 2015; Qin et al., 2019). It implies that importance of centrosome might be emphasized in selective cell types.

Cep215, a component of PCM, is also known as a causative gene for microcephaly (Bond et al., 2005). This phenotype is repeatedly observed in mutant mouse model (*Cep215*$^{an/an}$ mutant mouse; Lizarraga et al, 2010). Interestingly, this mutant mouse also showed developmental defects in male reproductive organ (Zaqout et al., 2017). The fact that Centrosomin, a ortholog of Cep215 in *Drosophila*, is also reported the essential factor for developing male germ cell is emphasized the importance of Cep215 in development of male reproductive organs (Li et al., 1998). However, the role of Cep215 in the development of male germ cells were not understood yet. Although the previous report suggests the role of Cep215 in embryonic germ cell, there are some limitations for understanding of the importance of Cep215 in this *Cep215*$^{an/an}$ mutant mouse. It is reported that *Cep215*$^{an/an}$ mutant mice express

the full length size of Cep215 protein (Lizarraga et al., 2010). Also, other *Cep215* mutant mice with mutations of very early exon in *Cep215* have leaky expression of full-length protein or express the fragments without the N terminal sequences although 2 alleles of *Cep215* gene are mutated (Barrera et al., 2010; Kraemer et al., 2015). These result indicate that there might be alternative transcripts of Cep215 due to its long DNA sequences and targeting only one site of the early exon, a common strategy of CRISPR-Cas9 system, is not sufficient to completely eliminate *Cep215* gene. In order to remove the entire putative alternative variants of Cep215, I established the strategy for generating *Cep215* total KO mice with *Cep215* gene which is excised from exon 2 to 36 via targeting two sites of allele.

Testis is a male reproductive organ which the spermatogenesis occurs in. The seminiferous tubule is composed of various developmental stages of germ cells and Sertoli cells. Spermatogenesis is a specific developmental process, which makes diploid (2n) spermatogonia to produce the haploid (n) mature sperm. The process of spermatogenesis can be categorized into 3 steps, proliferation and differentiation of spermatogonia (SG), meiosis of spermatocytes (SC), and spermiogenesis of post-meiotic spermatids (ST). This process begins at the post-natal stage and sustains until adulthood. In puberty, spermatocytes undergo two rounds of meiotic division, as a result, the haploid spermatids are generated. Although the germ cells undergo a series of divisions for a long period, each germ cells are connected by intercellular bridge for synchronized cell division and the compensation of haploid DNA contents (Greenbaum et al., 2011). Along with the development of germ cells, Sertoli cells mature after birth and form blood-testis barrier (BTB) in puberty which is a physical barrier to prevent germ cells from attack of immune cells or cytotoxic molecules from blood (Kaur et al., 2014). Although the importance of Cep215 in embryonic primordial germ cells was already reported, the importance and the role of Cep215 in testis development occurring after birth is not discovered yet.

In this study, I generated total *Cep215* KO mouse and investigated the importance of Cep215 in development of testis. It revealed that *Cep215* KO mice have severe developmental

defects in testis, especially progression of meiosis. In addition to germ cells, *Cep215* deletion also induces defects in formation of testis architectures.

MATERIALS AND METHODS

Animals

The animal experiments in this study were permitted by Institutional Animal Care and Use Committee at Seoul National University (SNU-211112-3-3). *Cep215* KO mouse were made by CRISPR/Cas9 system targeting for whole gDNA of *Cep215*. guide RNA sequences were shown in Table 2. Genotypes of *Cep215* mutant mouse (Cep215+/+, Cep215 +/-. Cep215 -/-) were determined with genomic PCR analyses using mouse tail. The PCR primers were shown in Table 2. Tissue preparation was carried out after euthanasia using CO2 and perfusion with 1× PBS.

Table 2. Sequences for guide RNA (gRNA) of CRISPR/Cas9 KO method and genotyping PCR primers.

	Sequence
gRNA #1	5'- TATTGGCTGACATTCAACCG -3'
gRNA #2	5'- AGTCATCATCCTTTTCACCA -3'
gRNA #3	5'- GACTACACCAGCAACCACAT -3'
gRNA #4	5'- GTGGTTGCTGGTGTAGTCGT -3'
Genotyping PCR primer #F	5'- CGATGTGTAGGCTAGGCAGG -3'
Genotyping PCR primer #R1	5'- TCCTGAAGATGACAAGGCACC -3'
Genotyping PCR primer #R2	5'- ATGCCCTTTCCCCAGAACAG -3'

Immunoblot analyses

The perfused mouse organs were homogenized and incubated with RIPA buffer (150mM NaCl, 1% Triton X-100, 0.5% sodium deoxycholate, 0.1% SDS, 50mM Tris-HCl at pH 8.0, 10mM NaF, 1mM Na_3VO_4, 1mM EDTA and 1mM EGTA) containing a protease

inhibitor cocktail (P8340; Sigma-Aldrich) for 10min on the ice. The tissue lysates were centrifuged with 12,000 rpm for 10 min at 4℃. The supernatants were mixed with 4×SDS sample buffer (250mM Tris-HCl at pH 6.8, 8% SDS, 40% glycerol and 0.04% bromophenol blue) and 400mM DTT (0281-25G; Amresco). Mixtures were boiled for 5 min and the protein samples were subjected to SDS-polyacrylamide gel electrophoresis. The gel was transferred to a nitrocellulose membrane. The membrane was blocked with 5% skim milk in 0.1% TBST (Tris-buffered saline TBS with 0.1% Tween 20) for 1-2 h. The membrane was incubated with primary antibody overnight at 4˚C. The membrane was incubated with horseradish peroxidase-conjugated secondary antibody for 30-40 min at room temperature. The ECL solution was treated onto the membrane, and then exposed to an X-ray film.

H & E staining

For the histological analyses, Hematoxylin and Eosin staining was also conducted on paraffin embedded mouse brain (5μm thickness) and testis tissue (3μm thickness). Hematoxylin stains acidic molecules such as nuclei with blue color, while eosin stains basic materials in cytoplasm in reddish color. This H&E staining was conducted by using automatic staining machine (Leica ST5010 Autostainer XL).

TUNEL Assay

The TUNEL assay was performed for detecting apoptotic germ cells. I used the FragELTM DNA Fragmentation Detection Kit (Calbiochem; Cat. No. Q1A39) and strictly followed the manufacturer's instruction. In brief, the paraffin embedded testis sections were rehydrated and permeabilized with proteinase K. The tissues were treated with 1×TdT (terminal deoxynucleotidyl transferase) equilibrium buffer to mark the exposed 3'-OH ends of DNA fragments formed during apoptosis. To estimate the cell type specific apoptotic rate, I counted the number of TUNEL-positive spermatogonia and spermatocytes and divided into the entire number of spermatogonia and spermatocytes, respectively.

Immunohistochemistry of tissue sections

The mouse tissues were fixed in 4% PFA (Paraformaldehyde) solution overnight at 4℃. After washing, the fixed tissues were embedded in paraffin and sectioned with 3μm thickness in case of testis. The testis sections were rehydrated and boiled for the antigen retrieval buffer pH 6 Citrate buffer or pH 9 Tris-EDTA buffer depending on the primary antibodies. And then, the tissues were permeabilized by incubation with 0.1% PBST (phosphate-buffered saline with 0.1% Triton X-100). The tissue sections were blocked with 3% bovine serum albumin in 0.5% PBST for 30 min and incubated with primary antibodies overnight at 4℃. The antibodies used for immunohistochemistry were described at the section of 'Antibodies'. After washing with 0.1% PBST for 3 times, the tissues were incubated with secondary antibodies for 30min, and them washed with 0.1% PBST 3 times. The tissues were mounted with cover glass using Prolong gold mounting solution (Invitrogen) after DAPI incubation.

Chromosome spreading and immunostaining analysis of mouse testis

Immunostaining analysis of chromosome spreading was performed following Lakshmi et al (Gopinathan et al., 2017) with minor modifications. In brief, the adult mice were sacrificed using CO2 and perfused with 1×PBS. The testes were excised and placed in PBS. The tunica albuginea was carefully removed and the seminiferous tubules were slightly teased apart with blunt forceps. The seminiferous tubules were incubated with hypotonic extraction buffer (30mM Tris pH 8.2, 50mM Sucrose, 17mM Trisodium Citrate Dihydrate, 5mM EDTA) with inverting for 30min to 1h on ice depending on the size of testis. The seminiferous tubules were placed in microtube with 250μl or 1ml of 100mM Sucrose pH 8.2 depending on the size of testis in WT and KO mouse, respectively. And then, the tubules were pipetted repeatedly around 50 times using a cut 1000μl and 200ul tips in turn until the solution turned cloudy. A poly-L-lysine coated slide was dipped in freshly prepared fixative solution (1% PFA, 30mM

Sodium Tetraborate, 0.15% Triton X-100 in PBS), 50μl of the seminiferous tubule suspension was added and suspended few times at the edge of the slide with droplets of fixative solution. The solution was allowed to spread along the length of the slide. Slides were placed in a humidified chamber at 4℃ for 6-7 h, and stored at -20℃ until further use.

For immunostaining analysis, slides with chromosome spreads were washed with PBS 3 times. The slides were permeabilized by incubation with 0.1% PBST, followed by blocking with 3% bovine serum albumin in 0.5% PBST for 1h. The slides were incubated with primary antibodies overnight at 4℃. The antibodies used for immunostaining were described below. After washing with 0.1% PBST for 3 times, the slides were incubated with secondary antibodies for 1h, and washed with 0.1% PBST 3 times. And then, third antibodies were prepared with Zenon Alexa fluor labeling kit following the protocol of the manufacturer. The cells were incubated with conjugated antibody for 2h and mounted with a cover glass using Prolong gold mounting solution after DAPI incubation.

Antibodies

The antibodies were commercially purchased as listed below: Cep215 (06-1398; Millipore), γH2AX (05-636; Upstate), SCYP3 (ab15093; abcam), centrin-2 (04-1624; Millipore), γ-tubulin (ab11316-100; Abcam), Claudin-11 (36-4500; Invitrogen), Connexin43 (3512; Cell signalling), Gapdh (AM4300; Invitrogen). The Pcnt antibody was previously described (Kim and Rhee, 2011). The Alexa-fluorescence secondary antibodies were purchased from Invitrogen. The mouse and rabbit IgG-HRP antibodies were purchased from Sigma and Millipore, respectively.

Image processing

Images of H&E staining were acquired from the light microscope (Olympus BX 51) and processed with ProgRes® CapturePro (JENOPTIK). The immunostained tissues were observed using fluorescence microscope with a CCD (CoolSNAP EZ CCD; Photometrics)

camera and processed with PVCamtest (Photometrics), Adobe Photoshop software and ImageJ software.

Statistical analyses

For statistical analyses, experiments were independently performed three times. To calculate *P* values, all data were analyzed using the Prism 6 software (GraphPad Software) including unpaired two-tailed *t*-test, one- or two-way analysis of variant (ANOVA). In the case of ANOVA, the Tukey's post-test or Sidak's post-test were performed if *p* value is lower than 0.05.

RESULTS

Generation and characterization of *Cep215* total KO mouse

Several lines of the *Cep215* deletion mice have been previously reported, but all of them were generated with small deletions at the early exons of the gene, risking the presence of alternative splicing variants of the Cep215 protein in the cells (Barrera et al., 2010; Kraemer et al., 2015). *Hertwig's anemia* (*an*) mutant which arose in the progeny of a heavily irradiated male mouse demonstrated an in-frame 111 bp deletion resulting from loss of exon 4 from the mRNA (Hertwig, 1942; Lizarraga et al., 2010). In order to avoid a possible interference of the residual Cep215 variants, Professor Young Hoon Sung in Asan Medical Center generated the KO mice in which the whole *Cep215* gene was removed. Total deletion of the *Cep215* gene was carried out with gRNAs targeting introns 1 and 37 using CRISPR/Cas9 system (Fig. 23a). The deletion was confirmed with the PCR genotyping (Fig. 23b). Immunoblot analysis was carried out to determine Cep215 expression in selected tissues. The Cep215 protein was detected in cerebrum, cerebellum, kidney and most abundantly in the testis (Fig. 23c). No specific band was detected in the tissues of the *Cep215* KO mice, indicating that the Cep215 protein is absent in the *Cep215* total KO mice.

I determined the gross phenotypes of the *Cep215* KO mouse. The heterozygote mating produced homozygote mutants less frequently than expected (Fig. 24a). This suggests that the total deletion *Cep215* had a slight lethality in their embryonic stage. The live homozygote mice were smaller than the wild type mice, but did not die early (Fig. 24b, c). Especially, the *Cep215* KO mice showed microcephaly, which had been reported with the $Cep215^{an/an}$ mutants (Fig. 24d; Lizarraga et al., 2010). The cortical thickness and cortical length were significantly reduced in the *Cep215* KO mice (Fig. 24e, f). In sum, the total *Cep215* KO mice which I had generated revealed general features which had been previously observed with the $Cep215^{an/an}$ mutant mice (Lizarraga et al., 2010).

Histological analysis of the developing testes in *Cep215* KO mouse

Microcephaly is the major phenotype of the *Cep215* KO mice. In addition, *Cep215* KO mice had defects in other organs, such as testes and eyes (Zaqout et al., 2017, 2020). Indeed, I observed that the *Cep215* KO male mice had testes with reduced volumes (Fig. 25a, b). Since mouse spermatogenesis starts at P10 and reached to meiosis at P17 (Nebel et al., 1961; McLean et al., 2003), I used P7, P17, and adult mice to determine male germ cell development. As expected, the P7 testes consisted of Sertoli cells and spermatogonia, and the P17 testes additionally included spermatocytes (Fig. 25c, d). The *Cep215* KO mice also included Sertoli cells and spermatogonia in P7 testes, and spermatocytes in P17 testes (Fig. 25c, d). However, the number of meiotic germ cells in the *Cep215* KO testes was significantly reduced and no post-meiotic germ cells were found in the *Cep215* KO mouse (Fig. 25c, d). These results indicate that the male germ cells of the *Cep215* KO testes may differentiate into premeiotic spermatocytes, but do not complete meiosis. It is different from *Cep215*$^{an/an}$ mutant mice in which the male germ cells are completely absent in postnatal testes (Zaqout et al., 2017).

Defects in the *Cep215* KO spermatocytes

Even if spermatocytes were detected at the *Cep215* KO testes, their number was greatly reduced in comparison to the wild type testes. This observation raises the possibility that the meiotic process may be impeded in the *Cep215* KO male germ cells. I immunostained the testes with the γH2AX antibody to determine meiotic prophase progression of the male germ cells. During the meiotic prophase, homologous chromosomes form bivalent via double strand break and repair, which are detected with the γH2AX antibody (Heyting, 1996). In fact, most of the seminiferous tubules in immature and adult testes included the γH2AX-positive germ cells (Fig. 26). However, only a half of the seminiferous tubules in the *Cep215* KO testes include γH2AX-positive germ cells, indicating that meiotic progression of the *Cep215* KO testes was significantly impeded (Fig. 26).

Seminiferous tubules in the *Cep215* KO testes include reduced numbers of germ cells and sometimes were devoid of any germ cell at all (Fig. 25c). This phenotype suggests that a fraction of male germ cells in the *Cep215* KO testes are discarded at a premeiotic stage. I performed TUNEL assays to determine apoptosis in male germ cells of the *Cep215* KO testes (Fig. 27). The results showed that premeiotic male germ cells of the *Cep215* KO mice underwent apoptosis more frequently than those of the wild type mice (Fig. 27). Apoptosis was most frequent at the spermatocyte stage (Fig. 27b). These results suggest that development of the male germ cells in the *Cep215* KO mice is blocked at meiotic prophase and the cell are eventually discarded by apoptosis.

Observation of the centrosomes in male germ cells at different developmental stages

Since Cep215 is a component of the centrosome, I observed centrosomes in the male germ cells of the *Cep215* KO mice. I performed coimmunostaining analyses with antibodies specific to a centriole marker (centrin2) and major PCM proteins (Cep215, pericentrin and γ-tubulin). As expected, centrioles were detected in all male germ cells at different developmental stages (Fig. 28). The PCM proteins were also visible in the male germ cells except the round spermatids right after meiosis (Fig. 28). In the *Cep215* KO testes, Cep215 signals were absent, and centrosomes were visualized with the centrosome marker antibodies at premeiotic germ cells (Fig. 28). The centrosomes were not precociously separated nor the centrosome intensities of pericentrin and γ-tubulin were not reduced in the male germ cells of the *Cep215* KO mice (Fig. 28). These results suggest that the centrosomes in the male germ cells are more or less intact even in the absence of Cep215.

Immunostaining of the isolated spermatocytes from the *Cep215* KO testes

In order to determine stages of the meiotic prophase precisely, I performed immunocytochemistry with isolated spermatocytes from wild type and *Cep215* KO testes. Spermatocytes were isolated from the testes, placed in a hypotonic solution for expansion and

fixed for immunostaining analysis. The stages of meiotic prophase I may be determined with the immunostaining patterns of Sycp3 and γH2AX (Fig. 29a). In the wild type testes, diplotene was the most prominent stage (Fig. 29b). However, zygotene was the most prominent in the *Cep215* KO testes (Fig. 29b). Spermatocytes at pachytene and diplotene stages were hardly detected in the KO testes (Fig. 29b). This result suggests that meiotic progression is specifically arrested after zygotene stage in the *Cep215* KO male germ cells.

In order to closely examine centrosomes during meiosis, I immunostained the isolated spermatocytes with the selected antibodies which detect centrosomes. It is recently reported that centrosome duplication and separation occur at zygotene and diakinesis of prophase I, respectively (Alfaro et al., 2021; Wellard et al., 2021). I also observed that two centrosome signals are present at zygotene and pachytene/diplotene spermatocytes and they are separated at diakinesis spermatocytes (Fig. 30). Two centrosome signals were also observed at the zygotene and pachytene/diplotene spermatocytes of the *Cep215* KO mice (Fig. 30). However, centrosome separation was not observed at the *Cep215* KO mice which had little spermatocytes at diakinesis. These results suggest that the meiotic defects in the *Cep215* KO male germ cells may not be attributed by anomaly in germ cell centrosomes.

Defects in the testis architecture of the *Cep215* KO mice

One of the germ cell characteristics is the presence of intercellular bridge which links cytoplasm of the neighboring germ cells, due to incomplete cytokinesis. While the function of intercellular bridge was not fully understood yet, the most suitable hypothesis is that intercellular bridge is important for synchronous cell division by sharing cytoplasm and some proteins or mRNAs (Greenbaum et al., 2011). Tex14 is known to be important for maintenance of intercellular bridge. In fact, germ cell death occurs and spermatogenesis fails in the *Tex14* KO mice (Greenbaum et al., 2006). I tested if the intercellular bridges were affected by loss of Cep215 in male germ cells. I immunostained the Tex14 protein and estimated the number of intercellular bridges in the 17-day-old testes of the wild type and *Cep215* KO mice. The

spermatogonia and spermatocytes were connected well through intercellular bridges which were marked by Tex14 (Fig. 31a). Intercellular bridges were also formed between the germ cells of the *Cep215* KO mice, but the number of Tex14 signals per one germ cell was significantly reduced (Fig. 31b). This result reveals that the premeiotic male germ cells were not connected stably by intercellular bridges in the *Cep215* KO mice.

Male infertility can be caused not only by the defects of germ cells, but also by disruption of the structural environments for germ cell development (Uhrin et al., 2000). Sertoli cells are important for progression of spermatogenesis by secretion of signaling molecules (Griswold et al., 2012; Griswold, 2016). Furthermore, Sertoli cells are important for formation of blood-testis barrier (BTB) to prevent passage of immune cells or cytotoxic molecules (Mruk and Cheng, 2015). The development of Sertoli cells and formation of BTB occurred in puberty. BTB divides the seminiferous tubule into the apical and adluminal compartments (Mruk and Cheng, 2015). The basal compartment includes spermatogonia and leptotene, zygotene spermatocytes, whereas the adluminal compartment includes pachytene spermatocytes and germ cells at afterword developmental stages. In young mouse before puberty, some marker proteins of BTB, such as claudin-11, diffused in entire seminiferous tubules (Hollenbach et al., 2018).

To determine whether BTB formation were affected by *Cep215* deletion, I immunostained the *Cep215* KO testes with the antibodies specific to claudin-11 and connexin 43, junctional proteins at Sertoli cells. I coimmunostained them with the γH2AX antibody to determine the stages of prophase I (Fig. 32a). In P17 testes, most of spermatocytes developed into pachytene stage and BTB was formed ring-like structures, which divided the tubules into basal and adluminal compartments (Fig. 32b-d). On the other hand, BTB in the *Cep215* KO testes were incomplete with diffused distribution of claudin-11 and connexin 43 (Fig. 32c, d; Hollenbach et al., 2018). These results suggest that BTB failure may attribute to defects in meiotic progression of male germ cells in *Cep215* KO mice.

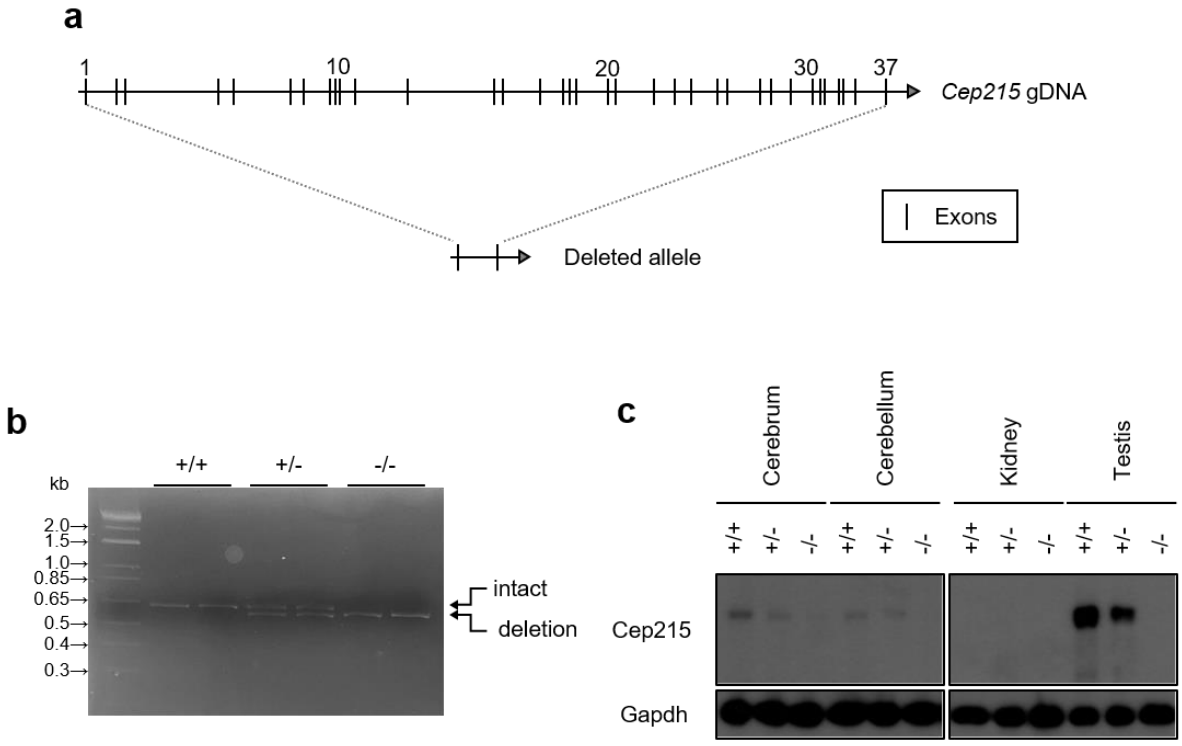

Figure 23. Generation of the *Cep215* total KO mouse (**a**) A schematic strategy for the *Cep215* gene deletion using the CRISPR-Cas9 system. Two different sets of the guide RNAs that target intron 1 and intron 37 were used for the total deletion of *Cep215*. (**b**) Genomic PCR products of the wild types (+/+), heterozygotes (+/-) and homozygotes (-/-) at the *Cep215* allele. The PCR products for the intact and deletion alleles of *Cep215* were 621bp and 569bp in size, respectively. (**c**) Adult mouse tissues of the *Cep215* mutant mice were subjected to immunoblot analysis with antibodies specific to Cep215 and Gapdh.

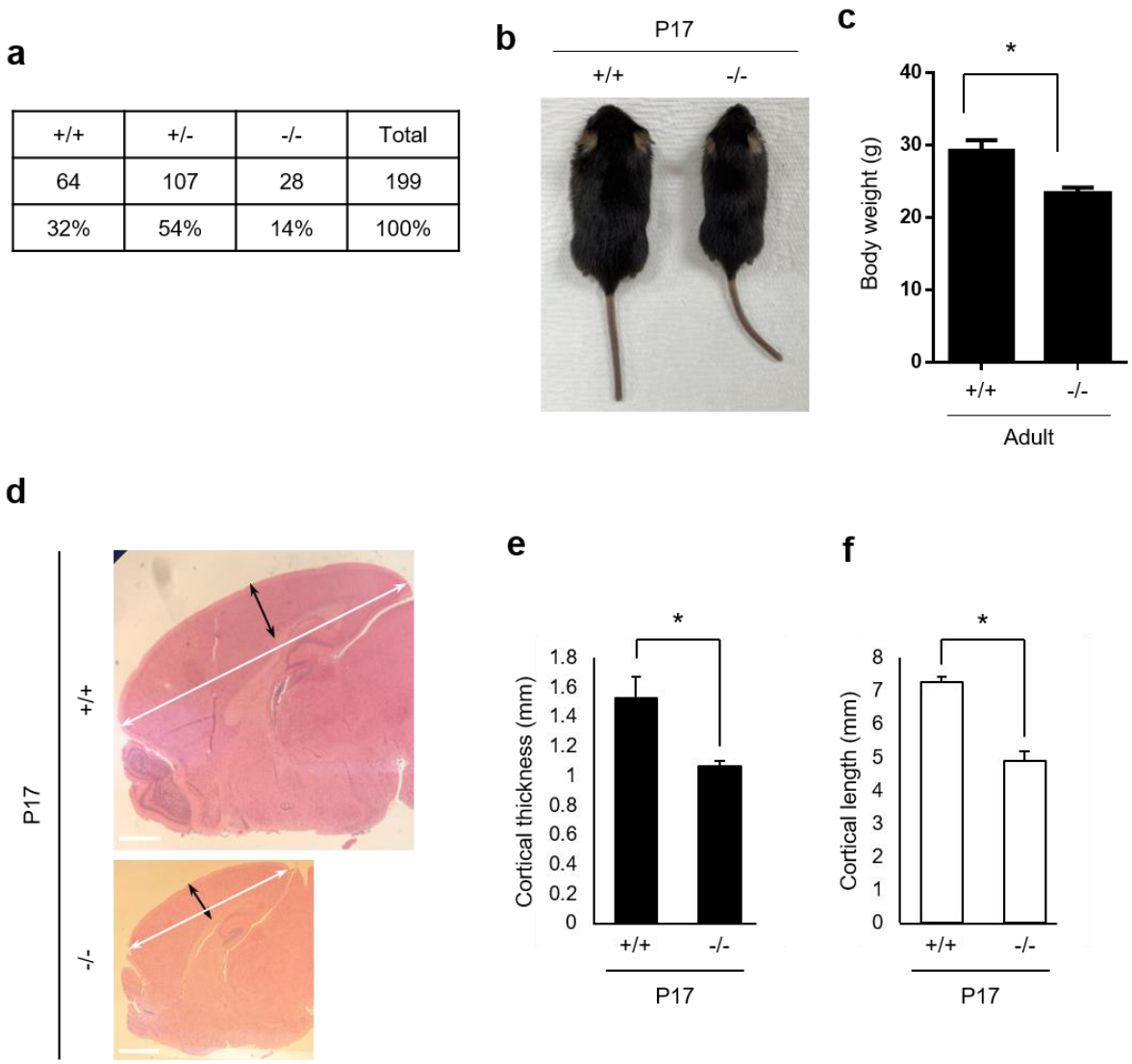

Figure 24. Gross phenotypes of the *Cep215* KO mice (**a**) The progeny genotypes after the *Cep215* heterozygote mating. (**b**) Size comparison of the wild type and *Cep215* mutant littermates at P17. (**c**) The body weights of the wild type and *Cep215* mutant littermates in adult. (**d**) The brain of the wild type and *Cep215* mutant littermates at P17 were subjected to H&E staining. The cortical thickness and length was marked with the black and white arrows, respectively. Scale bar, 1mm. (**e**, **f**) The cortical thicknesses (**e**) and cortical lengths (**f**) of the brains were measured. (**c**, **e**, **f**) At least three mice per experimental group were subjected to analysis. The statistical significance was determined by unpaired *t*-test. Error bars, SEM. *, P<0.05.

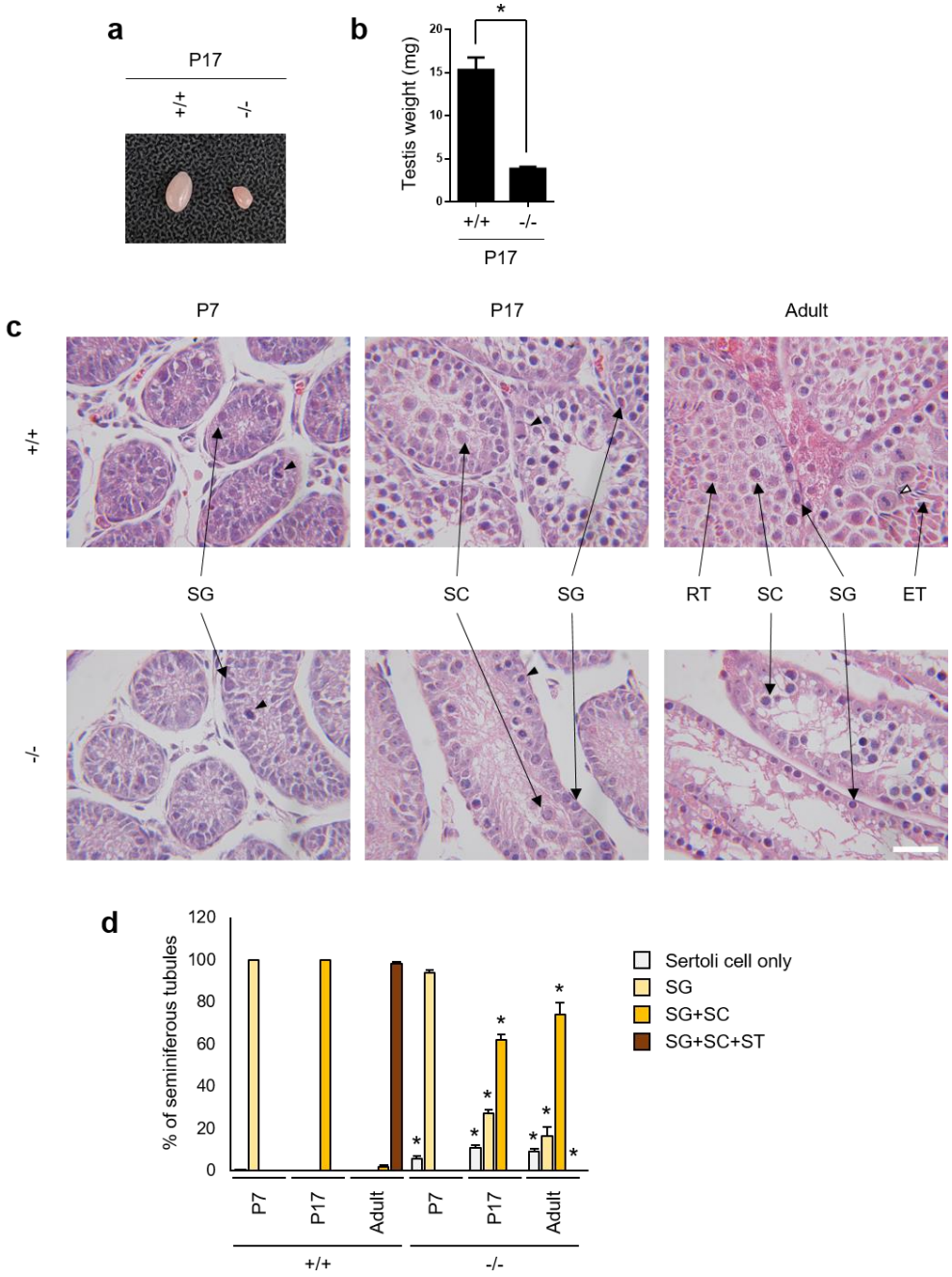

Figure 25. Histological analysis of the *Cep215* mutant testes (**a**) Testes of the wild type and *Cep215* mutant littermates at P17. (**b**) The weights of the testes at P17 mouse were measured and statistically analyzed (n=3 per groups). (**c**) The testes of the wild type and *Cep215* mutant littermates at P7, P17 and adult were subjected to H&E staining. SG, spermatogonia; SC, spermatocytes; RT, round spermatid; ET, elongated spermatid; filled arrowhead, mitotic spermatogonia; open arrowhead, meiotic spermatocytes. Scale bar, 50μm. (**d**) The number of seminiferous tubules with specific germ cells types were counted. At least 200 tubules per experimental group in three mice were subjected to analysis. (**b**, **d**) The statistical significance was determined by unpaired *t*-test (**b**) and two-way ANOVA (**d**). Error bars, SEM. *, P<0.05.

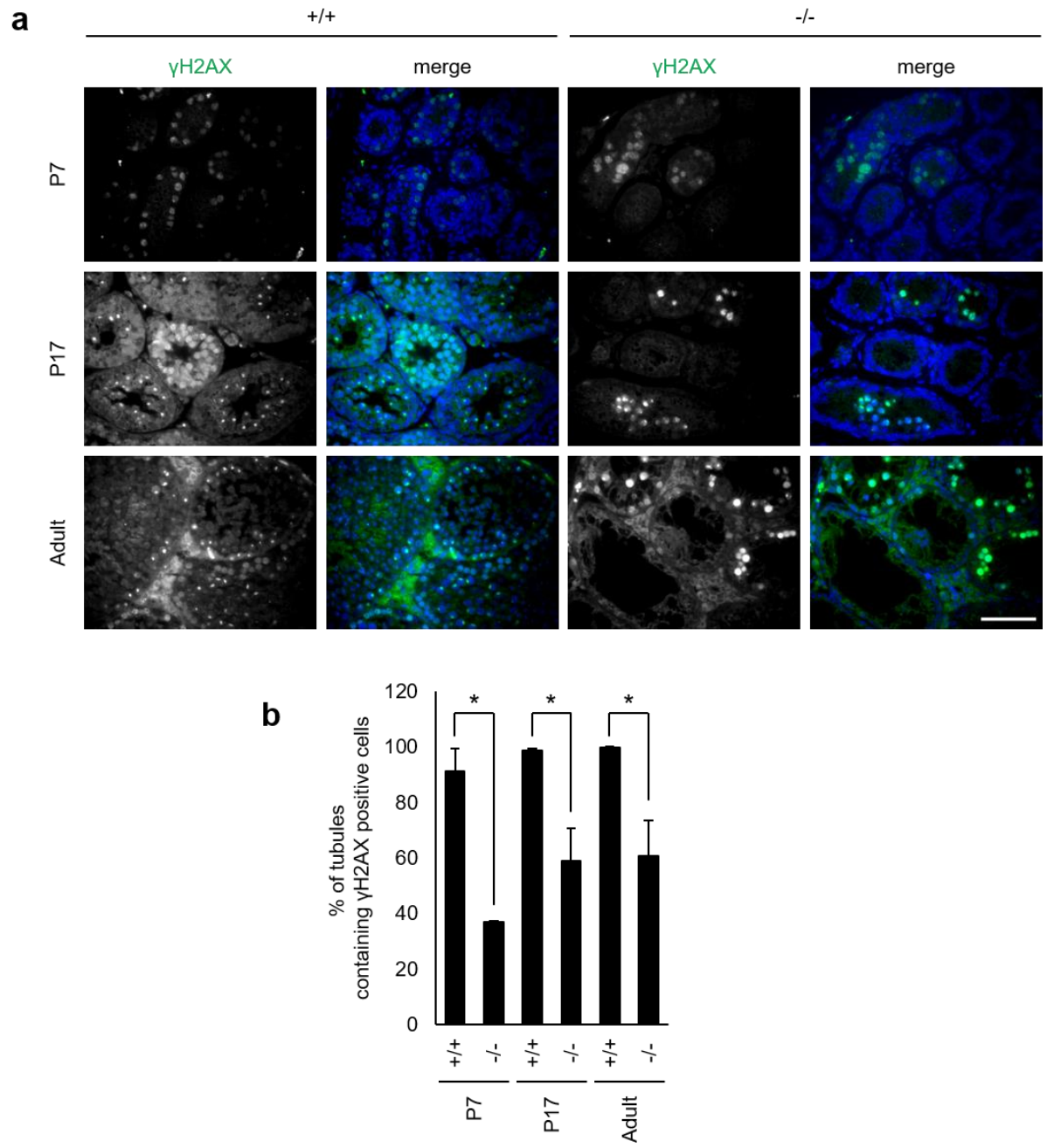

Figure 26. Defects in meiosis of the *Cep215* mutant testes (**a**) Testes of the wild type and *Cep215* mutant littermates at P7, P17 and adult were subjected to immunostaining analysis with the γH2AX antibody (green). Nuclei were stained with DAPI (blue). Scale bar, 50μm. (**b**) The number of tubules with γH2AX-positive meiotic cells were counted. Greater than 220 tubules per experimental group were counted in three mice. The statistical significance was determined by one-way ANOVA. Error bars, SEM. *, P<0.05.

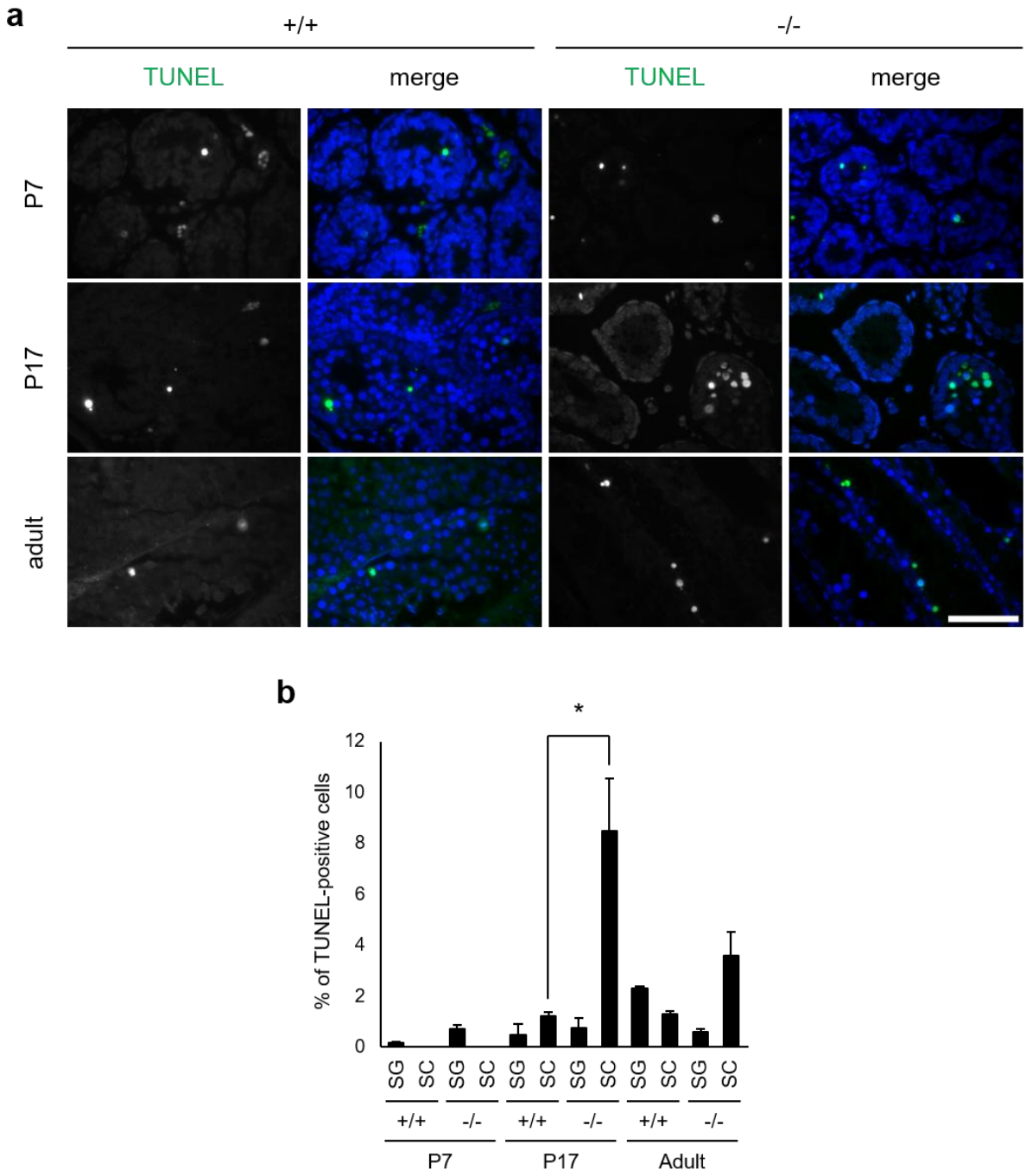

Figure 27. Cell death in the *Cep215* mutant testes (**a**) Testes of the wild type and *Cep215* mutant littermates at P7, P17 and adult were subjected to TUNEL analysis. Nuclei were stained with DAPI (blue). Scale bar, 50μm. (**b**) The number of TUNEL-positive spermatogonia (SG) and spermatocytes (SC) were counted. At least three mice per experimental group were used for the analyses. The statistical significance was determined by two-way ANOVA. Error bars, SEM. *, P<0.05.

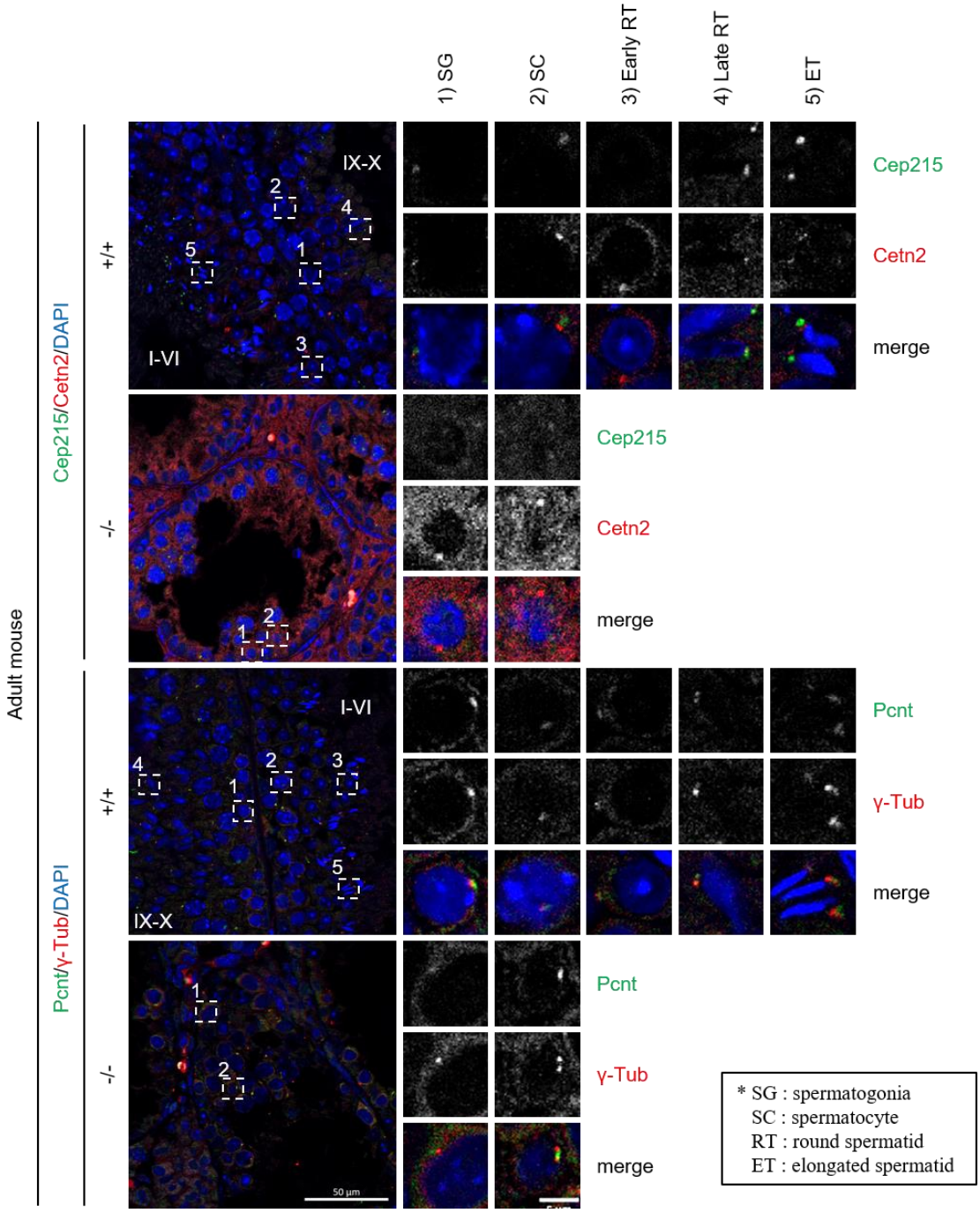

Figure 28. Expression patterns of the PCM proteins during spermatogenesis Testes of the wild type and *Cep215* mutant mice were subjected to coimmunostaining analyses with the antibodies specific to Cep215, Pcnt, γ-tubulin, and Centrin-2. Tubular stages were indicated with roman numbers. Nuclei were stained with DAPI (blue). Scale bar, 50μm in images of entire tissues, 5μm in magnified cell images. The results were repeatedly observed at least three mice per experimental group.

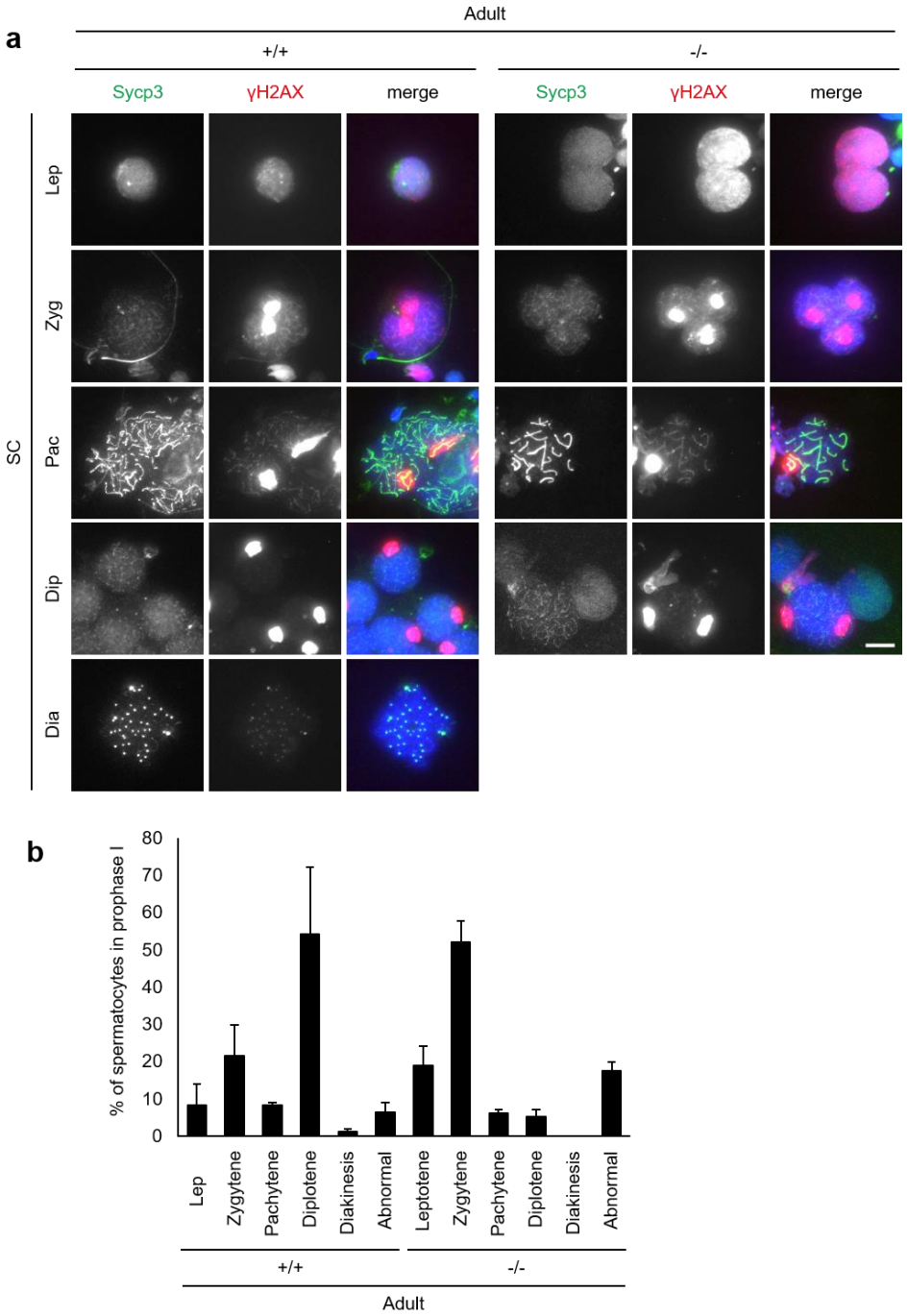

Figure 29. Spermatocyte spread analysis of the *Cep215* KO mice (**a**) Isolated spermatocytes of the adult wild type and *Cep215* KO mice were subjected to coimmunostaining analysis with the Sycp3 (green) and γH2AX (red) antibodies. Nuclei were stained with DAPI (blue). The stages of prophase I were determined based on the chromosome morphology. Scale bar, 10μm. (**b**) The number of spermatocytes at indicated stages of prophase I was counted. Greater than 200 cells per experimental group were counted in two independent experiments. Error bars, SEM.

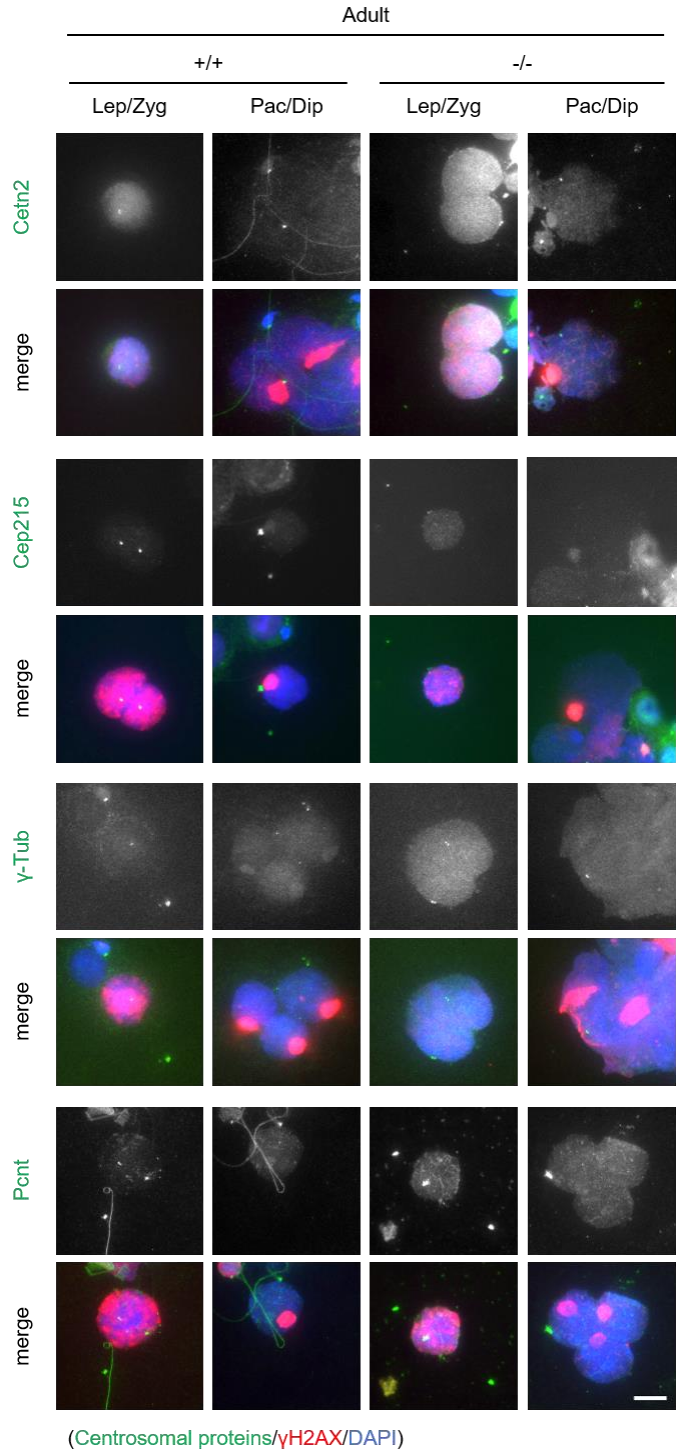

Figure 30. PCM proteins in the isolated spermatocytes of the *Cep215* KO mice The isolated spermatocytes from the wild type and *Cep215* KO mice were co-immunostained with the antibodies specific to the centrosomal proteins (centrin-2, Cep215, γ-tubulin, and Pcnt, green) along with γH2AX (red). The stage of prophase I was determined based on the staining patterns of γH2AX. Nuclei were stained with DAPI (blue). Scale bar, 10μm.

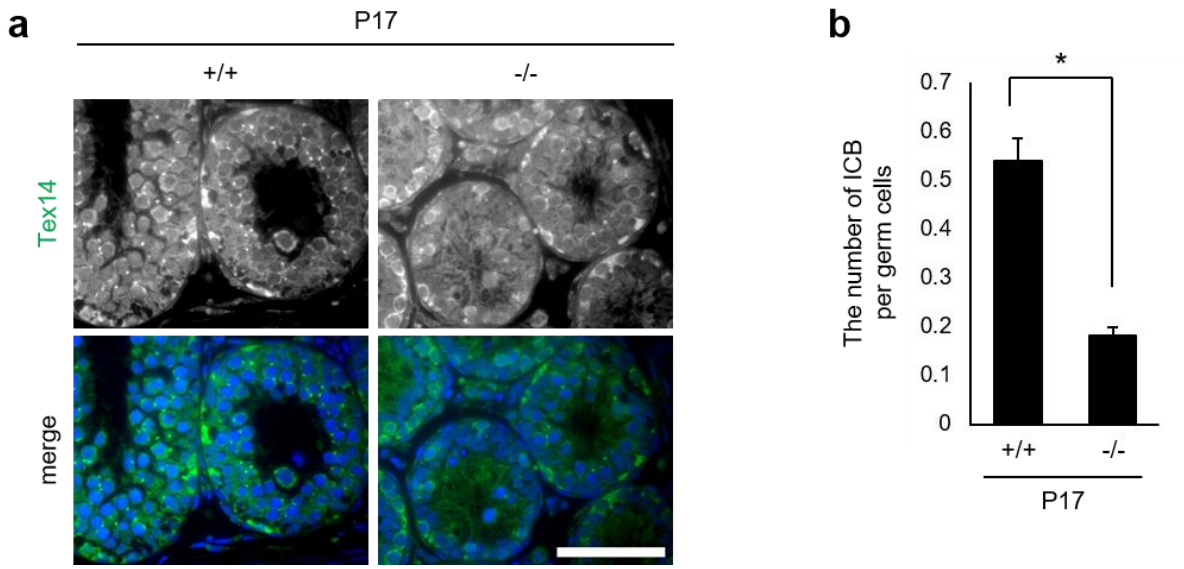

Figure 31. Disruption of the intercellular bridge in the *Cep215* KO mice (**a**) Testes of the wild type and *Cep215* KO mice at P17 were immunstained with antibody specific to Tex14 (green). Nuclei were stained with DAPI (blue). Scale bar, 50μm. (**b**) The number of intercellular bridge per germ cells were counted. At least three mice per experimental group were used for the analyses. The statistical significance was determined by unpaired *t*-test. Error bars, SEM. *, P<0.05.

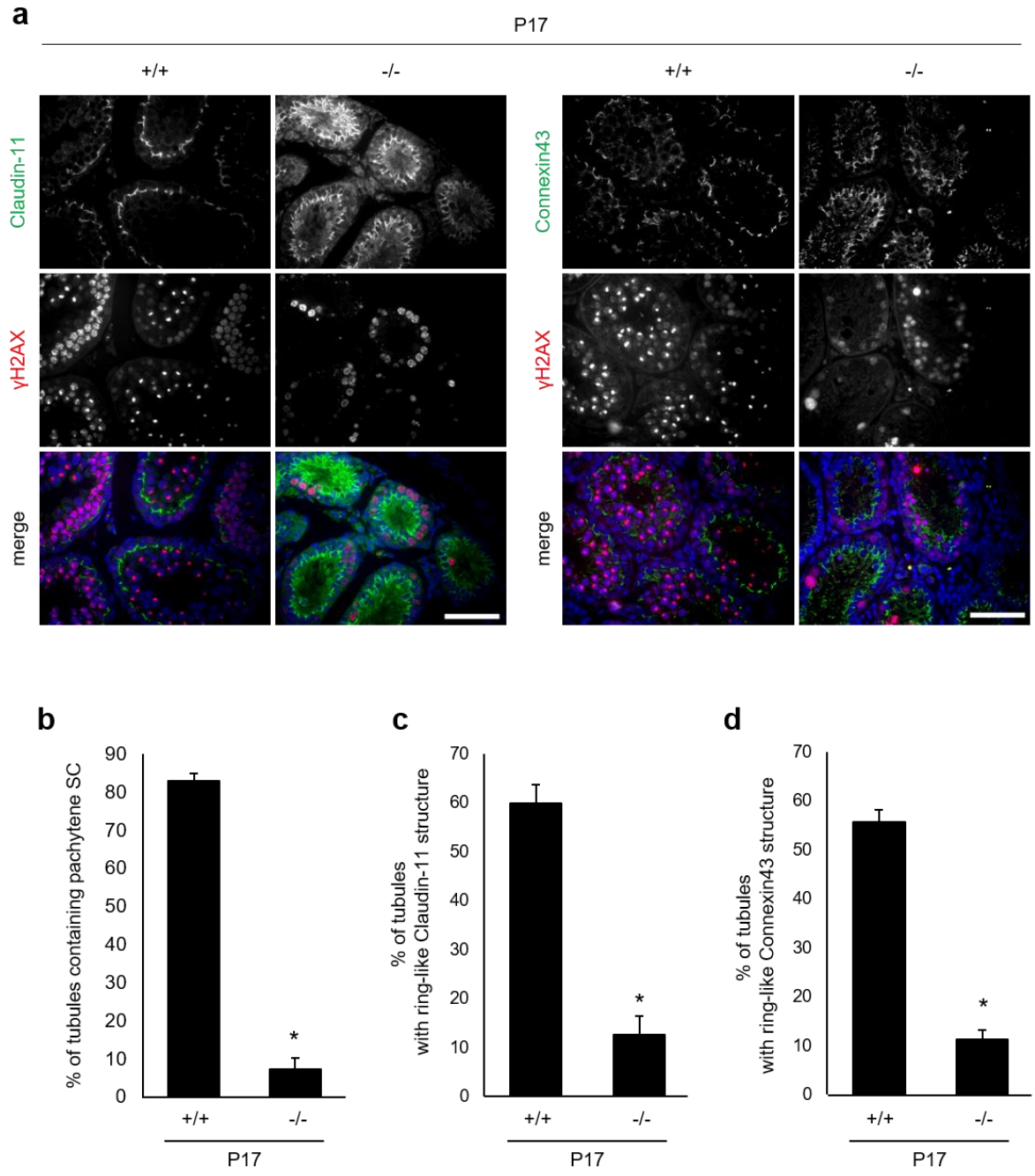

Figure 32. Disruption of the blood-testis-barrier in the *Cep215* KO mice (**a**) Testes of the wild type and *Cep215*-deleted littermates at P17 were subjected to coimmunostaining analysis with the antibodies specific to Claudin-11 or Connexin43 (green) along with γH2AX (red). Nuclei were stained with DAPI (blue). Scale bar, 50μm. (**b**) The number of seminiferous tubules with the spermatocytes undergoing pachytene stage were counted. (**c**, **d**) The number of tubules forming a ring-like structure of claudin-11(**c**) or connexin43 (**d**) were counted. (**b**-**d**) At least 190 tubules per experimental group were analyzed in three mice. The statistical significance was determined by unpaired *t*-test. Error bars, SEM. *, P<0.05.

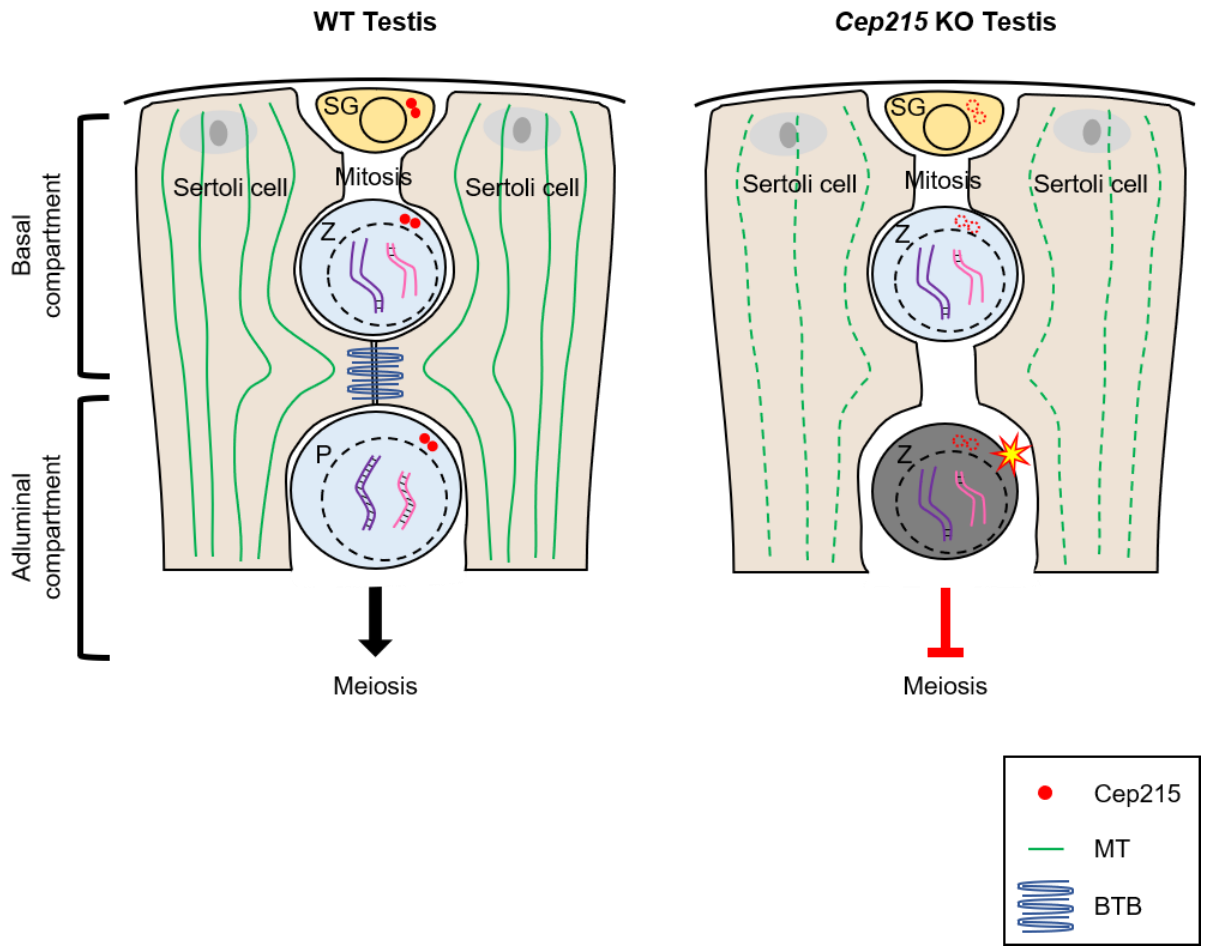

Figure 33. Model (**a**) Spermatogonial stem cells reside in the basal compartment. Once male germ cells initiate differentiation, they are forced to enter the adluminal compartment. Tight junctions between Sertoli cells form the blood-testis barrier which divides the basal and adluminal compartments. (**b**) In *Cep215* KO testis, tight junctions between Sertoli cells are not properly formed, probably due to abnormal microtubule networks within the Sertoli cells. As a result, differentiated spermatocytes were not protected by the blood-testis barrier and fail to complete meiosis but undergo apoptosis.

DISCUSSION

In this work, I investigated the phenotypes of *Cep215* KO mice in which the *Cep215* gene was totally removed, leaving no alternative splicing products. Overall phenotypes of my *Cep215* KO mice were more or less similar to that of the *Cep215*$^{an/an}$ mutant mice with typical microcephaly-like brains (Lizarraga et al., 2010). Nevertheless, we observed interesting phenotypes in the testes of the *Cep215* KO mice, details of which are distinct from those of the *Cep215*$^{an/an}$ mutant mice (Zaqout et al., 2017). For example, Zaqout et al. (2017) reported that Cep215$^{an/an}$ mutant mice were absent of the spermatogonial stem cells at the postnatal stage. However, I observed that *Cep215* KO mice had spermatogonia and early stages of spermatocytes, but fail to complete meiosis. It is not clear whether such difference stems from the presence of residual Cep215 truncate proteins in *Cep215*$^{an/an}$ mutant mice or simply from different mouse housing environments. Along with the phenotypes in germ cells, I also investigated the defects in microenvironment of germ cells. *Cep215* deletion caused the defects in BTB formation of Sertoli cells which is necessary for the immune privilege of germ cells (Fig. 32). The effects of Cep215 in Sertoli cells have not been reported so far.

The germ cells of *Cep215* KO mouse started to show developmental defects in timing of meiosis progression. In 17 days old *Cep215* KO mouse, the spermatocytes arrested mainly at the zygotene and eventually underwent cell death (Fig. 27 and 32). It is possible that the p53-dependent cell death pathway may be activated by a delay in meiotic progression of the *Cep215*-deleted spermatocytes (Barrera et al., 2010; Lee and Rhee, 2010). In fact, deletions of *CPAP*, a centrosome protein gene, results in embryonic lethal, due to the p53-dependent apoptosis caused by mitotic delays (Bazzi and Anderson, 2014; Phan et al., 2021). In the future, the studies related to p53 dependent apoptotic pathway will help to understand the intrinsic mechanism how *Cep215* deletion causes cell death in male germ cells.

I initially suspected that the centrosome of *Cep215*-deleted spermatocytes was not functional since Cep215 is a major component of the centrosome. To my surprise, the centrosomes in the male germ cells of the *Cep215* KO mice were intact and functional in point of PCM recruitment, cohesion of centrosome, and controlling the number of centriole as wild type (Fig. 28 and 30). These unexpected observations raise the possibility that the defects in spermatogenesis of *Cep215* KO mouse are not caused by malformation of the centrosomes in male germ cells.

Developmental arrest at a meiotic prophase of the *Cep215* KO male germ cells may be derived from an intrinsic defect within the male germ cells or from an extrinsic problem outside the germ cells. Both of intrinsic and extrinsic mechanisms may not be mutually exclusive but may occur simultaneously. In the case of cell intrinsic defects, the progression of prophase I would be affected by *Cep215* deletion. In prophase I, homologous chromosomes form bivalents via double strand breaks and repairs. At this point, movements of chromosomes depended on microtubules and microtubule-associated dynein-dynactin complex, which is mediated by interaction between KASH5 and telomere associated SUN1 (Morimoto et al., 2012; Alleva and Smolikove, 2017). Also, these movements are dependent on the microtubule networks. In zygotene, the microtubule networks are aggregated in defined area, and it is thought to be related to speed of chromosome movements (Lee et al., 2015). These observations suggest that the organization of microtubule networks in zygotene might affect to chromosome movements, and further, progression of synapsis formation. Because Cep215 in somatic cells can nucleates microtubule in the cytoplasm, cytoplasmic microtubules might be affected in zygotene of *Cep215*-deleted spermatocytes (Choi et al., 2010).

Sertoli cells are located adjacent to the germ cells. The importance of Sertoli cells in spermatogenesis have been already studied. It is reported that signaling molecules released from Sertoli cells are important for initiation and progression of meiosis (Griswold et al., 2012; Griswold, 2016). In addition, Sertoli cells form BTB between the proliferating spermatogonia and dividing meiotic spermatocytes to prevent cell death of germ cells (Kaur et al., 2014).

Collectively, it is possible that the failure of meiosis completion in *Cep215* KO mouse might be caused by defects in Sertoli cells (Fig. 32). In the testis of *Cep215* KO mouse, indeed, the proportion of seminiferous tubules with premeiotic germ cells was significantly reduced, and BTB formation was disturbed at the same time (Fig. 26 and 32). These observations suggest that maturation of Sertoli cells could be suppressed by *Cep215* deletion. The mutant study of AKAP9, a one of centrosomal protein, showed that the failure in maturation of Sertoli cells result in defects in male germ cell development and eventually infertility (Schimenti et al., 2013). Hence, it is worth to study the specific role of Cep215 in Sertoli cells. In the future, I may compare the testis phenotypes of the conditional *Cep215* KO mice specific to male germ cells and Sertoli cells.

Several centrosomal proteins have been associated with different kinds of human diseases, such as microcephaly, ciliopathy, and cancer (Jaiswal and Singh, 2021). There is the case that proteins which have different functions in the cellular level show the same phenotypes in the brain. PCM proteins, such as Cep152 and Pericentrin, are also identified as causative genes of microcephaly although their functions are quite different in the cellular level (Rauch et al., 2008; Cizmecioglu et al., 2010; Guernsey et al., 2010; Hatch et al., 2010). On the other hand, the proteins with similar functions in the cells can cause different defects in organisms. Although Cep192 and Cep152 function together in the centriole duplication, the phenotype is not same that mutations of Cep192 do not cause microcephaly (Sonnen et al., 2013). These results imply that the roles of centrosomal proteins in development of organisms would be various beyond its expected functions in cells. Comparison of the phenotypes caused by PCM proteins will be helpful to understand the role of the centrosome in developmental processes.

CONCLUSION

Since Cep215 is a centrosome protein, it has been intensely studied at cellular levels. Cep215 includes two important domains: The CM1 domain is for interaction with the γ-tubulin ring complex while the CM2 domain is for interaction with other proteins at specific subcellular locations. Therefore, the basic role of Cep215 may be to place microtubule organizing centers at specific locations within the cell, including the centrosome. In this study, I investigated Cep215 functions at organism levels, especially focusing on differentiation of astrocytes and male germ cells.

In chapter 1, I observed that deletion of *Cep215* caused the defects in differential morphogenesis of astrocytes. However, the *Cep215* KO did not affect neuronal differentiation, proliferation, and fate determination at least in the P19 embryonic carcinoma cell line. I also observed that the microtubule organizing function of Cep215 is critical for the glial process formation. Based on these results, I propose that Cep215 organizes microtubules for glial process formation during astrocyte differentiation.

In chapter 2, I observed that the testes in the *Cep215* KO mice were smaller than the wild type testes, suggesting defects in male germ cell development. Spermatogenesis in *Cep215* KO mouse was arrested at prophase I and the spermatocytes were vulnerable to cell death. The centrosomes of *Cep215*-deleted germ cells appeared to be intact, suggesting that the defects in progression of meiosis may be not caused by abnormal centrosomes in the *Cep215*-deleted male germ cells. Rather, the tight and gap junctions of Sertoli cells were disorganized and the intercellular bridges among germ cells were reduced in the *Cep215* KO testes. Based on the results, I propose that germ cell defects are attributed, in part, to disorganized architecture of the *Cep215* KO testis.

A prevailing hypothesis of Cep215 functions has described that the absence of Cep215 results in abnormalities in the centrosome functions, leading to defects in spindle formation

during mitosis. Delay in mitosis results in diverse outcomes, including mitotic arrest, aneuploidy and cell death. Once the stem cell populations are reduced in the *Cep215*-deleted organisms, the total numbers of differentiated cells should be reduced as well. However, my dissertation works revealed that phenotypes of the *Cep215* deletion are not directly linked to defects in mitosis. Rather, the phenotypes of the *Cep215* deletion is more linked to the morphological abnormalities of differentiated cells, at least in astrocytes of the brain and Sertoli cells of the testis. Based on the results, I propose that Cep215 is not only important for centrosome functions but also involved in cellular morphology by controlling the microtubule network in differentiated cells. I believe that my research opens a new aspect in roles of Cep215 at the organism levels.

REFERENCES

Abdullah, U., Farooq, M., Mang, Y., Marriam Bakhtiar, S., Fatima, A., Hansen, L., Kjaer, K.W., Larsen, L.A., Faryal, S., Tommerup, N.*, et al.* (2017). A novel mutation in CDK5RAP2 gene causes primary microcephaly with speech impairment and sparse eyebrows in a consanguineous Pakistani family. Eur J Med Genet *60*, 627-630.

Ahmad, F.J., Yu, W., McNally, F.J., and Baas, P.W. (1999). An essential role for katanin in severing microtubules in the neuron. J Cell Biol *145*, 305-315.

Alfares, A., Alhufayti, I., Alsubaie, L., Alowain, M., Almass, R., Alfadhel, M., Kaya, N., and Eyaid, W. (2018). A new association between CDK5RAP2 microcephaly and congenital cataracts. Ann Hum Genet *82*, 165-170.

Alfaro, E., Lopez-Jimenez, P., Gonzalez-Martinez, J., Malumbres, M., Suja, J.A., and Gomez, R. (2021). PLK1 regulates centrosome migration and spindle dynamics in male mouse meiosis. EMBO Rep *22*, e51030.

Alleva, B., and Smolikove, S. (2017). Moving and stopping: Regulation of chromosome movement to promote meiotic chromosome pairing and synapsis. Nucleus *8*, 613-624.

Azimzadeh, J., and Marshall, W.F. (2010). Building the centriole. Curr Biol *20*, R816-825.

Barker, J.E., and Bernstein, S.E. (1983). Hertwig's anemia: characterization of the stem cell defect. Blood *61*, 765-769.

Barrera, J.A., Kao, L.R., Hammer, R.E., Seemann, J., Fuchs, J.L., and Megraw, T.L. (2010). CDK5RAP2 regulates centriole engagement and cohesion in mice. Dev Cell *18*, 913-926.

Bazzi, H., and Anderson, K.V. (2014). Acentriolar mitosis activates a p53-dependent apoptosis pathway in the mouse embryo. Proc Natl Acad Sci U S A *111*, E1491-1500.

Beaudoin, G.M., 3rd, Lee, S.H., Singh, D., Yuan, Y., Ng, Y.G., Reichardt, L.F., and Arikkath, J. (2012). Culturing pyramidal neurons from the early postnatal mouse hippocampus and cortex. Nat Protoc *7*, 1741-1754.

Bertrand, N., Castro, D.S., and Guillemot, F. (2002). Proneural genes and the specification of neural cell types. Nat Rev Neurosci *3*, 517-530.

Bettencourt-Dias, M., Hildebrandt, F., Pellman, D., Woods, G., and Godinho, S.A. (2011). Centrosomes and cilia in human disease. Trends Genet *27*, 307-315.

Bond, A.M., Berg, D.A., Lee, S., Garcia-Epelboim, A.S., Adusumilli, V.S., Ming, G.L., and Song, H. (2020). Differential Timing and Coordination of Neurogenesis and Astrogenesis in Developing Mouse Hippocampal Subregions. Brain Sci *10*.

Bond, J., Roberts, E., Springell, K., Lizarraga, S.B., Scott, S., Higgins, J., Hampshire, D.J., Morrison, E.E., Leal, G.F., Silva, E.O., *et al.* (2005). A centrosomal mechanism involving CDK5RAP2 and CENPJ controls brain size. Nat Genet *37*, 353-355.

Buchman, J.J., Tseng, H.C., Zhou, Y., Frank, C.L., Xie, Z., and Tsai, L.H. (2010). Cdk5rap2 interacts with pericentrin to maintain the neural progenitor pool in the developing neocortex. Neuron *66*, 386-402.

Bunt, J., Lim, J.W., Zhao, L., Mason, S., and Richards, L.J. (2015). PAX6 does not regulate Nfia and Nfib expression during neocortical development. Sci Rep *5*, 10668.

Chandrasekaran, A., Avci, H.X., Leist, M., Kobolak, J., and Dinnyes, A. (2016). Astrocyte Differentiation of Human Pluripotent Stem Cells: New Tools for Neurological Disorder Research. Front Cell Neurosci *10*, 215.

Chavali, P.L., Chandrasekaran, G., Barr, A.R., Tatrai, P., Taylor, C., Papachristou, E.K., Woods, C.G., Chavali, S., and Gergely, F. (2016). A CEP215-HSET complex links centrosomes with spindle poles and drives centrosome clustering in cancer. Nat Commun *7*, 11005.

Chen, J.V., Buchwalter, R.A., Kao, L.R., and Megraw, T.L. (2017a). A Splice Variant of Centrosomin Converts Mitochondria to Microtubule-Organizing Centers. Curr Biol *27*, 1928-1940 e1926.

Chen, W.S., Chen, Y.J., Huang, Y.A., Hsieh, B.Y., Chiu, H.C., Kao, P.Y., Chao, C.Y., and Hwang, E. (2017b). Ran-dependent TPX2 activation promotes acentrosomal microtubule nucleation in neurons. Sci Rep *7*, 42297.

Ching, Y.P., Qi, Z., and Wang, J.H. (2000). Cloning of three novel neuronal Cdk5 activator binding proteins. Gene *242*, 285-294.

Choi, Y.K., Liu, P., Sze, S.K., Dai, C., and Qi, R.Z. (2010). CDK5RAP2 stimulates microtubule nucleation by the gamma-tubulin ring complex. J Cell Biol *191*, 1089-1095.

Cizmecioglu, O., Arnold, M., Bahtz, R., Settele, F., Ehret, L., Haselmann-Weiss, U., Antony, C., and Hoffmann, I. (2010). Cep152 acts as a scaffold for recruitment of Plk4 and CPAP to the centrosome. J Cell Biol *191*, 731-739.

Cunha-Ferreira, I., Chazeau, A., Buijs, R.R., Stucchi, R., Will, L., Pan, X., Adolfs, Y., van der Meer, C., Wolthuis, J.C., Kahn, O.I., *et al.* (2018). The HAUS Complex Is a Key Regulator of Non-centrosomal Microtubule Organization during Neuronal Development. Cell Rep *24*, 791-800.

de Anda, F.C., Pollarolo, G., Da Silva, J.S., Camoletto, P.G., Feiguin, F., and Dotti, C.G. (2005). Centrosome localization determines neuronal polarity. Nature *436*, 704-708.

Deneen, B., Ho, R., Lukaszewicz, A., Hochstim, C.J., Gronostajski, R.M., and Anderson, D.J. (2006). The transcription factor NFIA controls the onset of gliogenesis in the developing spinal cord. Neuron *52*, 953-968.

Doxsey, S. (2001). Re-evaluating centrosome function. Nat Rev Mol Cell Biol *2*, 688-698.

Endoh-Yamagami, S., Karkar, K.M., May, S.R., Cobos, I., Thwin, M.T., Long, J.E., Ashique, A.M., Zarbalis, K., Rubenstein, J.L., and Peterson, A.S. (2010). A mutation in the pericentrin gene causes abnormal interneuron migration to the olfactory bulb in mice. Dev Biol *340*, 41-53.

Eppig, J.T., and Barker, J.E. (1984). Chromosome abnormalities in mice with Hertwig's anemia. Blood *64*, 727-732.

Fish, J.L., Kosodo, Y., Enard, W., Paabo, S., and Huttner, W.B. (2006). Aspm specifically maintains symmetric proliferative divisions of neuroepithelial cells. Proc Natl Acad Sci U S A *103*, 10438-10443.

Fong, K.W., Au, F.K.C., Jia, Y., Yang, S., Zhou, L., and Qi, R.Z. (2017). Microtubule plus-end tracking of end-binding protein 1 (EB1) is regulated by CDK5 regulatory subunit-associated protein 2. J Biol Chem *292*, 7675-7687.

Fong, K.W., Choi, Y.K., Rattner, J.B., and Qi, R.Z. (2008). CDK5RAP2 is a pericentriolar protein that functions in centrosomal attachment of the gamma-tubulin ring complex. Mol Biol Cell *19*, 115-125.

Fong, K.W., Hau, S.Y., Kho, Y.S., Jia, Y., He, L., and Qi, R.Z. (2009). Interaction of CDK5RAP2 with EB1 to track growing microtubule tips and to regulate microtubule dynamics. Mol Biol Cell *20*, 3660-3670.

Fukasawa, K. (2007). Oncogenes and tumour suppressors take on centrosomes. Nat Rev Cancer *7*, 911-924.

Gopinathan, L., Szmyd, R., Low, D., Diril, M.K., Chang, H.Y., Coppola, V., Liu, K., Tessarollo, L., Guccione, E., van Pelt, A.M.M.*, et al.* (2017). Emi2 Is Essential for Mouse Spermatogenesis. Cell Rep *20*, 697-708.

Greenbaum, M.P., Iwamori, T., Buchold, G.M., and Matzuk, M.M. (2011). Germ cell intercellular bridges. Cold Spring Harb Perspect Biol *3*, a005850.

Greenbaum, M.P., Yan, W., Wu, M.H., Lin, Y.N., Agno, J.E., Sharma, M., Braun, R.E., Rajkovic, A., and Matzuk, M.M. (2006). TEX14 is essential for intercellular bridges and fertility in male mice. Proc Natl Acad Sci U S A *103*, 4982-4987.

Griswold, M.D. (2016). Spermatogenesis: The Commitment to Meiosis. Physiol Rev *96*, 1-17.

Griswold, M.D., Hogarth, C.A., Bowles, J., and Koopman, P. (2012). Initiating meiosis: the case for retinoic acid. Biol Reprod *86*, 35.

Guernsey, D.L., Jiang, H., Hussin, J., Arnold, M., Bouyakdan, K., Perry, S., Babineau-Sturk, T., Beis, J., Dumas, N., Evans, S.C.*, et al.* (2010). Mutations in centrosomal protein CEP152 in primary microcephaly families linked to MCPH4. Am J Hum Genet *87*, 40-51.

Hatch, E.M., Kulukian, A., Holland, A.J., Cleveland, D.W., and Stearns, T. (2010). Cep152 interacts with Plk4 and is required for centriole duplication. J Cell Biol *191*, 721-729.

Heyting, C. (1996). Synaptonemal complexes: structure and function. Curr Opin Cell Biol *8*, 389-396.

Hollenbach, J., Jung, K., Noelke, J., Gasse, H., Pfarrer, C., Koy, M., and Brehm, R. (2018). Loss of connexin43 in murine Sertoli cells and its effect on blood-testis barrier formation and dynamics. PLoS One *13*, e0198100.

Hosokawa, S., Furuyama, K., Horiguchi, M., Aoyama, Y., Tsuboi, K., Sakikubo, M., Goto, T., Hirata, K., Tanabe, W., Nakano, Y.*, et al.* (2015). Impact of Sox9 dosage and Hes1-mediated Notch signaling in controlling the plasticity of adult pancreatic duct cells in mice. Sci Rep *5*, 8518.

Issa, L., Mueller, K., Seufert, K., Kraemer, N., Rosenkotter, H., Ninnemann, O., Buob, M., Kaindl, A.M., and Morris-Rosendahl, D.J. (2013). Clinical and cellular features in patients with primary autosomal recessive microcephaly and a novel CDK5RAP2 mutation. Orphanet J Rare Dis *8*, 59.

Jaiswal, S., and Singh, P. (2021). Centrosome dysfunction in human diseases. Semin Cell Dev Biol *110*, 113-122.

Jones-Villeneuve, E.M., McBurney, M.W., Rogers, K.A., and Kalnins, V.I. (1982). Retinoic acid induces embryonal carcinoma cells to differentiate into neurons and glial cells. J Cell Biol *94*, 253-262.

Kang, P., Lee, H.K., Glasgow, S.M., Finley, M., Donti, T., Gaber, Z.B., Graham, B.H., Foster, A.E., Novitch, B.G., Gronostajski, R.M.*, et al.* (2012). Sox9 and NFIA coordinate a transcriptional regulatory cascade during the initiation of gliogenesis. Neuron *74*, 79-94.

Kaur, G., Thompson, L.A., and Dufour, J.M. (2014). Sertoli cells--immunological sentinels of spermatogenesis. Semin Cell Dev Biol *30*, 36-44.

Kim, K., and Rhee, K. (2011). The pericentriolar satellite protein CEP90 is crucial for integrity of the mitotic spindle pole. J Cell Sci *124*, 338-347.

Kim, S., and Rhee, K. (2014). Importance of the CEP215-pericentrin interaction for centrosome maturation during mitosis. PLoS One *9*, e87016.

Kollman, J.M., Merdes, A., Mourey, L., and Agard, D.A. (2011). Microtubule nucleation by gamma-tubulin complexes. Nat Rev Mol Cell Biol *12*, 709-721.

Kraemer, N., Issa-Jahns, L., Neubert, G., Ravindran, E., Mani, S., Ninnemann, O., and Kaindl, A.M. (2015). Novel Alternative Splice Variants of Mouse Cdk5rap2. PLoS One *10*, e0136684.

Kremneva, E., Kislin, M., Kang, X., and Khiroug, L. (2013). Motility of astrocytic mitochondria is arrested by Ca2+-dependent interaction between mitochondria and actin filaments. Cell Calcium *53*, 85-93.

Lawo, S., Hasegan, M., Gupta, G.D., and Pelletier, L. (2012). Subdiffraction imaging of centrosomes reveals higher-order organizational features of pericentriolar material. Nat Cell Biol *14*, 1148-1158.

Leduc, C., and Etienne-Manneville, S. (2017a). Intermediate filaments join the action. Cell Cycle *16*, 1389-1390.

Leduc, C., and Etienne-Manneville, S. (2017b). Regulation of microtubule-associated motors drives intermediate filament network polarization. J Cell Biol *216*, 1689-1703.

Lee, C.Y., Horn, H.F., Stewart, C.L., Burke, B., Bolcun-Filas, E., Schimenti, J.C., Dresser, M.E., and Pezza, R.J. (2015). Mechanism and regulation of rapid telomere prophase movements in mouse meiotic chromosomes. Cell Rep *11*, 551-563.

Lee, S., and Rhee, K. (2010). CEP215 is involved in the dynein-dependent accumulation of pericentriolar matrix proteins for spindle pole formation. Cell Cycle *9*, 775-784.

Li, K., Xu, E.Y., Cecil, J.K., Turner, F.R., Megraw, T.L., and Kaufman, T.C. (1998). Drosophila centrosomin protein is required for male meiosis and assembly of the flagellar axoneme. J Cell Biol *141*, 455-467.

Lizarraga, S.B., Margossian, S.P., Harris, M.H., Campagna, D.R., Han, A.P., Blevins, S., Mudbhary, R., Barker, J.E., Walsh, C.A., and Fleming, M.D. (2010). Cdk5rap2 regulates centrosome function and chromosome segregation in neuronal progenitors. Development *137*, 1907-1917.

Ma, Q., Chen, Z., del Barco Barrantes, I., de la Pompa, J.L., and Anderson, D.J. (1998). neurogenin1 is essential for the determination of neuronal precursors for proximal cranial sensory ganglia. Neuron *20*, 469-482.

Mahjoub, M.R. (2013). The importance of a single primary cilium. Organogenesis *9*, 61-69.

Mamber, C., Kamphuis, W., Haring, N.L., Peprah, N., Middeldorp, J., and Hol, E.M. (2012). GFAPdelta expression in glia of the developmental and adolescent mouse brain. PLoS One *7*, e52659.

Marjanovic, M., Sanchez-Huertas, C., Terre, B., Gomez, R., Scheel, J.F., Pacheco, S., Knobel, P.A., Martinez-Marchal, A., Aivio, S., Palenzuela, L.*, et al.* (2015). CEP63 deficiency promotes p53-dependent microcephaly and reveals a role for the centrosome in meiotic recombination. Nat Commun *6*, 7676.

McLean, D.J., Friel, P.J., Johnston, D.S., and Griswold, M.D. (2003). Characterization of spermatogonial stem cell maturation and differentiation in neonatal mice. Biol Reprod *69*, 2085-2091.

Medrano, S., and Steward, O. (2001). Differential mRNA localization in astroglial cells in culture. J Comp Neurol *430*, 56-71.

Meiring, J.C.M., Shneyer, B.I., and Akhmanova, A. (2020). Generation and regulation of microtubule network asymmetry to drive cell polarity. Curr Opin Cell Biol *62*, 86-95.

Mohammad, M.H., Al-Shammari, A.M., Al-Juboory, A.A., and Yaseen, N.Y. (2016). Characterization of neural stemness status through the neurogenesis process for bone marrow mesenchymal stem cells. Stem Cells Cloning *9*, 1-15.

Morimoto, A., Shibuya, H., Zhu, X., Kim, J., Ishiguro, K., Han, M., and Watanabe, Y. (2012). A conserved KASH domain protein associates with telomeres, SUN1, and dynactin during mammalian meiosis. J Cell Biol *198*, 165-172.

Mruk, D.D., and Cheng, C.Y. (2015). The Mammalian Blood-Testis Barrier: Its Biology and Regulation. Endocr Rev *36*, 564-591.

Muroyama, A., and Lechler, T. (2017). Microtubule organization, dynamics and functions in differentiated cells. Development *144*, 3012-3021.

Nasser, H., Vera, L., Elmaleh-Berges, M., Steindl, K., Letard, P., Teissier, N., Ernault, A., Guimiot, F., Afenjar, A., Moutard, M.L.*, et al.* (2020). CDK5RAP2 primary microcephaly is associated with hypothalamic, retinal and cochlear developmental defects. J Med Genet *57*, 389-399.

Nebel, B.R., Amarose, A.P., and Hacket, E.M. (1961). Calendar of gametogenic development in the prepuberal male mouse. Science *134*, 832-833.

Oakley, B.R., Paolillo, V., and Zheng, Y. (2015). gamma-Tubulin complexes in microtubule nucleation and beyond. Mol Biol Cell *26*, 2957-2962.

Ori-McKenney, K.M., Jan, L.Y., and Jan, Y.N. (2012). Golgi outposts shape dendrite morphology by functioning as sites of acentrosomal microtubule nucleation in neurons. Neuron *76*, 921-930.

Paridaen, J.T., and Huttner, W.B. (2014). Neurogenesis during development of the vertebrate central nervous system. EMBO Rep *15*, 351-364.

Paz, J., and Luders, J. (2018). Microtubule-Organizing Centers: Towards a Minimal Parts List. Trends Cell Biol *28*, 176-187.

Phan, T.P., and Holland, A.J. (2021). Time is of the essence: the molecular mechanisms of primary microcephaly. Genes Dev *35*, 1551-1578.

Phan, T.P., Maryniak, A.L., Boatwright, C.A., Lee, J., Atkins, A., Tijhuis, A., Spierings, D.C., Bazzi, H., Foijer, F., Jordan, P.W.*, et al.* (2021). Centrosome defects cause microcephaly by activating the 53BP1-USP28-TP53 mitotic surveillance pathway. EMBO J *40*, e106118.

Qin, Y., Zhou, Y., Shen, Z., Xu, B., Chen, M., Li, Y., Chen, M., Behrens, A., Zhou, J., Qi, X.*, et al.* (2019). WDR62 is involved in spindle assembly by interacting with CEP170 in spermatogenesis. Development *146*.

Robinson, B.V., Faundez, V., and Lerit, D.A. (2020). Understanding microcephaly through the study of centrosome regulation in Drosophila neural stem cells. Biochem Soc Trans *48*, 2101-2115.

Roper, K. (2020). Microtubules enter centre stage for morphogenesis. Philos Trans R Soc Lond B Biol Sci *375*, 20190557.

Sakers, K., Lake, A.M., Khazanchi, R., Ouwenga, R., Vasek, M.J., Dani, A., and Dougherty, J.D. (2017). Astrocytes locally translate transcripts in their peripheral processes. Proc Natl Acad Sci U S A *114*, E3830-E3838.

Sanchez-Huertas, C., Freixo, F., Viais, R., Lacasa, C., Soriano, E., and Luders, J. (2016). Non-centrosomal nucleation mediated by augmin organizes microtubules in post-mitotic neurons and controls axonal microtubule polarity. Nat Commun *7*, 12187.

Sanchez-Martin, F.J., Fan, Y., Lindquist, D.M., Xia, Y., and Puga, A. (2013). Lead induces similar gene expression changes in brains of gestationally exposed adult mice and in neurons differentiated from mouse embryonic stem cells. PLoS One *8*, e80558.

Sanchez, A.D., and Feldman, J.L. (2017). Microtubule-organizing centers: from the centrosome to non-centrosomal sites. Curr Opin Cell Biol *44*, 93-101.

Schatten, H., and Sun, Q.Y. (2011). New insights into the role of centrosomes in mammalian fertilization and implications for ART. Reproduction *142*, 793-801.

Schatten, H., and Sun, Q.Y. (2018). Functions and dysfunctions of the mammalian centrosome in health, disorders, disease, and aging. Histochem Cell Biol *150*, 303-325.

Scheer, U. (2014). Historical roots of centrosome research: discovery of Boveri's microscope slides in Wurzburg. Philos Trans R Soc Lond B Biol Sci *369*.

Schimenti, K.J., Feuer, S.K., Griffin, L.B., Graham, N.R., Bovet, C.A., Hartford, S., Pendola, J., Lessard, C., Schimenti, J.C., and Ward, J.O. (2013). AKAP9 is essential for spermatogenesis and sertoli cell maturation in mice. Genetics *194*, 447-457.

Shin, W., Yu, N.K., Kaang, B.K., and Rhee, K. (2015). The microtubule nucleation activity of centrobin in both the centrosome and cytoplasm. Cell Cycle *14*, 1925-1931.

Sonnen, K.F., Gabryjonczyk, A.M., Anselm, E., Stierhof, Y.D., and Nigg, E.A. (2013). Human Cep192 and Cep152 cooperate in Plk4 recruitment and centriole duplication. J Cell Sci *126*, 3223-3233

Stiess, M., Maghelli, N., Kapitein, L.C., Gomis-Ruth, S., Wilsch-Brauninger, M., Hoogenraad, C.C., Tolic-Norrelykke, I.M., and Bradke, F. (2010). Axon extension occurs independently of centrosomal microtubule nucleation. Science *327*, 704-707.

Stolt, C.C., Lommes, P., Sock, E., Chaboissier, M.C., Schedl, A., and Wegner, M. (2003). The Sox9 transcription factor determines glial fate choice in the developing spinal cord. Genes Dev *17*, 1677-1689.

Uhrin, P., Dewerchin, M., Hilpert, M., Chrenek, P., Schofer, C., Zechmeister-Machhart, M., Kronke, G., Vales, A., Carmeliet, P., Binder, B.R.*, et al.* (2000). Disruption of the protein C inhibitor gene results in impaired spermatogenesis and male infertility. J Clin Invest *106*, 1531-1539.

Ventura, R., and Harris, K.M. (1999). Three-dimensional relationships between hippocampal synapses and astrocytes. J Neurosci *19*, 6897-6906.

Wang, Z., Wu, T., Shi, L., Zhang, L., Zheng, W., Qu, J.Y., Niu, R., and Qi, R.Z. (2010). Conserved motif of CDK5RAP2 mediates its localization to centrosomes and the Golgi complex. J Biol Chem *285*, 22658-22665.

Wellard, S.R., Zhang, Y., Shults, C., Zhao, X., McKay, M., Murray, S.A., and Jordan, P.W. (2021). Overlapping roles for PLK1 and Aurora A during meiotic centrosome biogenesis in mouse spermatocytes. EMBO Rep *22*, e51023.

Woodruff, J.B., Wueseke, O., and Hyman, A.A. (2014). Pericentriolar material structure and dynamics. Philos Trans R Soc Lond B Biol Sci *369*.

Yalgin, C., Ebrahimi, S., Delandre, C., Yoong, L.F., Akimoto, S., Tran, H., Amikura, R., Spokony, R., Torben-Nielsen, B., White, K.P.*, et al.* (2015). Centrosomin represses dendrite branching by orienting microtubule nucleation. Nat Neurosci *18*, 1437-1445.

Yoon, J., Park, K., Hwang, D.S., and Rhee, K. (2017). Importance of eIF2alpha phosphorylation as a protective mechanism against heat stress in mouse male germ cells. Mol Reprod Dev *84*, 265-274.

Yoon, J.S., Lee, M.Y., Lee, J.S., Park, C.S., Youn, H.J., and Lee, J.H. (2009). Bis is involved in glial differentiation of p19 cells induced by retinoic Acid. Korean J Physiol Pharmacol *13*, 251-256.

Zaqout, S., Bessa, P., Kramer, N., Stoltenburg-Didinger, G., and Kaindl, A.M. (2017). CDK5RAP2 Is Required to Maintain the Germ Cell Pool during Embryonic Development. Stem Cell Reports *8*, 198-204.

Zaqout, S., Blaesius, K., Wu, Y.J., Ott, S., Kraemer, N., Becker, L.L., Rosario, M., Rosenmund, C., Strauss, U., and Kaindl, A.M. (2019). Altered inhibition and excitation in neocortical circuits in congenital microcephaly. Neurobiol Dis *129*, 130-143.

Zaqout, S., Ravindran, E., Stoltenburg-Didinger, G., and Kaindl, A.M. (2020). Congenital microcephaly-linked CDK5RAP2 affects eye development. Ann Hum Genet *84*, 87-91.

ABSTRACT IN KOREAN
(국문 초록)

중심체는 대부분의 동물세포에 보존되어 있는 세포 소기관으로 주로 미세소관 형성 중심으로서 역할을 한다. 중심체는 다양한 세포 활동에 관여하고 있는데, 가장 대표적인 역할은 세포의 모양 형성, 세포 분열, 일차 섬모 형성 등이다. 중심체는 두 종류의 중심립과 그 주변을 둘러 싸고 있는 단백질 덩어리인 pericentriolar material (PCM) 으로 이루어져 있다. 그 중 Cep215 는 PCM 의 골격단백질로서 다른 PCM 단백질들이 잘 모일 수 있도록 해주는 역할을 하고 있으며, 특히, 중심체에서 미세소관이 자라날 수 있게 하는데 있어서 필수적인 감마 튜불린을 중심체로 끌어오는 역할을 하고 있다. Cep215 는 중심체뿐만 아니라 골지 등에도 존재하고 있으며 Cep215 가 위치하는 세포 소기관에서 미세소관을 뻗어내게 만들어주는 능력을 가지고 있다. 이러한 Cep215 의 역할은 분열하는 체세포를 이용하여 주로 연구가 되어 왔으며, 특정 장기 형성 과정에서의 Cep215 역할은 상대적으로 잘 알려지지 않았다. 본인은 박사학위 과정 동안 뇌와 정소 발생 과정에서 Cep215 의 역할에 대해 연구를 수행했다.

제 1 장에서는 배아암종세포에서 유래한 P19 세포와 생쥐 태아로부터 초대 배양한 해마 유래 세포를 이용하여 성상세포의 분화과정에서 Cep215 의 중요성을 확인하였다. Cep215 는 성상세포의 중심체뿐만 아니라 세포질, 특히 가지에서도 관찰되었다. P19 세포에서 Cep215 유전자를 완전히 없앤 결실세포주는 성상세포로의 분화가 저하되고, 가지를 형성하지 못하여 성상세포 특유의 세포 모양을 형성하지 못했다. 하지만 Cep215 결실세포주는 신경세포로의 분화, 세포의 분열 능력, 세포 운명 결정에는 영향을 미치지 않았다. Cep215 는 미세소관 형성을 통해서 성상세포의 가지 형성을 촉진한다는 것을 확인하였다. 이러한 결과들을 토대로 성상세포 분화 과정에서 Cep215 가 미세소관형성을 조절함으로써 성상세포의 형태를 형성한다는 것을 확인하였다.

제 2 장에서는 Cep215 결실 생쥐를 이용하여 Cep215 가 남성생식세포의 발생에 미치는 영향을 확인하였다. Cep215 유전자를 완전히 제거하기 위해서 첫번째와 마지막 인트론을 타겟팅하는 전략을 이용하여 결실을 유도하였다.

이렇게 제작한 Cep215 결실 생쥐를 이용하여 다양한 장기에서 보이는 표현형을 관찰하였다. Cep215 결실 생쥐는 이전 보고된 Cep215 돌연변이 생쥐와 마찬가지로 소두증과 같은 표현형을 보였으며, 야생형 생쥐와 비교했을 때, 작은 크기의 정소를 가지는 것으로 보아 남성생식세포의 발생에 문제가 있다는 것을 확인하였다. 실제로 Cep215 결실 생쥐의 정소에는 감수분열 이후에 관찰되는 생식세포들이 전혀 관찰되지 않았다. 이 결실 생쥐에서 일어나는 감수분열 과정은 초기에 해당하는 prophase I 과정에서 멈추는 것을 확인하였고, 이 정모세포들은 세포 사멸에 취약하다는 것을 확인하였다. 흥미롭게도, Cep215 결실 생쥐의 다양한 남성생식세포에서 중심체가 잘 형성되어 있다는 것을 확인하였고, 이를 통해서 이 결실 생쥐에서 보이는 표현형이 중심체의 결함에 의해서 유도된 것이 아닐 수도 있다는 것을 확인하였다. 대신에 sertoli 세포에 의해 형성되는 혈액-고환 장벽이 제대로 형성되어 있지않고, 생식세포끼리 연결시켜주는 세포간결합체의 형성이 감소되어 있다는 것을 확인하였다. 이러한 결과들을 토대로 본인은 Cep215 결실 생쥐의 정소에서 제대로 형성되지 않은 정소의 구조적인 환경이 어느 정도 남성생식세포의 발생에 영향을 미칠 수 있다는 것을 확인하였다. Cep215 는 주로 중심체에서 미세소관을 형성하는데 중요한 역할을 하기 때문에, Cep215 가 결실되어 나타나는 표현형이 이렇게 다양한 방식을 통해서 나타난다는 것이 아주 흥미로운 결과였다. 이 연구는 중심체 단백질의 사소한 변화로 인해 얼마나 다양한 세포 활동이 조절될 수 있는지 제시하였다.

주요어 : 중심체, Cep215, 미세소관, 분화, 성상세포, 남성생식세포

학번 : 2017-24251